GEO-3900

MASTER'S THESIS IN GEOLOGY

POLYMETAMORPHIC EVOLUTION OF NEPHELINE NORMATIVE ROCKS IN THE SKATTØRA MIGMATITE COMPLEX, TROMSØ, NORTH NORWAY

Marianne Leinan Knutsen

June, 2012

FACULTY OF SCIENCE AND TECHNOLOGY
Department of Geology
University of Tromsø

GEO-3900

MASTER'S THESIS IN GEOLOGY

POLYMETAMORPHIC EVOLUTION OF NEPHELINE NORMATIVE ROCKS IN THE SKATTØRA MIGMATITE COMPLEX, TROMSØ, NORTH NORWAY

Marianne Leinan Knutsen

June, 2012

FACULTY OF SCIENCE AND TECHNOLOGY
Department of Geology
University of Tromsø

Preface

First and foremost, I would like to thank my supervisor professor Erling J.Krogh Ravna for all his help, feedback, time and patience during the work with this thesis. I also wish to thank co-supervisor professor Holger Stunitz for good advice, Pritam Nasipuri for great guidance with the Perple_X software, and Edel Ellingsen for production of thin section and general guidance on the laboratory. And Will, thanks for reading through and for general help with the language barrier.

En stor takk går også til ekspertisen på blå brakka – spesielt hurtigtast ekspert'n, CorelDraw ekspert'n og målestokk ekspert'n.

Takk til både den avtroppede Bachelor-gjengen og Master-gjengen, som har gjort studietida her i Tromsø riktig så trivelig. Og spesielt til alle på kontor 14, og dem som har hatt det for vane å stikke innom, for mang en kaffepause med høy underholdningsverdi. Spesielt heldig føler jeg meg som har fått dele kontor med ikke mindre enn to drevne ballerinaer.

En spesiell takk går selvfølgelig også hjem til Alta. Ingen plass finnes bedre støtte enn på bakketoppen i Hjemmeluft.

Tromsø, Juni 2012

Marianne Leinan Knutsen

Abstract

The Skattøra migmatite complex (SMC) in the north Norwegian Caledonides is a slightly nepheline normative migmatitic meta-cumulate rock sequence, which experienced anatexis under water saturated conditions. *In situ*- and local crystallization of melt is reflected by leucosomes and the numerous anorthositic dykes net veining the rock complex.

Studies of quartz-free rocks gives challenges for implying P-T conditions by traditional geothermobarometric methods. Phase transitions during metamorphism, partial melting metasomatism in the SMC has been studied through optical petrography and bulk chemistry, and pseudosection-modelling has been the main tool for investigating phase topologies and quantifying P-T conditions during evolution of the SMC. Minimum limit for metamorphic peak conditions in the anorthositic part of the complex is suggested to be approximately 1.18 GPa in the temperature interval 800-850 ^{0}C. In more complex chemical systems onset of melting occurred at lower temperatures.

In the context of the tectonometamorphic evolution of the Upper Most Allochthon results for high grade metamorphism are supportive of earlier work, while for the late retrogressive stage additional suggestions are presented.

The discovery of cross-cutting dolerite dykes in the SMC adds a new feature that should be addressed in future studies.

Key-words: Skattøra migmatite complex; nepheline-normative; cumulate rocks; high-T-P metamorphism; partial melting; phase transitions; P-T pseudosections.

Contents

1 Introduction

1.1 Geographical location of the study area

The area of study is situated on the northern part of the Tromsø Island in Troms county, northern Norway (Figure 1.1; 1.2). The area is located within the city limits and parts of it are densely populated. Human inventions such as road cuts and industrial sites create large exposures of the rocks. All locations are easily accessible within a distance of 4,5 km of each other on the north-eastern side of the island. Mapsheet 1:50 000, Tromsø (1543-3), covers the area.

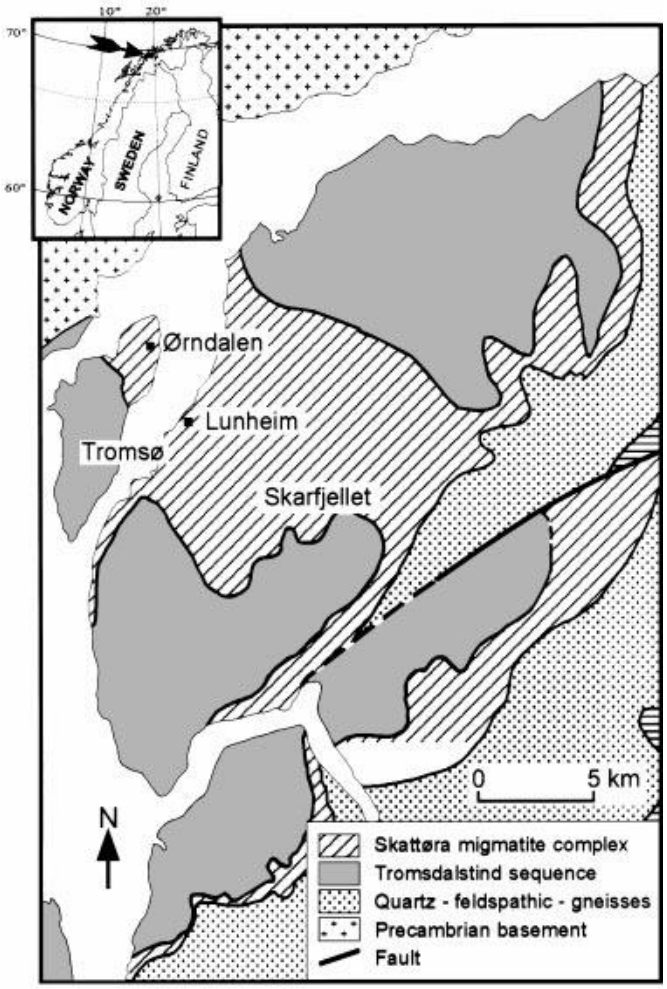

Figure 1.1: Geological mappe with nappe distribution in the Tromsø area, showing the occurrence of Skattøra migmatite complex on the Tromsø Island and the mainland lose to Tromsø. Field area is on the NE side of the Tromsø Island with four localities close to Ørndalen (simplified by Selbekk, Skjerlie & Pedersen (2000) from Krogh et al.(1990) and Zwaan & Grogan (1998)).

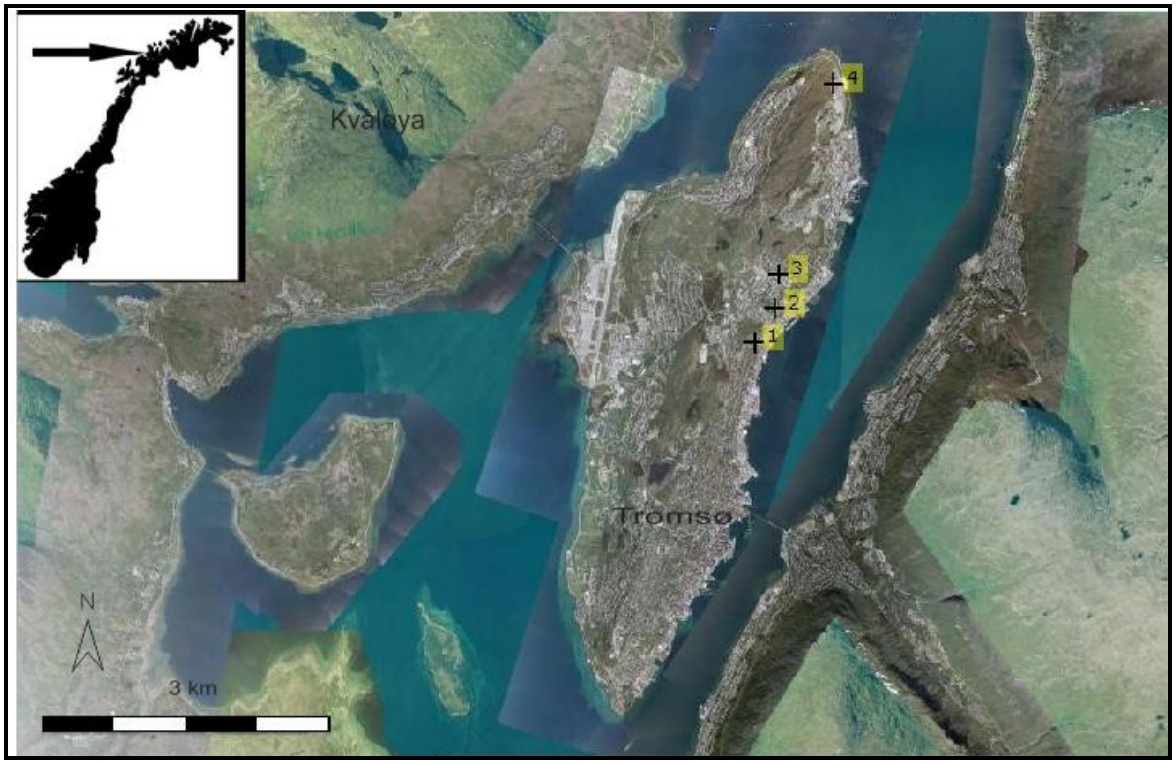

Figure 1.2: Overview of the study area showing the locations on the Island of Tromsø. Digital satellite image is obtained through www.norgei3d.no.

1.2 Purpose of the study

The main objective of this study is to do petrography, petrological surveys, and chemical analysis of metamorphic rocks in the Skattøra migmatite complex (SMC), with the focus to on extraction and interpretation of new data, which can help constrain the P-T conditions during the metamorphic evolution. The information obtained is aimed to contribute to the understanding of the tectonmetamorphous development of the rocks in the Uppermost Allochthton.

Approach:

- Studies of literature, earlier work, and research on the SMC and the mechanisms of migmatization and high-grade metamorphism.
- Field observations and rock sampling.
- Laboratory work: Studies and description of sampled rocks in hand-specimen, and selected samples in thin sections. Preparation of a selection of samples for further XRF analysis for major elements.
- Processing geochemical data using modeling software (Perple_X6.6.6) for construction of pseudosections.
- Interpret the obtained results in order to put them into a larger context of the development history of the SMC, and the Upper Most Allochthon.

1.3 Regional geology

1.3.1 Regional geological setting

The cover rocks in Norway are part of the Caledonian orogen that formed as a result of the collision of the palaeocontinents Laurentia and Baltica, when the Iapetus Ocean closed 500- 405 Ma years ago (Roberts & Gee, 1985).

The evolution of the Scandinavian part of the orogen was explained by Roberts & Gee (1985) by four major phases. Their opinion was that the first signs of convergence in the Iapetus Ocean could be recognized in rocks from late Cambrian time in what was called the *Finnmarkian* phase. Both the *Finnmarkian* and the 25 million year later *Trondheim* phase was characterised by ocean-ward subduction of the Baltica margin and accretion of Iapetan arc-systems and/or microcontinents. Arc-accretion and tectonthermal activity in the Mid to Late Ordovician on the margin of Laurentia is referred to as the Taconian phase, before the main collision event, known as the Scandian phase, in Late Silurian-Early Devonian. The margin of Baltica was rapidly subducted beneath Laurentia causing, exhumation, crustal overthickening, extensive thrusting and transportation of nappes before emplacement on to the Baltic craton and the belonging sedimentary succession. Subsequent to the collision phase there was extensional deformation (ductile and brittle), shearing and folding. On the basis of isotopic age-determination and biostratigraphic data, the Caledonian nappe succession was divided into the Lower-, Middle-, Upper- and Upper Most Allochthon.
The Lower- and Middle Allochthon were interpreted by Roberts (2003) to be rocks that originally belonged to the Baltic margin and shelf succession. The Upper Allochthon was regarded to be an association of rocks with oceanic (ophiolitic), magmatic arc system and marginal basin origin within or peripheral to the Iapetus ocean, whereas the rocks of the Upper Most Allochthon were interpreted to be exotic and derived from Lauretia.

However, it should be noted that the interpretation of the Middle Allochthon to be of Baltic origin is controversial. Corfu et al. (2007) suggested that the present model needed to be modified as the evolution seems to be more complex than first thought. Evidence based on U-Pb data showed that the Kalak Nappe complex, in the Middle Allochthon in the north Norwegian part of the Caledonides, was not likely to have formed as a part of the Baltic margin as interpreted by earlier workers, but rather representing an exotic terrane juxtaposed during the Scandian phase of the orogeny. This was supported by Kirkland et al. (2007). With these new evidences, the fundamental

argument for the earliest phase of the orogeny could no longer be valid and termination of the use of the term *Finnmarkian phase* was proposed by Corfu et al. (2007).

Due to the ongoing debate around the idea of terranes form an exotic mobile belt represented in the Scandinavian Caledonides, the classical tectonstratigraphic model will serve the purpose of this thesis (Fig 1.3). Bedrockmap 1:250 000, Tromsø, published by the Geological Survey of Norway in 1998 covers the area of focus.

1.3.2 Tectonostratigrapichal overview of Troms

The bedrock in Troms has all four Caledonian allochthonous units represented on top of a parautochthon sedimentary unit and the autochthon Precambrian crystalline basement (Roberts & Gee 1985).

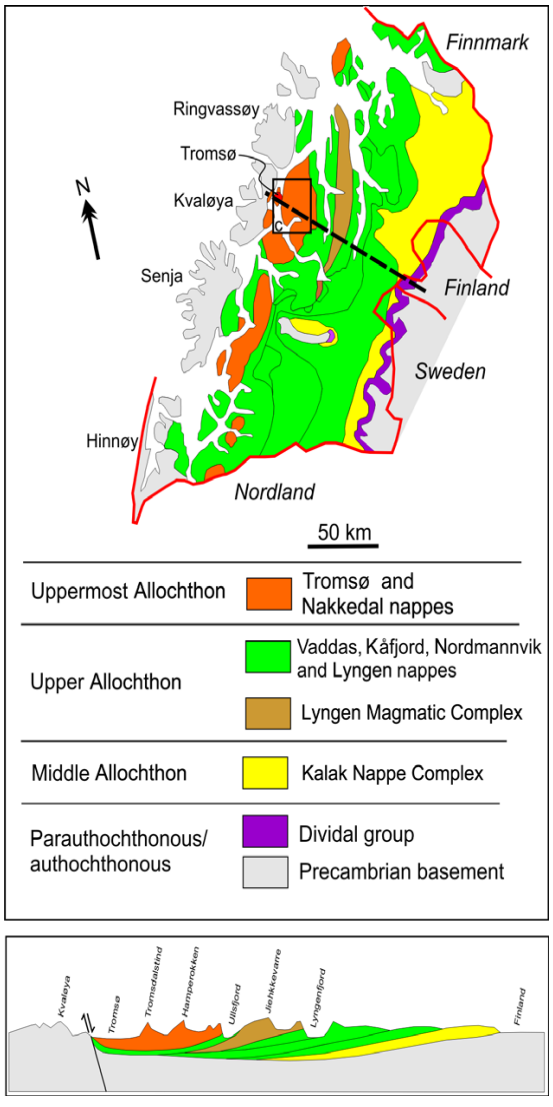

Figure 1.3: Tectonostratigraphy of the bedrock in Troms with profile showing the tectonic relation allochthonous units along NW-SE traverse (modified by Janká et al. (2012) after Krogh (1992)).

It is noted that nappes and nappe complexes within the allochthonous sequence have been given various names by different workers. Allocation of nappes into allochthons also varies with workers, and local names are presented by some authors to avoid incorrect correlations in cases where units have not been mapped continuously.

The autochthon unit is mainly exposed in the West-Troms Basement complex which is the dominating rock formation on the outer islands of Troms. Another location is the basement window in Mauken. The unit includes Archaean migmatites, tonalitic and quartzdioritic gneisses, Archaean-Early Proteozoic metasupracrustal rocks and Early Proterozoic intrusive bodies and dyke swarms. Late Vendian-Early Cambrian shale unconformably resting on the Precambrian basement represents the parautochthon unit, the Dividal group. Outcrops of these rocks are limited in Troms but they occur in the tectonic window of Mauken (Zwaan et al. 1998).

The allochthonous units have all been displaced by thrusting and transported a considerable distance, for the upper most units presumably more than 600 km, before being stacked together in the order they are occurring in the present tectonostratigraphy. Different formation environments give large geological variations between the units in the allochthonous sequence (Zwaan et al.1998).

The Lower Allochthon in Troms is referred to as Målselv Nappe complex which is mainly exposed in the area of Mauken (Andresen et al. 1985).
The unit consists of dolomites and quartzites of Late Riphean age, hornblende-schist and amphibolite assumed to be Precambrian basement rocks, and variety of mylonitic rocks. The unit became tectonically mixed and metamorphosed under low grade conditions (Index mineral, IM: Chl) under the Caledonian orogeny (Zwaan et al. 1998).

The controversial *Kalak Nappe Complex* is the Middle Allochthon.
It outcrops on the peninsula of Lenvik as meta-arkosis and garnet-micaschist assumed to be of Late Proterozoic age. In the area of Nordkjosbotn the unit occurs with a minor thrust contact towards granodioritic gneiss presumed to be a slice of the Precambrian basement. The lower part of the complex is of intermediate metamorphic grade (IM:Grt+Bt) while higher grade (IM:Hbl) metamorphism is recognized in the upper part (Zwaan et al. 1998).

The Upper Allochthon, mainly exposed in the inner region of Troms, is divided by Zwaan et al.

(1998) into four nappes which together constitute the Reisa Nappe complex.
From lower to upper nappe;
The Vaddas Nappe – Intermediate-high grade metasedimentary rocks presumably of Ordovician age.

The Tamok Nappe – High grade metasedimentary, metavolcanic (IM:Hbl) and metaintrusive rocks presumably of Ordovician age.

The Kåfjord Nappe- High grade metasedimentary (IM: Ky + St), metavolcanic and metaintrusive (IM: Grt + Tur) rocks presumably of Ordovician age.

The Hei Nappe (Zwaan et al 1998) / The Nordmannvik Nappe (Andresen et al. 1985)- Polymetamorphic unit consisting of Early Ordovician or older metasedimentary rocks of high metamorphic grade (IM: Ky), highly metamorphosed parts of the Middle Allochthon tectonically mixed with mafic and ultramafic intrusive rocks (IM:pyroxene) (Zwaan et al.1998).

The Lyngsfjell Nappe is by Zwaan et al. (1998) placed in the Upper Most Allochthon. Andresen et al. (1985) notes a distinct structural and metamorphic break between this unit and the overlying Tromsø Nappe Complex and refers to it as the upper part of the Upper Allochthon.

The Lyngen Nappe (after Andresen et al. 1985) – Is composed of a lower sequence of metasedimentary rocks, the Lyngen magmatic complex (LMC), and the unconformably overlying metasedimentary Balsfjord group (Bergh & Andresen 1985). The LMC comprises ophiolite- and arc related rocks. Tonalites in parts of the complex are interpreted by Selbekk et al. (2001) to have formed by anatectic processes. Metamorphic grade ranges from low- to intermediate in the lower parts of the Upper Ordovician- Mid Silurian Balsfjord group to high grade close to the contact towards the Upper Most Allochthon (Zwaan et al. 1998).

Several workers (e.g Andresen et al. 1984, Zwaan et al. 1998) stresses the uncertainties related to the division of the Upper Most Allochthon, which in some cases is referred to as the Tromsø Nappe Complex. The unit and includes a wide variety of exotically derived metamorphosed rocks, and main exposures of the are on the Island of Tromsø, the Island of Reinøya and on the mainland in the sentral region of Troms (Zwaan et al 1998).However, there is a clear tectonical contact between the Tromsø Nappe and the Nakkedal Nappe leading to the subdivision:

The Nakkedal Nappe –

This unit comprises a sequence of Early Silurian and older metasedimentary rocks cross-cut by pegmatites (the Nakkedal schist), the SMC, and a group of felsic- and mafic intrusive rocks (Zwaan et al. 1998). Metamorphic grade in the nappe is high (IM: Grt + Hbl), and rocks have experienced several phases of metamorphism (Broks 1985). Similarly to the tonalites in the LMC, leucocratic dykes in the SMC, in the upper part of the nappe, are interpreted by Selbekk et al. (2000) to have formed by anatexis.

The Tromsø Nappe –

The upper most nappe in the Caledonian nappe complex comprises the metasupracrutal Tromsdalstind sequence, felsic intrusives, and ultramafic rocks (Zwaan et al., 1998). The unit has polymetamorphic development and contains retro-eclogites as evidence of high pressure conditions (IM: Grt,Ky, Px) (Bryhni & Andréasson,1985). U-Pb ages of titanites and zircons suggest sedimentation to be Early Ordovician or older, while the eclogites in the nappe are of Late Ordovician age (Corfu et al., 2003).

1.4 Skattøra Migmatite Complex

1.4.1Migmatites

The rocks of interest are part of a migmatite complex. Some terms related to the melting of rocks are included as they are used for descriptive purposes.

A migmatite is by E.W Sawyer (2008, pp.3- 4) defined as:

a rock that is found in medium- and high-grade metamorphic areas that can be heterogeneous at the microscopic to macroscopic scale and consist of two, or more petrographically different parts. One of these parts must have formed by partial melting and contain rocks that are petrogenetically related to each other and to their protolith through partial melting or segregation from the solid fraction.

Partial melting changes a one-phase **protolith (paleosome)** to a two-phase (solid + melt) **neosome** which may, or may not, undergo segregation. The part derived from segregated partial melt is the light-colored **leucosome** which is dominantly of quartzofeldspathic or feldspathic composition.

The solid, dark-colored residual rock is, when enriched in ferromagnesian minerals, referred to as **melanosome (restite)**. The part of a migmatite complex that is not the neosome, generally with the appearance of an ordinary metamorphic rock is the **mesosome** (Ashworth, 1985).

If the partial melting, **anatexis**, is of moderate degree so that leucosome is subordinate to non-leucosome and pre-migmatization structures are preserved it is termed **metatexis**. **Diatexis** is a more extensive partial melting where the volume of the leucosome becomes comparable or dominant over, non-leucosome. The pre-migmatization structures are disrupted and mafic minerals are prominent in the leucosome (Ashworth 1985).

According to Bucher & Frey (1994) the beginning of melting is included in the field of metamorphism as long as a rock remains predominantly in their solid state. The estimation for the high-temperature limit of metamorphism of rocks therefor is given by determination of the melting temperature. In the presence of aqueous fluids, melting temperature for a granitic rock is ca. 660°C, while for a basaltic rock the temperature must be ca. 800^0C. Under dry conditions melting temperatures rises to ca. 1000^0C for granite and ca. 1120^0C for basalt. However, solid state metamorphic processes such as recrystallization and various phase transitions in the mantel takes place in excess of 1500^0C.

Earlier descriptions of the Skattøra Migmatite Complex have been done according to both the terminology of: (1) Mehnert (1968), (2) Ashworth (1985).

Rindstad's (1992) descriptions refer to (1). Description by Selbekk et al. (2000) has references to both (1) and (2).

1.4.2 Earlier work

Karl Pettersen is the first known geologist that did systematic surveys of the bedrock in the Tromsø area. He produced several publications with profiles and maps based on his work in the region in the period 1865-1890.

In his work from1868, the rocks on the northern part of the Tromsø Island (north of Breivika on the east side and north Sandnes on the western side) are described as hornblende-gneiss and grey-gneiss that frequently is cut across by light colored veins of feldspar. A year later he includes this area in a

more widespread rock type with eastward continuation of Tromsøysundet called Bjørnskarets norite. Light coloured feldspars are dominating this rock type but hornblende, mica and quartz are also present. He describes zones of feldspar in irregular alternation with hornblende-dominated rock, sometimes the two occur as alternating bands. Zones of more massive hornblende rock also occur. He speculates in the eruptive formation of the norite, but stresses that the sub-horizontal occurrence between schist is not compatible with this idea.

Landmark (1973) published his « Descriptions to the geological map «Tromsø» and « Målselv» ». In addition to re-description of the geology, he presented a tectonstratigraphic order (Lower-, Middle-, and Upper Allochthon) for the main rock types together with tectonic interpretations of the area.

The norite described by Pettersen almost hundred years earlier then became part of a more extensive unit with the name Skulgam gneiss (after Skulgam on Rinvassøya north of Tromsø) in the lower level of the upper allochton. It is described as an amphibolite-oligoclase complex. Even though presented as one unit, Landmark stressed the strong petrological and structural differences within the Skulgam gneiss. He finds that the composition of the light veins on the Tromsø Island area does not contain any quartz, while there is 20-30 % quartz in the oligoclase rock further north. He also describes that oligoclasite and amphibolite are occurring with close to migmatitic structures on the island of Tromsø, and interpreted the history of these rocks to be polymetamorphic. First the formation of gneissic fabric, secondly the intrusive process causing the numerous veins and dykes. However, he could not be certain if the magma had originated as a primary magma or from anatexis.

Binns (1978) made correlations of the Caledonian nappe pile in the Tromsø region and northwards.

He distinguished between seven nappes or nappe complexes. In this model Landmarks Upper Allochthon was included in nappe number seven, called Tromsø Nappe complex. Binns found the migmatitic gneiss in the Tromsø area not to be identical with the Skulgam gneiss on Ringvassøya and renamed it Skattøra gneiss. He considered it to be a slice of basement rock that was partly deformed and metamorphosed during the Caledonian orogeny.

Andresen et al. (1985) divided the Tromsø Nappe complex into the lower-, middle- and upper unit, where the Skattøra gneiss represented the middle one, Nakkedal Nappe, described as amphibolites cut by dioritic and oligoclasitic amfibol- bearing dykes.

The lower contact of the Nakkedal Nappe was described as gradual, going from quartz-feldspathic gneiss into amphibolitic gneiss and amphibolites. The upper contact to the Tromsø Nappe was

described as tectonic on the basis of a mylonitic fabric and the fact that none of the dykes from the Skattøra gneiss are seen to cut through to the overlying high- pressure metamorphic sequence.

Broks (1985) did a cand. scient. thesis on the bedrock in the Tromsø Nappe Complex. He concluded that the Skattøra gneiss was of magmatic origin and that it has gone through three episodes of deformation. In addition to descriptions that coincide with Andresen et al. (1985) he points out that diabase dykes and ultramafic layers occur at locations on the Tromsø Island.

Krogh et al. (1990) did K-Ar datings on amphiboles from the Skattøra gneiss that gave ages of 436±20 Ma and 448±20 Ma

Rindstad (1992) did discuss in her cand. scient. thesis that the Skattøra gneiss of the Tromsø Island originated as a layered cumulate rock, which later was partly migmatized. She described the rocks to be foliated in places and cut through by a network of light coloured plagioclase veins with either oligoclastic or dioritic composition. She also noted serpentinised lenses, and veins and layers rich with epidot and prehnite.

She divided the mesosome part of the complex into: meta-anorthosite and meta-gabbro,

with further divisions of the latter one into: anorthositic gabbro, leuco-gabbro and amphibolite

All parts of the complex where found to be nepheline-normative.

Zwaan et al. (1998) refined the geological map of Tromsø (1: 250 000) where the Nakkedal Nappe is divided into three lithological groups; the 432± 7 Ma and older Nakkedal schist, the Skattøra gneiss (of unknown age), and a group of intrusive rocks, including the 432± 7 Ma Reinøygranite. The Skattøra gneiss is described as hornblende-rich gneiss with oligoclase pegmatites, dark veins and gabbroic lenses.

Selbekk et al. (2000) renames an area of about 200 km² where the Skattøra gneiss is mainly migmatized to the Skattøra Migmatite Complex. They did dating of an anorthositic dyke and a leucosome by the U/Pb method on titanite that gave the age of 456±4 Ma.

With focus on the petrogenesis of the anorthositic dykes of the complex, Selbekk and Skjerlie (2001) describes the migmatized rocks to be mafic, with anorthositic to leucodioritic leucosomes and mesosomes of amphibolite. They suggested that the anorthositic dykes formed by anatexis of alkaline gabbro in the presence of a H_2O-bearing fluid phase at about 1.0 GPa and 900 to 950 °C. The paleosome to the SMC remains regarded to be a layered mafic igneous complex(unknown age).

1.4.3 General description of the rock types based on earlier work

Meta-anorthosite occurs as m-scale layers that consist of 40-90% plagioclase, 5-30% clinozoisite/epidote, 0-30% white mica and < 10% amphibole. Layers are fine grained and have a foliation defined by light mica- and/or mm-scale amphibole-bearing bands and also zones enriched in epidote (Rindstad 1992).

Metagabbro consists of 40-65% plagioclase (An72-90) and amphibole, and are generally medium-grained to pegmatitic. Most usual is inequigranular texture, without preferred crystal orientation, but modal layering occurs in some places. Plagioclase is commonly saussuritized. Accessory minerals are Fe-Ti oxides, sulphides and titanite (Selbekk et al., 2000).

Amphibolites consist of 70-100% amphibole, 0-30 % plagioclase, and 0-5% Fe-Ti-oxides. They are commonly medium- to coarse grained and show nematoblastic textures (Selbekk et al., 2000).

The leucocratic dykes are characteristic for the SMC and form up to 90% of the complex, on average 50%. Thickness varies from a few cm up to several meters. In general grain size increase with dyke thickness. In places dykes form an anastomosing network. They also occur as foliation parallel or with random orientation, but in general thicker dykes are straight and cross-cutting the foliation with a steep NNE-SSW striking dip. In most cases the dykes have sharp and rather planar contacts with the country rocks. Compositionally dykes are 85-100% plagioclase and 0-15% amphibole (Selbekk et al., 2000).

Plagioclase crystals are generally unzoned with grain size ranging from fine grained to pegmatitic. Compositions of crystals from a single dyke are uniform, but inter-dyke composition varies from An15 to An50 (mainly in the range of An20-An35).

Amphibole grain size varies across dykes but crystals are found with size up to 10-15 cm. Distribution is irregular. The composition of amphibole is ferropargasitic.

Accessory minerals are apatite, muscovite, biotite, iron-oxides/-sulphides, titanite and epidote or clinozoisite (Selbekk et al., 2000).

Ultramafic lenses occur locally. Un-weathered rock fragments are black, fine-grained and consist of partly serpentinized olivine (10-80% olivine, 10-60% antigorite). Needle shaped amphibole (0-1%) and talc (5-30%) are present in reaction zones towards surrounding rocks. 0-30% magnesite, 0-10% chlorite and 0-2% clinopyroxene is also present in these lenses (Rindstad 1992).

Epidot- and prehnite layers/veins occuring in the SMC have heteroblastic texture, with 70-90% epidote (occurs both as 0.1-5.0 mm idioblastic grains and as a fine-grained matrix mineral), 10-30% prehnite (both as matrix mineral and 0.1-0.3 idiomorphic grains in mm- thick prehnite-veins) and 0-3% chlorite. Calsite crystals are observed in relation with the late prehnite veins (Rindstad 1992).

Metasediments occur in lenses either as garnet-biotite schist with feldspar and accessory zircon, or epidote-garnet-calcite skarn-like rocks. They are interpreted to be xenoliths in the original mafic introusion (Selbekk et al., 2000).

1.5 Abbreviations and symbols

Minerals (Kretz, 1983):

Ab	albite
Act	actionlite
Adr	andradite
Aln	allanite
An	anothite
Ap	apatite
Atg	antigorite
Ath	anthopyllite
Brc	brucite
Bt	biotite
Cal	calcite
Chl	chlorite
Cpx	clinopyroxene
Crn	corundum
Ctl	chrysotile
Czo	clinozoisite
Di	diopside
Ep	epidote
Fa	fayalite
Fo	forsterite
Grs	grossular
Grt	garnet
Hem	hematite
Hbl	hornblende
Ilm	ilmenite
Kfs	K-feldspar
Ky	kyanite
Mca	mica
Ms	muscovite
Mrg	margarite
Ne	nepheline
Ol	olivine
Omph	omphacite
Opx	orthopyroxene
Pg	paragonite
Phl	phlogopite
Pl	plagioclase
Qtz	quartz
Rt	rutile
Sa	sanidine
Sph	sphene
Spl	spinel
Srp	serpentine
St	staurolite
Tlc	talc
Tr	tremolite
Ttn	titanite
Tur	turmaline
Zo	zoisite
Zrn	zircon

Others:

Amph	amphibole
IM	index mineral
LMC	Lyngen Magmatic Complex
Op	opaque minerals
P	pressure
PPL	plane polarization light
REE	rare earth elements
SMC	Skattøra Migmatite Complex
T	temperature
TN	Tromsø Nappe
UM	ultramafic
XPL	crossed polarized light

2 Methods

2.1 Field observations and sampling

Field observations were done to get an overview of the lithologies within the SMC. A total of 24 samples were selected from the four locations on the Island of Tromsø (locations are shown in fig.1.2). Sampling was done with the purpose of extracting metamorphic information from the SMC, and the main focus has been on the cumulate lithologies, reaction zones between cumulate rocks and migmatitic rocks, and to a smaller extent on the felsic and mafic dykes. Hand specimens were studied and described in order to select samples for more detailed examination. All measurements are done with a Silva compass, using the right-hand rule. Pictures are taken with a Canon EOS 400D DSLR camera.

2.2 Microscopy

16 samples were selected for further studies in thin section with the aim of identifying metamorphic mineral assemblages, and micro-textures related to them which could be used for further interpretation and thermodynamic calculation purposes. Specimens were prepared by the use of available rock saws at UIT, and 1* 2*3cm chips were handed over to the thin section laboratory at Department of Geology, UIT, for further production. All non-isotropic samples sections were cut normal to foliation and parallel to lineation. 15 thin sections were successfully completed, and further examinations of them have been done by the use of a "Leitz Laborlux 11 Pol S" polarization microscope. Descriptions in chapter 3 are mainly given according to Børge Brattli's (1992) terminology. Heinrich (1965), Shelly (1993) and MacKenzie & Adams (1994) are other reference work used during petrographical studies. Microphotographs are taken with Leica DMLP camera.

Samples are presented in table A1 in the appendix with respect to their sample number, location, lithology, and when applicable, thin section number, XRF-analysis number and figure number.

2.3 X-ray fluorescence (XRF)

Analyses of bulk rock compositions of three selected samples were done using Bruker S8 Tiger XRF at the Department of Geology, UIT, with respect to major- and minor elements (Si, Ti, Al, Fe, Mn, Mg, Ca, Na, K, P and Cr). Using this method the prepared samples are irradiated with x-rays which results in emission of fluorescent x-rays. Each element emits x-rays with a characteristic energy/ wavelength, which is distributed through an oriented crystal before measured by a detector and subsequent electronic processing (for basic principles of the method see for example Van Grieken & Markowicz 2002).

Preparing the samples for whole-rock analysis:

Samples were selected for XRF-analysis with respect to homogeneity, cut clean of weathered surfaces and other visible alteration (veins etc.) before crushing with a "Retsch ® type type BB2/A" jaw crusher. Material was crushed to <1,5 cm pieces before further grinding into powder by a swing mill. Equipment was cleaned and dried after standard procedure between each sample.

Rock powder and flux (Li-tetraborate; $Li_2 B_4 O_7$) was weighed in a 1:7 ratio, by the use of the electronic balance "Mettler AE160".

Amount rock powder: 0.6000 g. Amount flux: 4,2000 g. Accuracy was ± 0.0002 g. Two parallels were made for each sample in order to detect any errors during preparation.

After weighing the mix, it was transferred to glasses, labeled and homogenized by shaking. Then the mix was melted in platinum crucibles covered with lids over a "Turbotorc" gas burner at approximately 1200^0C. Total melting time was 6 min.; 3 min. of melting and checking that no material was left on the wall of the crucible, then another 3 min of melting and homogenization before the sample was poured into the lid/mold, and placed on a ceramic plate (on the electric heater-at 300^0C) for cooling. When loose, beads were transferred to a cold plate for further cooling in room temperature, before labeling and storing in an exicator. Equipment was cleaned after standard procedure between each sample.

Before the analysis was performed on the glass beads “Standard AGV-1” was used for calibration and compared to reference values given in Børre Davidsen (1991). Calibration-, reference- and analytical values are presented in table A2 in the appendix.

All analyzes were successful with less than 1-1,5 wt% deviation between parallel samples.

2.4 CIPW norm calculation

The CIPW norm is a commonly used calculation scheme for working out mineralogy of igneous rock from chemical analyses. Software computes the ahydrouse mineral assemblage that could crystallize from a given bulk (Glazner,1984). Since the calculations are based entirely on chemistry it is not a tool for determining mineralogy – igneous fine grained, coarse grained and even metamorphosed igneous rock with same bulk while have the same normative composition. In this thesis the normative composition are calculated for dolerite and felsic dyke. This is done using the CIPW normative calculation software available through U.S Geological Survey web-page: http://volcanoes.usgs.gov/yvo/aboutus/jlowenstern/other/software_jbl.html

2.5 Pseudosection construction

Pseudosections are mineral stability diagrams calculated for a specific bulk composition in a chosen P-T window. Calculations were carried out on two of the metamorphic lithologies to model metamorphic conditions. In addition calculations were performed on unaltered samples with the aim to gain information of the anatectic processes in the SMC.

“Without thermodynamics, metamorphic petrology is a descriptive science” - is one of Frank S. Spears concluding remarks in his book “Metamorphic Phase Equilibria and Pressure-Temperature -Time Path” from 1993. The basis for understanding pseudosection calculations can be studied through the thorough review of the fundamental laws of thermodynamics and their derivations in this book. Even though slightly different approaches are used for calculations of phase equilibria to geologic systems (e.g THERMOCALC, Perple_X) the main objective is the same; to determine the internal energy with P and T as independent variables. This is achieved through the integration of the Fundamental equation (First- and

Second law of thermodynamics) and the Gibbs –Duhem equation, which after transformation with respect to variables is expressed by Gibbs free energy:

$$(1)\quad dG = -SdT + V\,dP + \sum \mu_i\, dn_i \qquad \text{(Spears, 1993)}$$

where G= Gibbs free energy, S= entropy, T= temperature, V= volume, P=pressure, μ_i =chemical potential of component i, n_i =moles of component I.

For the purpose of this study Perple_X 6.6.6 (Connolly, July 2011) software package was used to produce pseudosections. It works by the approach of finding the lowest absolute G for a selected number of points(nodes) and P-T space, to predict the most stable configuration of phases of the given bulk composition. At each point the composition and properties of the phases, and the thermodynamical properties of the system are uniquely determined (Connolly & Petrini, 2002). General work flow of problem solving with Perplex_X6.6.6 is shown schematically in figure 2.1.

Before running BUILD, output data from XRF analyses were converted from weight % to normalized mole proportions. FeO values are calculated from stoichiometry from initial Fe2O3. TiO2 and MnO have been set to 0, to simplify pseudosection complexity. " hp04ver.dat" was used as thermodynamic database, "solution_model.dat" as solution model file, and all pseudosections presented in this thesis were run with the number of x-and y nodes set to 40-60. Graphical outputs were modified in "CorelDRAW X5".

Uncertainty limits related to thermodynamic modelling are large and must always be taken into considerations. The Perple_X software does not provide uncertainty limits for calculations, and so all P-T implications given in this thesis based on pseudosection construction must be considered with error limits: ± 65°C and ± 0.32GPa, given by Ravna & Terry (2004).

Other general sources of errors during this study could be related to:

- How representative the selected sample is for the rock of interest.
- Homogenisation of selected samples used for XRF analyses.
- Zoned minerals.
- Relicts of different equilibria assemblages.
- Contamination during any part of the preparation.
- Inaccuracy in the weighing process.
- Wasting during transfer of material.

- Errors related to thermodynamic modeling (for details se section 2.5 above)

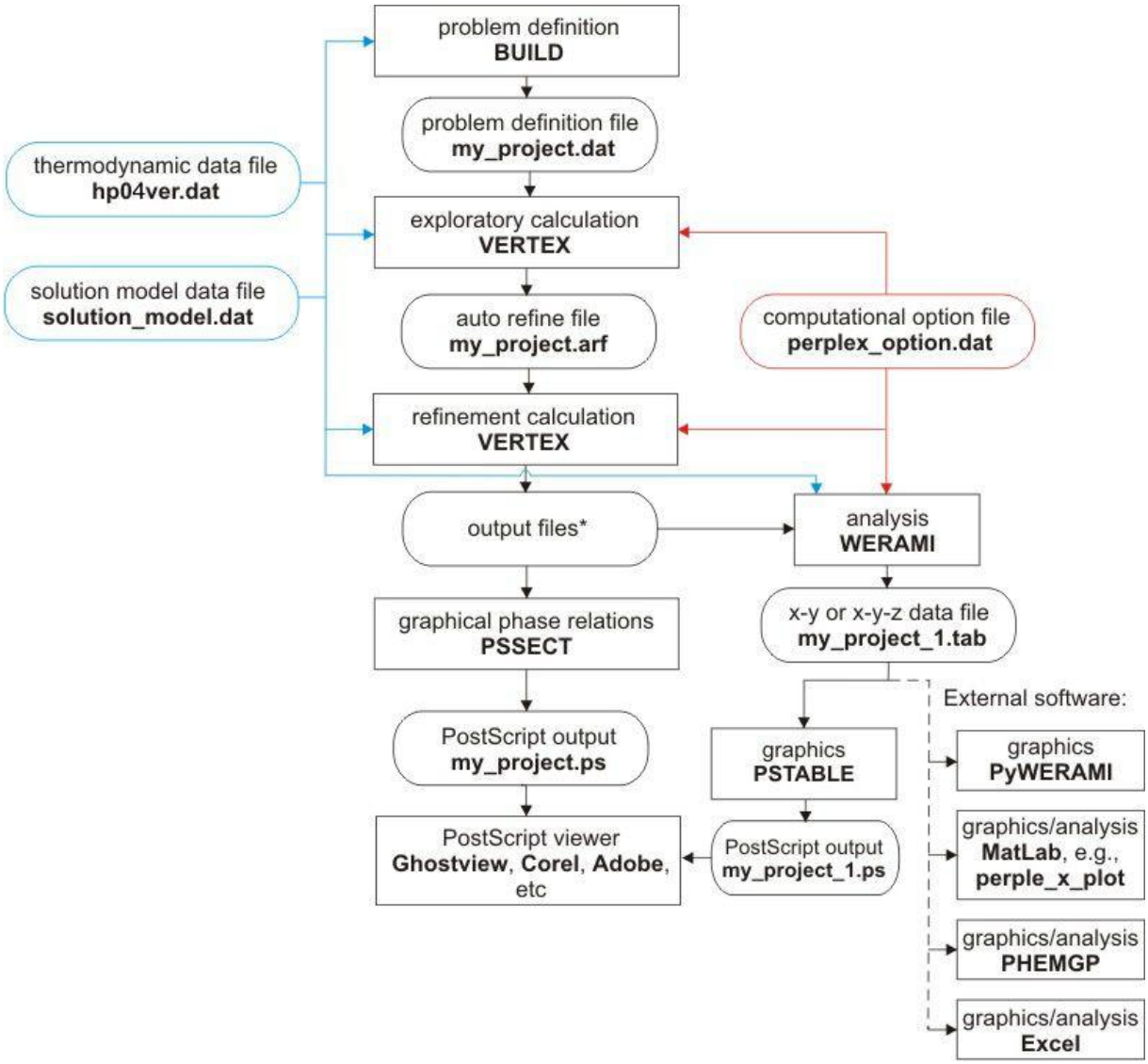

Figure 2.1: Perple_X6.6.6 program structure for minimization calculations. Calculations and interpretations are done through; BUILD (problem definition), VERTEX (computation), PSSECT (depiction), WERAMI (digital interpretation), PSTABLE (graphical representation). Modified after Perple_X documentation; web-based tutorials (http://www.perplex.ethz.ch/perplex_666_seismic_velocity.html**).**

3 Descriptions of lithologies

This chapter presents descriptions of rocks based on field relations, hand-specimens and thin sections. An attempt has been done to strategically select rocks useful for the purpose of this study within the large specter of rock types in the SMC, rather than to establish a detailed overview of field relations between them. For that reason it is important to stress that descriptions only are valid for the restricted area of the locations. The aim has been to investigate the minerals in the different lithologies with respect to metamorphic mineral assemblages and phase transitions. Petrology is emphasized, and rock types are described based on the overall classification:

1) **Felsic rocks**:- Meta-anorthosite(3.1.1)
   -Felsic dykes (3.1.2)
2) **Mafic rocks: -**Migmatite gneiss (3.2.1)
   -Cpx-Grt amphibolite (3.2.2)
   -Dolerite (3.2.3)
3) **Ultramafic roks: -**Amphibole-rich rock (3.3.1)
   -Serpentinite (3.3.2)

Reaction zones that occur between ultramafic rocks and felsic dykes are described in a separate section (3.3.3).

Structural data are summarized at the end of the chapter, and is otherwise only included when it is of direct interest.

4) **Structural data:** - Summary of structural elements for each lithology, with brief descriptions (3.4.1)

5) **Summary and interpretation of petrographical observations**

3.1 Felsic rocks - Field relations

Meta-anorthosite main outcrop is at location 3, the bus terminal just north of the University Hospital of North-Norway. The rock type occurs as m-thick layers in alternation with dm-thick mafic layers. Transitions between the alternating layers are sharp. The rock sequence is cut by steeply dipping mafic- and felsic dykes, and has undergone both brittle and ductile deformation.

Felsic dykes are characteristic for SMC. They occur at all four locations but are most abundant at location 3 and 4. Dyke thickness varies from mm-to m–scale, and grain size generally increases with dyke thickness, from fine grained to pegmatitic. The abundance of amphibole varies between dykes. Thin veins commonly terminate in the larger dykes. Some dykes have a white color, while others are purple-grey. On location 4, by the Remiks Miljøpark AS, well-developed reaction patterns are preserved in contact zones between felsic dykes and ultramafic rocks (described separately in section 3.3.3). Deformation is mainly recorded in smaller scale dykes, while thicker dykes have a straight appearance.

Figure 3.1: Image showing outcrop of meta-anorthosite and its relation to felsic and mafic dykes at location 3.

Figure 3.2: Image that shows field relation of white-and purple-grey colored felsic dykes on location 4.

3.1.1 Meta-anorthosite: hand specimens and microscopy

Hand-specimens of the rock are dominated by light-colored minerals. Fine-medium grained feldspar, white mica and chlorite is identifiable with hand lens. Samples are either massive or have well-developed foliation defined by mm-thin layers of fine grained, white mica in alternation with mm-thin layers rich in green-dark colored, fine grained minerals.

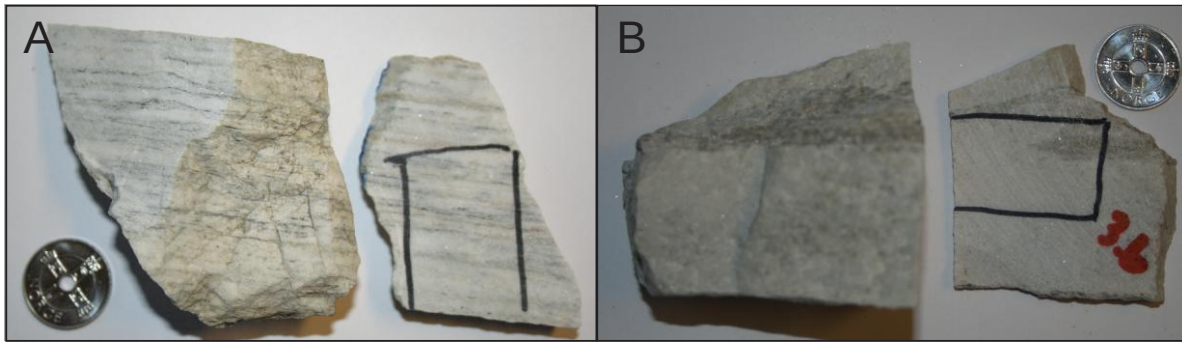

Figure 3.3: Hand specimens of meta-anorthosite. A) Sample 3.4 has penetrating foliation. B) Sample 3.6 showing massive meta-anorthosite with abundant white mica. Black boxes are for thin section preparation. Coin diameter= 2 cm.

In thinsections the meta-anorthosite has hetrogranular texture. The massive sample predominantly consists of zoisite and white mica, with chlorite and epidote/clinozoisite enriched in zones. Samples with penetrating fabric have feldspar as the dominating mineral,

and foliation is defined by lepidoblastic white mica and chlorite together with nematoblastic clinozoisite/epidote.

Mineralogy:

Plagioclase (40-90%) is colorless and has low relief in PPL. Grains are anhedral- to subhedral (0,05mm-1mm) and often contain impurities. Interference colors are 1st order and polysynhtetic albite twinning is common. Massive varieties of the rock have plagioclase with irregular contact surfaces towards eipdote/clinozoisite, mica or granular zoisite. In foliated samples grain boundaries between plagioclase and other minerals are less complex. Triple-junctions and straight crystal surfaces occur between plagioclase grains.

Zoisite(30-70%) is colorless but has high positive relief relative to the plagioclase. Interference colors up to middle 1storder are observed. Zoisite has a granular habit with a chaotic distribution, and no distinct preferred orientation. Boundaries towards other minerals are irregular.

White mica (10-60%) is colorless in PPL, has low- medium relief and lamellar habit with perfect (001) cleavage. Grain size ranges from <0,05 mm-0,9mm. Interference colors are upper 2nd order to lower 3rdorder. White mica most commonly occurs in clusters with epidote/clinozoisite and chlorite, which defines a foliation. In the massive sample the white mica appear without any notable preferred orientation, and with a tendency to cut across grain boundaries of other minerals.

Clinozoisite/ Epidote (10-30%): Clinozoisite occur with pale green color in PPL. Grains (0,005mm-1,5mm) are elongate subhedral with high relief. Cleavage is observed in the larger sized grains, and extinction angle is parallel. Interference colors are 1th order or anomalous (blue) in XPL. Epidote resembles clinozoisite, but a weak pleochroism (pale-green to green) is sometimes present. Interference colors are upper 2nd to lower 3rd, and individual grains show multiple colors. In massive samples there is little consistency in distribution, but in foliated rock these minerals are strongly directional.

Chlorite (< 5%) has pale-green to green pleochroism, medium relief, lamellar habit with perfect (001) cleavage, and lower 1st order interference colors. Mainly occur together with white mica.

In addition small clusters of mixed, fine grained, green-brown unidentified minerals occur (<5%).

Table 3.1: Intergranular relations of the minerals present in samples of meta-anorthosite; S= straight grain boundaries, L=lobate grain boundaries, C= complex grain boundaries, CC= cross-cutting, P=poikolitic, I= inclusion. Table should be read with emphasis on the numbered minerals.

Mineral	Pl	Zo	Mca	Ep/Czo	Chl
1.Pl	S/L	C/I	S/C	C/I	S/C
2.Zo	P	S/C	S/P/C	P	C
3.Mca	S/CC	S/CC/I	S/CC	C/CC/I	S/CC
4.Ep/Czo	C/P	C/I	P/C	C/S	C
5.Chl	S/CC	CC	S/CC	CC	S/CC

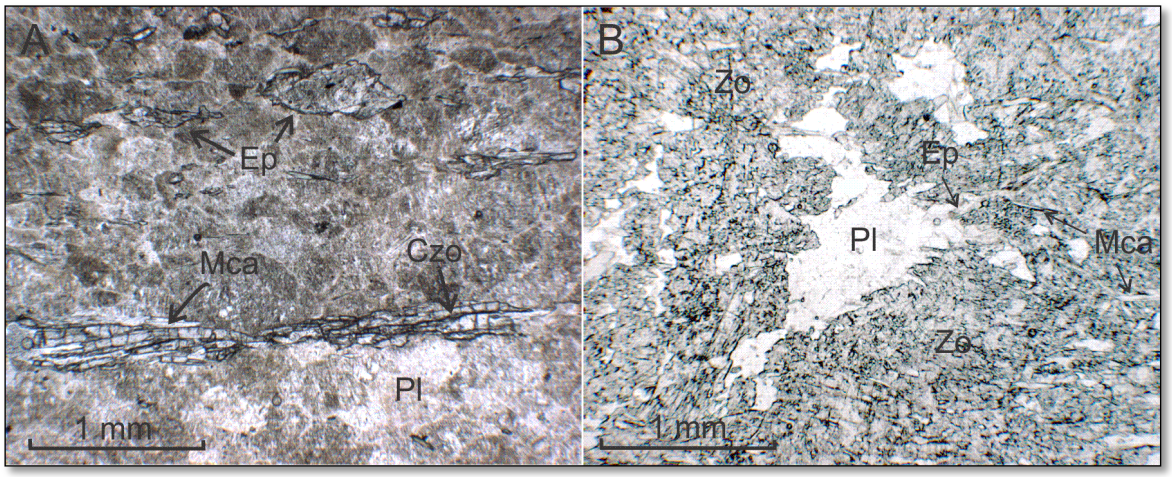

Figure 3.4: Micrographs of meta-anorthosite; A) Image is showing nematoblastic clinozoisite and lepidoblastic white mica, in the foliated sample 3.4. B) Showing poikolitic zoisite with irregular grain boundaries towards plagioclase.

3.1.2 Felsic dykes: hand specimens and microscopy

Hand specimens of felsic dykes are massive and predominantly consist of medium- to coarse grained plagioclase and amphibole. Plagioclase is either close to white or purple-grey, and two cleavages at ~90º are recognized. Long-prismatic, dark green amphibole grains (up to 2 cm), with visible ~60º-120º intersection cleavage, are distributed throughout samples. Along grain boundaries thin white veinlets occur.

Figure 3.5: Sample 4.24 showing a coarse-grained, purple-grey variation of felsic dykes with white veinlets. Black box is for thin section preparation. Diameter of coin= 2cm.

Thin sections of the purple-grey felsic dykes are heterogranular, with plagioclase as dominating mineral. Other minerals are hornblende, calcite, phlogopite and chlorite, which all commonly occur along boundaries between large grains of plagioclase. In white dykes plagioclase grains contain a larger amount of zoisite inclusions in addition to epidote/clinozoisite and white mica (see figure 3.6).

Mineralogy of purple-grey dyke:

Plagioclase (80-100%) is colorless and has low relief in PPL. Grains (0.5mm- 7mm) are anhedral- subhedral. Interference colors are middle 1st order, extinction angle is inclined and polysynthetic albite-twinning is a prominent feature. Weak zoning is common and boundaries between plagioclase grains are generally straight- to lobate.

Hornblende (5-10%) is yellow-green to olive green pleochroic. Grains (0,25mm- 5mm) are anhedral or elongate-subhedral. Two cleavages at ~60°-120° are observed. Interference colors are upper 2nd order, and extinction is inclined.

Calcite (<1%) occur as colorless anhedral grains (<0,05mm- 0.35mm) with low relief. In XPL grains have various shades of pastel (high order) interference colors, and polysynthetic twinning. In large grains two cleavages are visible ~70° to each other.

Phlogopite (< 1%) is light-brown to orange pleochroic. Grains (0.2mm-1mm) have lamellar habit, (001) cleavage, and moderately high relief. Interference colors are middle-upper 2nd order. Extinction is pebbly and parallel.

Chlorite (<1%) is colorless to pale green pleochroic. Grains (0.2mm-0.6mm) have lamellar habit with perfect (001) cleavage. Relief is moderately high, and interference colors are lower 1st order. Occur as lamellas in phlogopite.

Table 3.2: Intergranular relations of minerals in purple-grey felsic dykes; S= straight grain boundaries, L=lobate grain boundaries, C= complex grain boundaries, I= inclusion. Table should be read with emphasis on the numbered minerals.

Mineral	Pl	Hbl	Phl	Cal	Chl
1.Pl	S/L	L/C	S/C	S/C	
2.Hbl	L/I	C	S/L	S/C	
3.Phl	S/I	S/L	S/C	S/L	C
4.Cal	S/C	S/C	S/L	S	
5.Chl			I		

Mineralogy of white colored dyke:

Plagioclase (80-100%) is colorless with low relief in PPL. Grains (0.06mm- 3mm) have cleavage intersection at ~90º. Under crossed nicols colors are lower 1st order, and polysynthetic albite-twinning is common. Large anhedral grains are surrounded by smaller subhedral grains with polygonal mosaic texture.

Zoisite (5-10%) is colorless with high relief. Grains (<0.2mm) are elongate subhedral with 1st order interference colors, and extinction is straight. The mineral occur with a systematic distribution within plagioclase grains in white felsic dykes (figure 3.4).

Hornblende (<5%) has yellow-green to olive green pleochroism. Grains (0,25mm- 5mm) are anhedral or elongate-subhedral. Two cleavages at ~60º-120º are observed. Interference colors are upper 2nd order, and extinction is inclined.

White mica (<5%) is colorless in medium relief in PPL. Habit is lamellar with (001) cleavage. Grains (0.02mm-0.3mm) have bright 2nd order interference color. Extinction is parallel and pebbly.

Epidote/clinozoisite (<5%) is colorless with high relief. Grains (0.02mm-0.35mm) are anhedral to elongate-subhedral. In XPL clinozoisite has anomalous blue or yellow interference colors. Individual grains of epidote have multiple bright 2nd order interference colors.

Table 3.3: Intergranular relations of minerals in white variation of felsic dykes; S= straight grain boundaries, L=lobate grain boundaries, C= complex grain boundaries, CC= cross-cutting, P=poikolitic, I= inclusion, E= embaying. Table should be read with emphasis on the numbered minerals.

Mineral	Pl	Zo	Mca	Ep/Czo	Hbl
1.Pl	S/L/C	P	S/C	I/C	L/C
2.Zo	I	S/CC	S/CC	C	
3.Mca	S/CC	S/CC	S/CC	S/CC	
4.Ep/Czo	CC/E/P	C	S/CC	S/C	C
5.Hbl	L/C			C	S/C

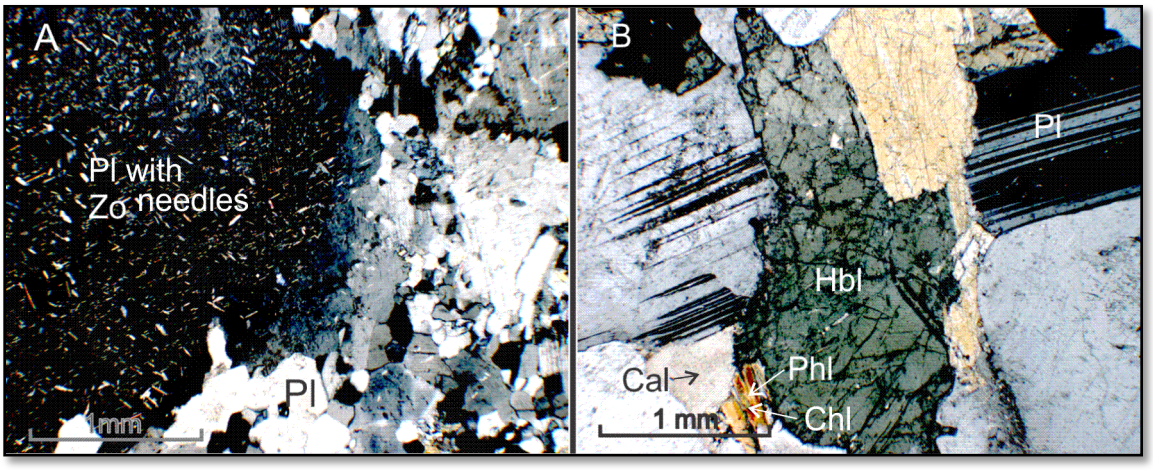

Figure 3.6: Micrographs of leucocratic dykes. A) Thin section of sample 3.5 (white dyke) showing large plagioclase grain with numerous zoisite inclusions, surrounded by smaller inclusion-free plagioclase grains. B) Thin section of sample 4.24(purple-grey dyke) showing hornblende surrounded by plagioclase, calcite and phlogopite with lamella of cholorite. Plagioclase grains are pure relative to plagioclase in image A, and grain boundaries between them are straight.

3.2 Mafic rocks - Field relations

Rocks of mafic composition in the SMC are mainly amphibolites or varieties of gneiss. Composition and textures are diverse, and transitions between rock types are gradual. One exception is the cross-cutting meta-doleritic dykes, which have sharp contacts to surrounding rocks.

Migmatite gneiss mainly occurs at location 2, and 4. Compositional banding is easily recognized by the alternating light-and dark colored mm- to cm- scale bands. On location 2, at entrance of the Tromsøysund tunnel, banding is parallel to overall layering of the rock sequence (alternating dm-mm thick felsic and mafic layers). In places the migmatite has a stromatic appearance.

Main locality for the **Cpx- Grt bearing amphibolite** is at the entrance of the Tromsø intra-island tunnel at Breivika, locality 1. These rocks are situated close to the tectonic contact to the Tromsdalstind sequence. Rock texture changes gradually from strongly foliated, to having a more gneissic apperance. In both cases fabric is folded. Rocks of felsic composition occur either as thin veins parallel to foliation (less then cm scale), or thicker veins (1-10 cm) that are discontinues and crosscut foliation. Veins are also folded (fig. 3.22).

Meta-doleritic dykes have been studied at location 3, where they are steeply dipping (45-60^0) and have a cross-cutting relationship to the meta-anorthosite and mafic layers. Felsic dykes occurs in relation to the meta-dolerite as an additional truncating component (figure 3.7). Thickness of the mafic dykes varies from dm- to m-scale. Contacts to the meta-anorthosite are irregular with chilled margins. Felsic dykes are observed to cross-cut mafic dykes, the contacts between them are sharp, and no change in grain size is recognized in the contact zone. The rock has a weak fabric, defined by amphibole, with orientation sub-parallel or oblique to dyke edge.

Figure 3.7: Image is showing field relations of mafic rocks. To the left-migmatite gneiss (loc. 2), middle- Cpx-Grt bearing amphibolite(loc.1), right-doleritic in meta-anothositeto dyke cross-cut by felsic dyke(loc.3). Pen/pencil is 15 cm.

3.2.1 Migmatite-gneiss: hand specimens and microscopy

Hand-specimens of the rock have gradual transitions from massive amphibolite to gneiss with alternating bands of fine- to medium grained plagioclase and fine- to medium grained amphibole. Rock character changes over a few cm. Bands are up to 3 mm in thickness, and generally light colored bands are thicker than dark colored ones. Bands often stop abruptly but without any structural interference.

Figure 3.8: Sample 4.21 is showing the characteristic compositional banding of the migmatite gneiss. Black box is for thin section preparation. Diameter of coin=2cm.

In thin section the light colored bands are made up of heterogranular feldspar and epidote/clinozoisite while dark bands essentially consist of nematoblastic hornblende whit minor plagioclase. Thin straight or anastomosing veins (<0,05 mm) filled with light colored minerals transects the thin section.

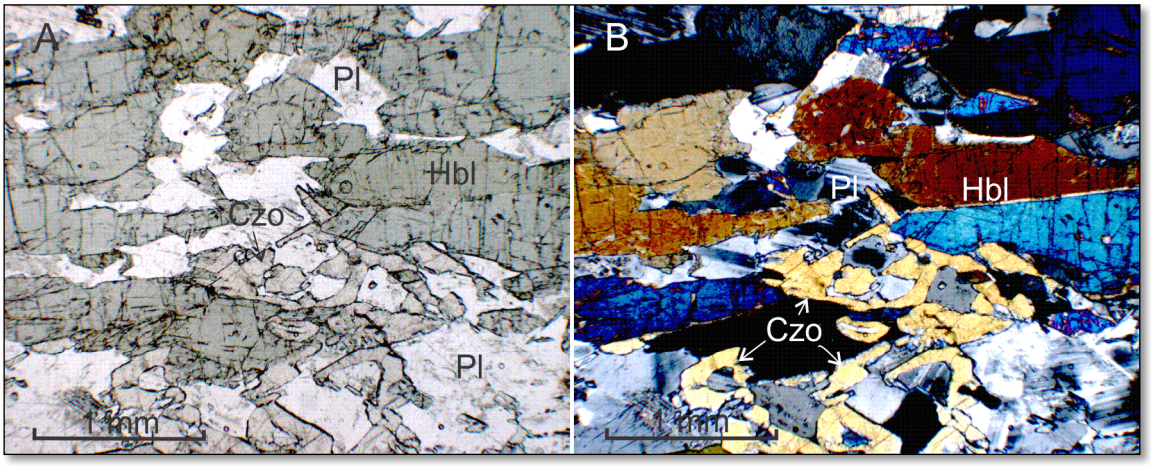

Figure 3.9: Thin section of sample 4.21. A) PPL micrography showing nematoblastic hornblende surrounded by anhedral plagioclase and clinozoisite. B) XPL micrograph showing the zoning of plagioclase, twinning of hornblende and the embaying distribution of clinozoisite.

Mineralogy:

Hornblende (50-80%) occurs as yellow-green pleochroic, anhedral to elongate-subhedral grains (0,05mm - 0,8mm). Relief is moderately high, and interference colors are 2nd order with inclined extinction. Some grains have twinning.

Feldspar (40-70%) is colorless and has low relief. Under crossed nicols feldspar has 1st order interference colors and inclined extinction. Grains (0.02mm-3mm) are commonly zoned and twinning is mostly according to albite-law, but some pericline- and Carlsbad-twinning also occur. Plagioclase is often contaminated with light colored fine grained unidentifiable minerals. Smaller subhedral grains with polygonal mosaic texture around lager grains is observed, but it is not a dominating feature.

Epidote/Clinozoisite(10-30%) has a pale grey-green color and high relief. Grain size ranges from 0,01mm- 1,25mm. Large grains are anhedral often with inclusions of feldspar, while smaller grains are elongate-subhedral. Vermicular texture is observed in contact to hornblende. Clinozoisite have anomalous (blue-yellow) interference colors while epidote grains often have multiple 2nd order colors. Subhedral grains go extinct parallel to elongation. Zoning occurs as epidote core and clinozoisite rim. Distribution is generally along grain

boundaries between hornblende and plagioclase, but it is also common to see these minerals with cross-cutting or embaying relationship to other minerals.

Zoisite(< 10%) occurs with granular habit, pale green color and high relief. Grains (<0.02mm-0.07mm) have 1st order grey interference color, or sometimes slightly anomalous blue.

Titanite(<1%) grains (<0,02mm) have oval shape, and brown color both in PPL and XPL. Distribution is disseminated.

Table 3.4: Intergranular relations of minerals in migmatite gneiss; S= straight grain boundaries, L=lobate grain boundaries, C= complex grain boundaries, P=poikolitic, I= inclusion, E= embaying. Table should be read with emphasis on the numbered minerals.

Mineral	Hbl	Pl	Ep/Czo	Zo	Ti
1.Hbl	S/L	S/L	C		
2.Pl	S/L	S/L	C/I	C/I	P
3.Ep/Czo	C	CC/P/E	S/L	C	
4.Zo		C/P	C		
5.Ti		I			

3.2.2 Cpx-Grt-Amphibolite:hand specimens and microscopy

Hand-specimens are porphyroblastic with foliation defined by thin, medium grained amphibole and other fine grained dark colored minerals. Light colored minerals are present in the fine grained matrix or as mm-thick bands/veins parallel to foliation. In more gneissic sample dark colored and light colored minerals occur as mm-thick, alternating bands or lenses. Garnets are distributed across samples, but occur in different textural settings:

(1) As porhpyroblasts where foliation bends around the garnet.
(2) Inside light colored veins
(3) Cross-cutting light colored veins

Figure 3.10: Sample 1.1 of foliated Cpx-Grt bearing amphibolite with porphyroblastic texture, and leucocratic vein. Black box is for thin section preparation. Diameter of coin= 2cm.

Thin sections of the rock are dominated by nematoblastic hornblende defining the fabric. Matrix is heterogranular and consists of feldspar, epidote/clinozoisite and hornblende. In addition garnet-porphyroblasts occur, and disseminated opaque minerals and titanite is common. There is also minor allanite.

Mineralogy:

Hornblende (50-90%) occurs as anhedral to elongate-subhedral grains (0,05mm – 0,5mm) in shades of green, and two varieties of pleochroism is observed: yellow to olive green, and pale green to green-blue. Zoned grains have olive green center and green-blue rims. Relief is moderately high and cleavage is ~60°-120°. Interference colors are 2nd order and extinction angle is inclined or symmetrical in basal section. Hornblende occurs in several textural ways:

(1) As nematoblastic grains defining the fabric, which have a tendency to bend around garnet porphyroblasts.
(2) As inclusion in poikilitic garnet porphyroblasts.
(3) As smaller grains in intermixed zones with other minerals.
(4) Around the rim of clinopyroxene.

Plagioclase(10-30%) is colorless with low relief in PPL. Grains are anhedral-subhedral and size ranges from <0,05mm- 1,2mm. Smaller grains occur with polygonal mosaic texture around larger anhedral grains. Two cleavages at ~90° are visible in the larger grains. Interference colors are 1st order, and plagioclase is distinguished by albite twinning. Plagioclase often contains unidentifiable impurities, and zoning is common.

Epidot/clinozoisite (10-30%) is pale green and has high relief in PPL. Epidote has multiple bright 1st – 2nd order interference colors, while clinozoisite have 1st order or anomalous colors (yellow-blue). There are gradual transitions between them. Vermicular habit in symplectites with quartz in close relation to hornblende or garnet is most common, but subhedral grains also occur (<0,1 mm). Clinozoisite embaying plagioclase is also observed.

Garnet (5-20%) porphyroblasts range from 1mm- 4,5mm. They are light pink in color, anhedral-subhedral in shape and have medium-high relief. In XPL they have total extinction. Commonly garnets are cracked or poikilitic with inclusions of hornblende, epidote/clinozoisite, plagioclase and clinopyroxene. Inclusions define an internal foliation which is slightly oblique to the main foliation in the rock.

Clinopyroxene (<10%) is pale green and have two cleavages approximately perpendicular to each other. Relief is moderately high, and grains are anhedral-subhedral (<0,05mm -0,5mm). Under crossed nicols grains have middle 2nd order interference colors and go extinct at ~ 45°. In some cases clinopyroxene is rimmed by the blue-green variety of hornblende.

Titanite (<5%) is light brown, eye-shaped grains (<0,1 mm) with high relief. The color stay brown in XPL, and grains go extinct parallel with elongation. Occurrence is disseminated and most commonly as individual grains.

Opaque (<5%) minerals are anhedral grains (<0,05 mm-0,75mm) with disseminated occurrence.

Quartz (<5%) is colorless with low relief in PPL. Interference colors are lower 1st order, often with undulating extinction. Grains (<0.2mm) are anhedral and occur with vermicular habit in symplectitic growth with epidote.

Allanite (<1%) is pale brown, elongate in shape and have low-medium relief. Occur as grains (<0.02mm) included in clinozoisite or hornblende. When present in hornblende allanite is surrounded by brown halo.

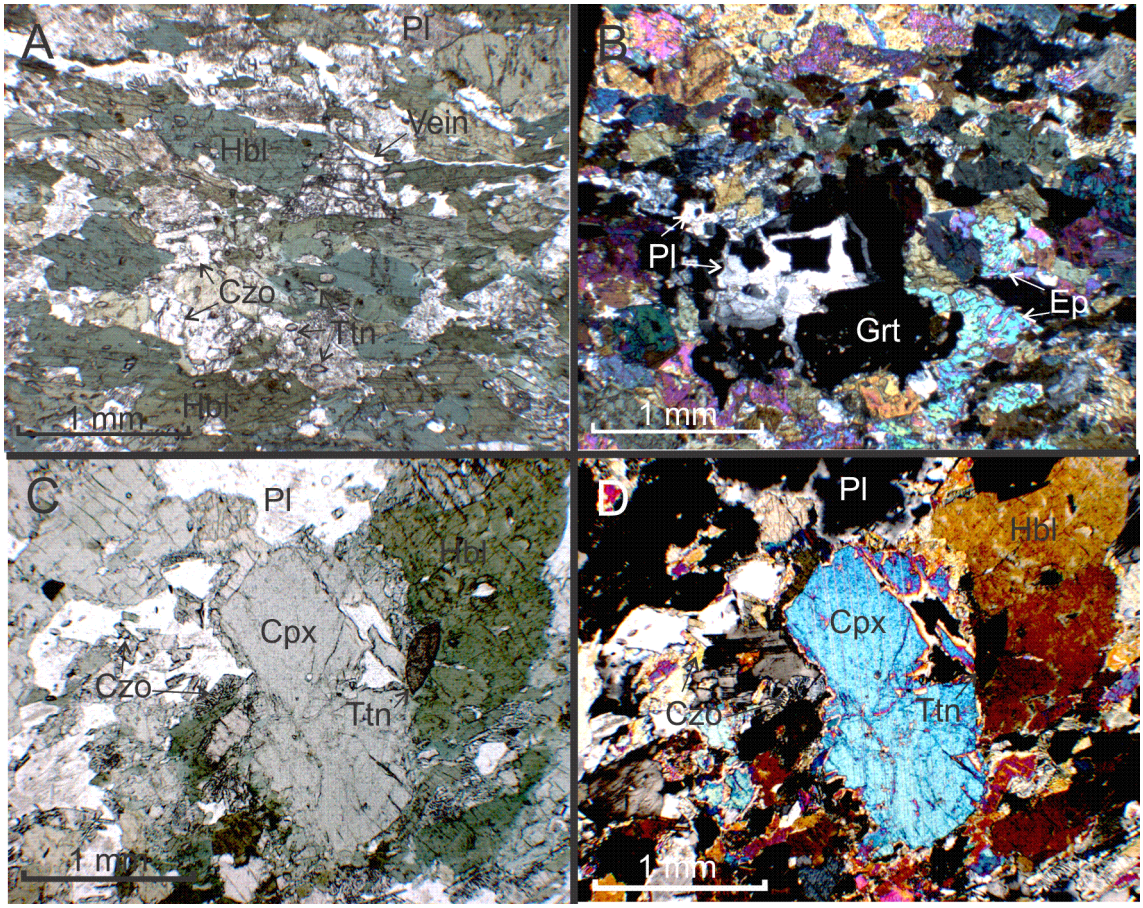

Figure 3.11: Micrographs of thin section 1.1; A) Image of hornblende in PPL shows how the mineral occur in two different shades of green (upper Hbl is green-blue to pale green pleochroic, lower Hbl is olive green to yellow-green pleochroic). A thin vein is transsecting the section. B) Image taken in XPL where plagioclase is filling the space between garnet grains, and epidote has a symplectitic texture with vermicular quartz. C) Image of Cpx in PPL with relation to Hbl, Ttn, Pl (zoned) and Czo (symplectite texture).

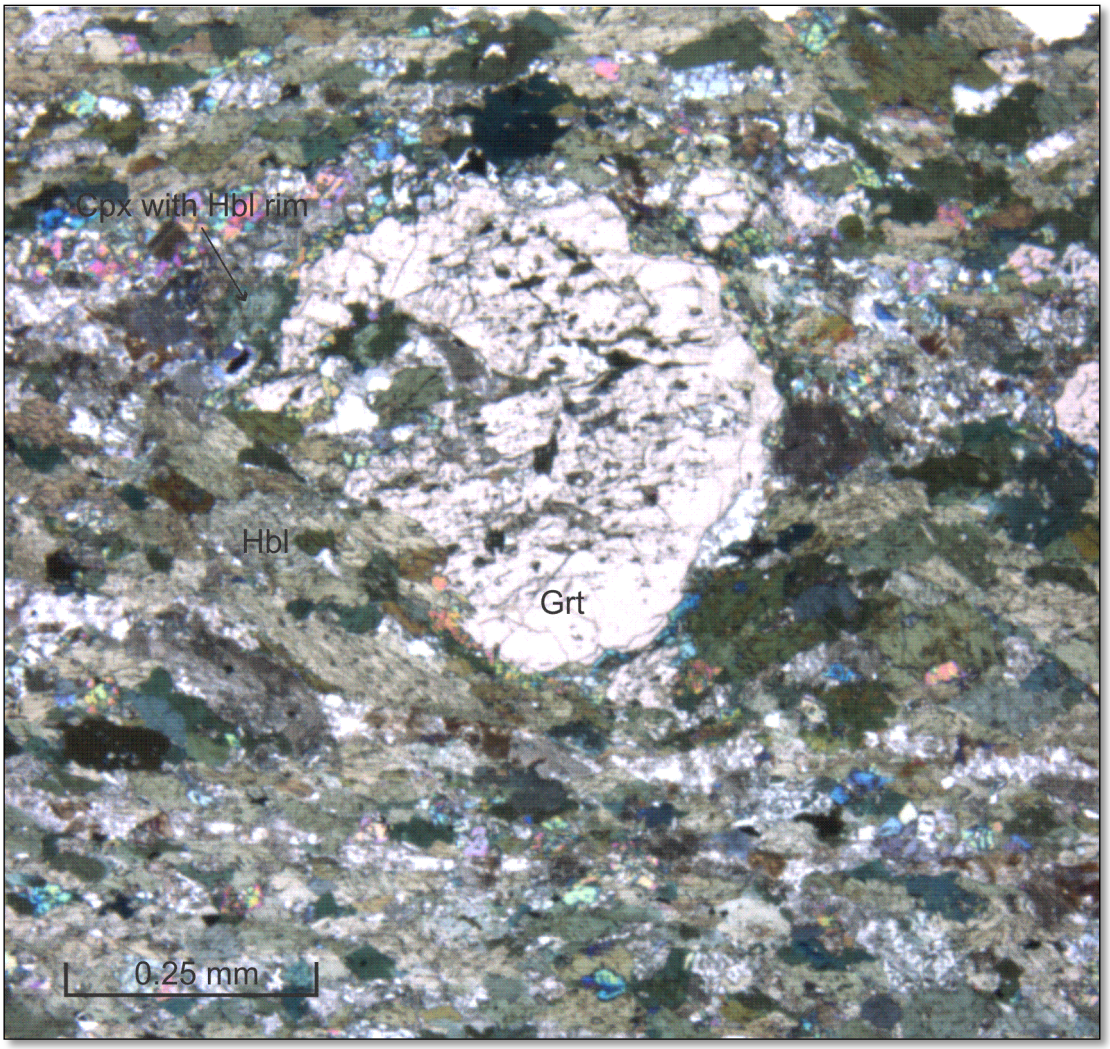

Figure 3.12: Image of poikilitic garnet porphyroblast. Inclusions of plagioclase, hornblende, titanite, clinopyroxene and epidote/clinozoisite define an internal foliation which is slightly oblique to the main foliation. Foliation bends around the lower edge of the garnet, and mid-way up on the right side of the garnet there is a zone of very fine grained matrix.

Table 3.5: Intergranular relations of minerals in Cpx-Grt bearing amphibolite; S= straight grain boundaries, L=lobate grain boundaries, C= complex grain boundaries, P=poikolitic, I= inclusion, E= embaying, Sy= symplectitc,. Table should be read with emphasis on the numbered minerals.

Mineral	Hbl	Pl	Ep/Czo	Grt	Cpx	Ti	Op	Qtz	Aln
1.Hbl	S/L	S/L	C	S/C/I	S/C/I	C/P	C		C
2.Pl	S/L	S/C	C	L/C/I	L/C	C/P	L		
3.Ep/Czo	C	C/E	Sy	C/I	C/S	C	C	Sy	P
4.Grt	S/P/C	L/C/P	C/P		P	P	P		
5.Cpx	S/C/P	L/C	C/Sy	I	L/C	C/P	P		
6.Ti	CC/I	CC/I	CC	I	CC/I	S	S/L		
7.Op	C	L	C	I	I	S/L	S/L		
8.Qtz			Sy						
9.Aln	I		I						

3.2.3 Meta-dolerite

Hand-specimens of meta-dolerite are fine- to medium grained with a weak foliation which is defined by elongate amphibole grains. Grain size of minerals increases with distance from the edges of the dykes. Ratio of light colored and dark colored minerals is approximately 1:3. Through hand lens small clusters of a fine grained, red-brown mineral occur in relation to light colored minerals.

Figure 3.13: Image of sample 3.5 showing dolerite dyke with sharp contact towards felsic dyke. Foliation is weak and oblique to dyke edge. Black box is for thin section preparation. Diameter of coin = 2cm.

In thin section meta-dolerite has heterogranular texture. Foliation is defined by nematoblastic hornblende. Matrix mainly consists of fine- grained feldspar, epidote/clinozoisite, hornblende. Titanite, rutile, zircon and opaque minerals have disseminated distribution. Several< 0.05 mm thin veins transect the thin section.

Mineralogy:

Hornblende (40-60%) occur as anhedral to elongate-subhedral (0,05 mm-2,5 mm) grains with medium high relief. Zoned grains have green-brown pleochroic center and green-green blue pleochroic rim. Interference colors ranges from middle 1st order to middle 2nd order, and

extinction is inclined. Grains are fractured and often have irregular grain boundaries towards other minerals. Smaller aggregates of hornblende are present in matrix. In some cases grains of other minerals are included in hornblende giving a poikilitic texture.

Plagioclase (30-50%) is colorless and has low relief in PPL. Grains (0,06mm -0,5mm) are most commonly anhedral and have two perpendicular cleavages. Interference colors are 1st order and plagioclase is distinguished by polysynthetic albite-twinning. Extinction angle is inclined. Boundaries are irregular, and large grains are often surrounded by clusters of smaller grains. Some of the plagioclase grains are zoned, and together with impurities this helps to distinguish small grains not to be quartz.
Plagioclase occurs in several ways:

(1) Anhedral poikilitic grains
(2) Subhedral grains with polygonal mosaic texture
(3) Inclusions in hornblende
(4) Symplectitic with clinozoisite

Clinozoisite/epidote (10-30%): 0,01mm- 1, 2 mm large grains of clinozoisite are anhedral-euhedral, have pale green color and high relief in PPL. Interference colors are 1st order or anomalous (blue-grey). Epidote grains have multiple bright 1st -2nd order interference colors. Generally smaller grains are euhedral and occur with systematic distribution inside plagioclase, while larger grains are anhedral- to subhedral and often have symplectite texture in relation to plagioclase.

Titanite(<5%) occur as 0,02mm- 0,3 mm rounded/oval grains, or cluster of small grains with somewhat elongate shape. Relief is high and distribution is disseminated. The mineral is brown both in PPL, and in XPL, and elongate grains have parallel extinction.

Allanite (<1%) occur as light brown,< 0.2mm, zoned, sometimes twinned, elongate subhedral grains inside clinozoisite. Interference colors are 1st order yellow-brown. Allanite often has corona of clinozoisite with radial fracturing-pattern.

Zircon (<1%)occur as euhedral-subhedral prismatic,< 0,05 mm, pale brown grains with high relief. Interference colors are strong but often mottled. Grains occur as inclusions in hornblende, often with a brown halo in PPL.

Opaque mineral (<1%) are disseminated with anhedral form. Grains are 0,05mm – 1,5 mm. Often occur as inclusions in hornblende, and commonly there is a irregular rim of rutile around the grain.

Rutile (<1%) grains are anhedral with red-brown color, that stays brown under crossed nicols. Relief is high and individual grains ranges in size from <0.05mm-0.1mm, however the dominating occurrence is around the rim of opaque minerals.

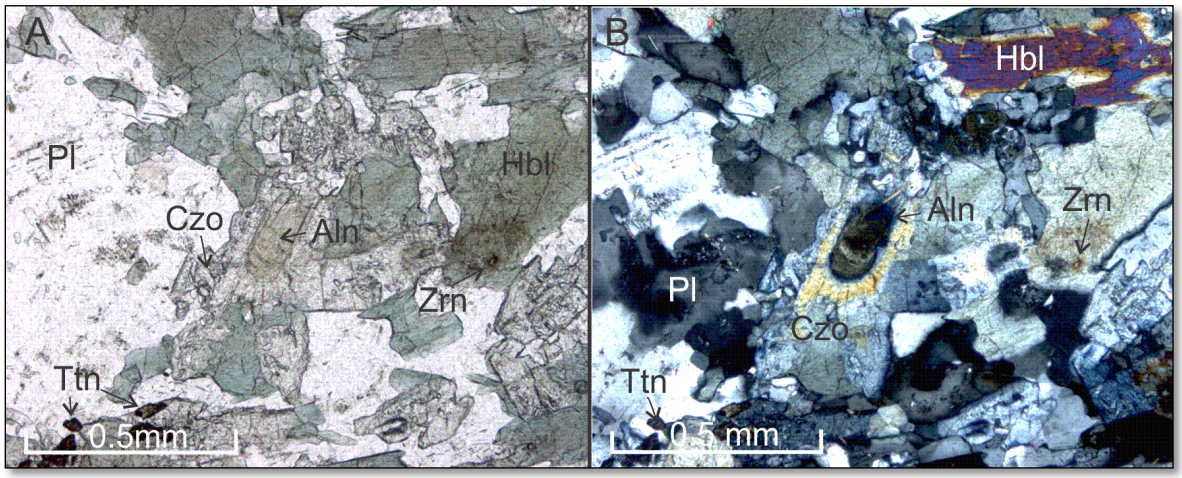

Figure 3.14: Micrography of thin section 3.5. A) Image showing Aln surrounded by clinozoisite in PPL. Zrn has a brown halo and is included in Hbl. B) Section A in XPL; showing the radial fracture pattern around Aln, and the zoned nature of plagioclase.

Table 3.6: Intergranular relations of minerals in meta-dolerite; S= straight grain boundaries, L=lobate grain boundaries, C= complex grain boundaries, P=poikolitic, I= inclusion, Sy= symplectitc,. Table should be read with emphasis on the numbered minerals.

Mineral	Pl	Hbl	Ep/Czo	Ti	Al	Zi	Op	Rt
1.Pl	S/L	C/I	P/Sy	C			C	C
2.Hbl	C/P	C	C/P	C/P	P	P	C/P	C
3.Ep/Czo	Sy/I/CC	C/I	C	C	C		C	
4.Ti	I	I	C					
5.Al		I	I					
6.Zi		I						
7.Op	C	I/C	C					C
8.Rt	C	C					C	

3.3 Ultra mafic rocks - Field relations

The ultramafic rocks that have been studied can be divided into serpentinite and amphibole rich rocks. Transitions between the two rock types are gradual. Main exposures are at location 4, where the ultramafic rocks occur as lenses in outcrops that have a high number of inconsistently oriented felsic dykes. Commonly ultramafic xenoliths (cm-dm scale) are seen in the felsic dykes.

Amphibolite-rich rock is green both weathered and freshly cut. The rock is massive or with foliation. When present, foliation is sub-parallel to the gradual transition between the two ultramafic rock types.

Serpentinite is generally massive. In some cases well preserved reaction zones towards felsic dykes occur. Weathered surfaces of the serpentinite are commonly brown, while fresh cuts expose a black-green colored rock.

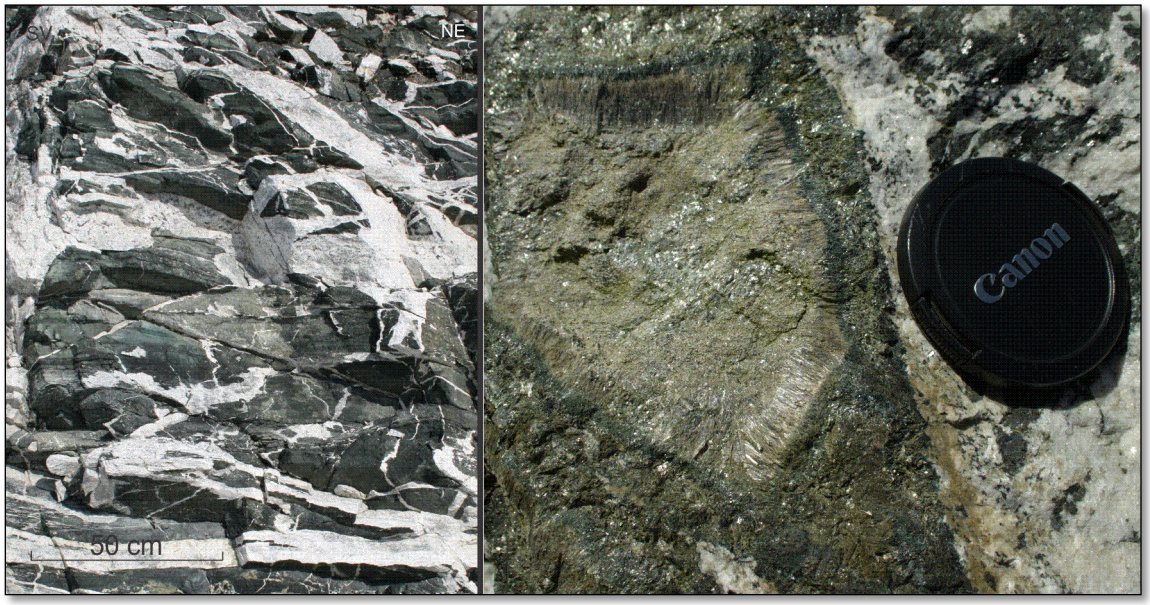

Figure 3.15: Image to left is showing occurrence of ultramafic rocks with irregular or sharp contacts to felsic dykes at location 4. Image to the right is of a reaction zone between serpentinite and a felsic dyke at location 4. Diameter of lens cap = 4cm.

3.3.1 Amphibole-rich ultramafic rock

Hand specimens of the rock are fine- to medium grained. Texture is massive or foliated. Amphiboles occur either with green color, acicular shape and without distinct preferred orientation, or as dark green-black elongate grains that defines the fabric in foliated samples. Fine grained dark-colored mica is present.

Figure 3.16: Image of sample 4.13 showing a weakly foliated variety of the amphibole-rich rock. Black box is for thin section preparation. Diameter of coin= 2cm.

In thin section texture is granoblastic or hetrogranular. Foliation, when present, it is defined by nematoblastic amphibole in a matrix of fine- grained amphibole, biotite and chlorite. Acicular amphibole is randomly distributed across sections with cross-cutting relationship to the overall fabric. Opaque minerals, commonly rimmed by rutile have disseminated distribution.

Mineralogy:

Amphiboles (80-100%) generally occur with occur with colorless to pale-green pleochroism, and moderately high relief, but pale-green to yellow-brown pleochroism is also observed. Two habits exist:

1) Subhedral prismatic (0,1 mm-2mm) with and moderately high relief. Typical cleavage intersection of ~60°-120^{0}is observed. Interference colors up to middle 2nd order with inclined extinction angle.

2) Acicular (0,2mm-2mm) with moderately high relief, 2nd to 3rd order interference colors, and inclined extinction.

Both habits are commonly zoned. Several variations occur:

- Colorless center and pale-green rim
- Pale-green center and colorless rim
- Yellow-brown center and pale-green or colorless rim.
- Yellow-brown center, colorless middle part and pale green rim

The mineralogy of the amphiboles is further discussed in section 5.3

Chlorite (10-20%) has pale green- green pleochroism, medium relief, perfect (001) cleavage, and lamellar habit. Grains size ranges from 0,1mm-1mm. Interference colors are lower 1st order and extinction is parallel.

Phlogopite (<10%) is pleochroic in shades of brown, have moderately high relief and perfect (001) cleavage. Grains have lamellar habit and grain size ranges from 0,1mm-0,6mm.Interference colors are upper 3rd order. Biotite occurs in clusters with smaller aggregates of amphibole and chlorite.

Opaque (<5%) is disseminated with anhedral shape. Grains (<0.02mm-0.1mm) often occur with rims of rutile.

Rutile (<1%) grains are anhedral with red-brown color, that stays brown under crossed nicols. Relief is high and individual grains ranges in size from <0.05mm-0.1mm, however the dominating occurrence is around the rim of opaque minerals.

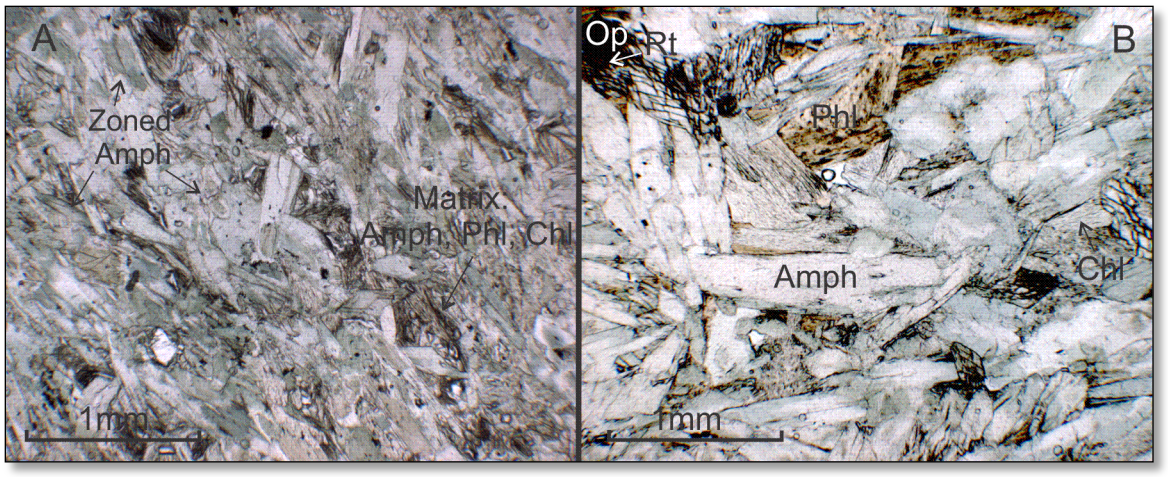

Figure 3.17 : Micrographs of amphibole-rich rock; A) Image is showing variations of zoned amphibole in fine-grained sample (4.13). Matrix of Amph, Phl and Chl occur between amphiboles. B) Image of fine- to medium-grained sample(4.18), whit zoned Amph, Phl, Chl, Op and Rt.

Table 3.7: Intergranular relations of minerals in amphibolite-rich ultramafic rock; S= straight grain boundaries, L=lobate grain boundaries, C= complex grain boundaries, P=poikllitic, I= inclusion. Table should be read with emphasis on the numbered minerals.

Mineral	Amph1	Amph 2	Chl	Phl	Op	Rt
1.Amph1	S/L	C	S/I	S/I	C	C
2.Amph2	CC	S	CC	S/CC	C	C
3.Chl	S/P	C	S/L	C	C	C
4.Phl	S/C	S/CC	C	S/C	C	C
5.Op	C/I	C/I	C/I	C/I	C	C/I
6.Rt	C/I	C/I	C/I	C/I	C	C

3.3.2 Serpentinite

Hand specimens are massive and consist of light green, light-reflecting fragments (mm-scale) without any recognizable habit or cleavage, in a fine grained dark colored matrix. The rock smells of sulfur.

Figure 3.18: Sample 4.15 of massive serpentinite with brown weathered surface. Black box is for thin section preparation. Diameter of coin= 2 cm.

Thin sections are heterogranular, and dominated by minerals of the serpentine group. Olivine is present as fractured grains where serpentine fills the cracks. A considerable amount of opaque minerals also occur, in addition to chlorite and minor spinel.

Mineralogy:

Serpentine (70-90%) occurs in two varieties:

1) *Chrysotile* (0.02mm-0.1mm) is fibrous with a grey color in PPL. Relief is high and interference color is up 1st order grey. Fibers are aligned across veins in fractured olivine.
2) *Antigorite* (0.04mm-1mm) is colorless with lamellar habit and medium high relief. Interference colors are anomalous blue(Fe-rich) and light brown(Mg-rich).

Opaque (5-20%) occur with anhedral shape. Grains size ranges from 0.02 mm-1mm. Opaque minerals are often surrounded by antigorite, or they are situated in the center of the serpentine veins.

Olivine (< 10 %) is colorless in PPL. Relief is moderately high. Grains (0.05mm-2mm) are often strongly fractured, with serpentine minerals filling the veins between the aggregates of olivine. Interference colors are upper 2nd –lower 3rd order. Impurities makes olivine appear yellow/orange in PPL.This color also masks the interference color.

Spinel (<5%) is deep green, non-pleochroic. Grains (<0.02mm- 0.3mm) are anhedral and have high relief. Under crossed nicols grains are black.

In addition amphibole starts to appear gradually towards amphibole-rich ultramafic rock.

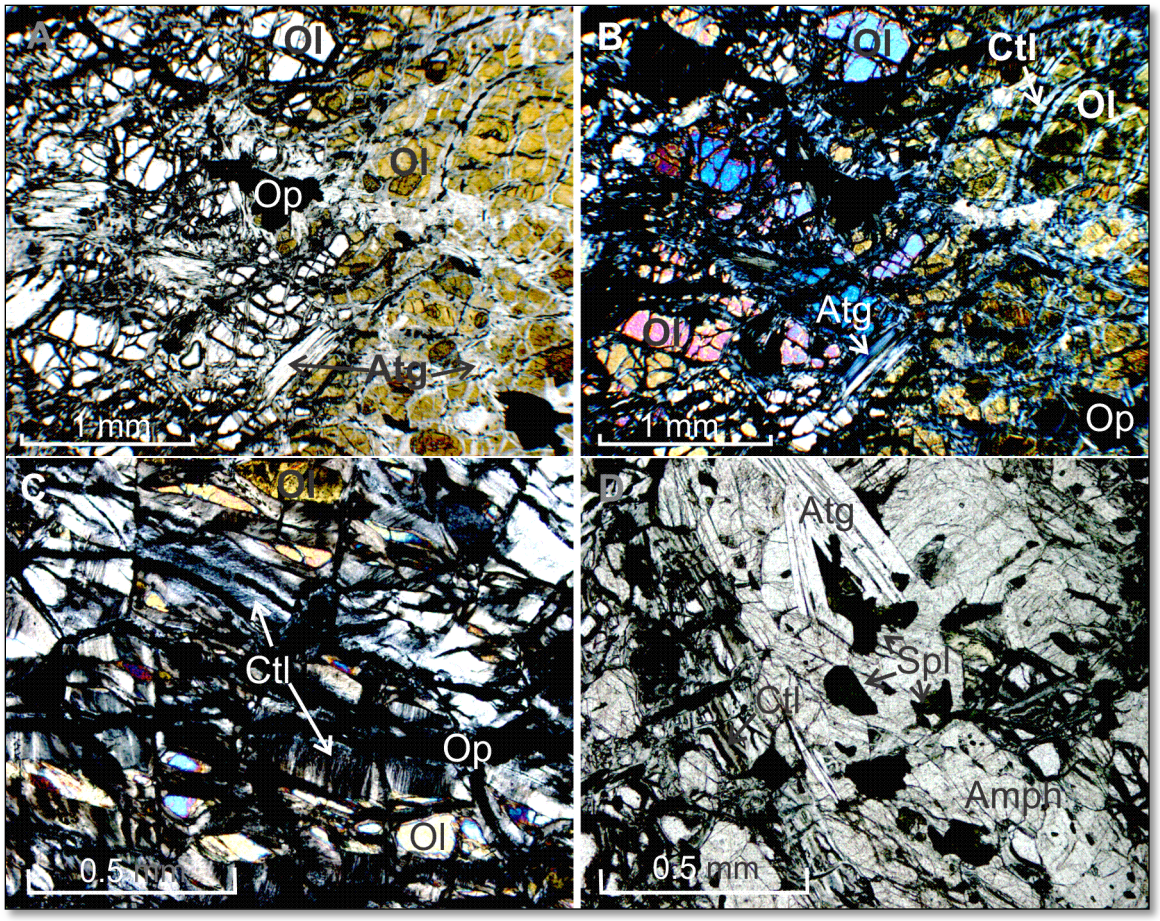

Figugre 3.19 : Micrographs of serpentinite; A & B) Sample 4.23 showing part of serpentinite with large amount of olivine grains. Chrysotile, antigorite and opaque minerals are filling the veins between aggregates of olivine. C) Image of sample 4.22 showing the fibrous habit of chrysotile. D) Image showing the occurrence of spinel and amphibole in sample 4.15 (transition between serpentinite and amphibole-rich ultramafic rock).

Table 3.8: Intergranular relations of minerals in amphibolite-rich ultramafic rock ; S= straight grain boundaries, L=lobate grain boundaries, C= complex grain boundaries, P=poikilitic. Table should be read with emphasis on the numbered minerals.

Mineral	Ol	Atg	Ctl	Spl	Op
1.Ol		C	S/C	C/P	S/C
2.Atg	C/CC	S/CC	C/CC	C	C
3.Ctl	S/CC	C	S/L	C	S/C
4.Spl	I/C	C	C		
5.Op	S/C/CC	C	S/C		S/C

3.3.3 Reaction zones between ultramafic rock and felsic dykes

In the contact zone between felsic dykes and serpentinite it is observed reaction zones, where texture and mineralogy changes through several zones in mm-cm scale. There is a strong parallel alignment of minerals, often oriented perpendicular to contact surface. In some cases minerals form radial reaction pattern, from an ultramafic/completely altered center towards the felsic dyke. The change of mineralogy is clearly recognized through the change of color and habit in hand-specimens, and sub-division into zones is done according to figure 3.20:

Figure 3.20: Sample 4.22 showing how color, habit and texture change in through five zones from serpentinite towards felsic dyke. Diameter of coin =2 cm.

Starting from the serpentinite; a zone with massive, black to dark brown rock **(1)**, before a clear transition into a zone enriched in a light grey, massive, softer and soapy mineral, recognized to be talc **(2)**. Subsequent a zone of strongly aligned, light brown needle-shaped (< 5mm) amphibole **(3)**, with gradual transition into shorter (<2mm) amphibole needles with green color **(4)**. Closest to the felsic dyke a zone dominated of chlorite that is identifiable visibly from its green color and well-developed cleavage, together with a fair bit of talk in a flaky habit **(5)**.

Further studies in thin sections show that transitions between zones are intermixed. Texture is heterogranular in all zones, but mineral orientation changes from being random in the lower two zones, to strong parallel alignment of minerals in zone 3,4 and 5.

Mineralogy:

Zone (1): The mineralogical composition in this zone coincides the sepentinite described above; Serpentine (antigorite + chrysotile), olivine, opaque minerals and minor spinel (for more details see section 3.3.2.

Transition: Amount of olivine and chrysotile decrease towards zone (2), while there is an increase of antigorite. Spinel disappears completely while talc enters the assemblage. Opaque minerals continue to occur without any noticeable change.

Zone (2)*:*
Talc (50-80%) is pale brown with medium relief in PPL. Habit is lamellar with (001) cleavage. Grains (0.1mm-0.7mm) have random orientation. Interference colors are upper 2^{nd} – upper 3^{rd} order, and extinction is pebbly.

Antigorite (20-30%) is colorless with lamellar habit and medium high relief. Grains (0.04mm-1mm) occur with random orientation in clusters with talc, or in close relation to opaque minerals. Interference colors are anomalous blue (Fe-rich) and light brown (Mg-rich).

Opaque minerals (10-20%) are disseminated with anhedral shape. Grains size ranges from 0.02mm-2mm, and larger grains are often surrounded by antigorite.

Transition: Towards zone (3) there is a decrease in talc and antigorite, and amphibole is introduced. Opaque minerals continue through the transition zone without any noticeable change.

Zone (3):

Anthophyllite/Gedrite (90-100%) is pale tan in color, prismatic elongate habit. Grains (0.3mm- 4mm) are subhedral and have moderately high relief. (110) cleavage is often visible. Interference colors are upper 1st order, and extinction is parallel to elongation. There is a strong parallel alignment of grains within the zone.

Opague minerals (< 10%) occur as anhedral grains with random distribution. Grain size ranges from 0.02mm- 1.5mm.

Transition: Intermixed zone with anthophyllite/gedrite and tremolite/actinolite. Opaque minerals decrease towards zone (4).

Zone (4):

Tremolite/Actinolite (60-100%) is pale green, has elongate prismatic habit and medium relief. Amphibole cleavage (~60 º -120º) is recognized. Grain size ranges from 0.02mm- 1.5mm, and there is a strong parallel alignment. Interference colors are 2nd order and extinction is inclined.

Hornblende (20-40%) is yellow to light green pleochroic with medium relief. Amphibole cleavage (~60 º -120º) is observed. Grains (0.1mm- 1.25 mm) are anhedral to elongate subhedral. Zoned grains occur, with yellow-green pleochroic center and pale green-colorless rim. Interference colors are upper 2nd order, and extinction is inclined. Elongate grains have preferred orientation parallel to actinolite.

Opaque minerals (<5%) occur as anhedral grains with random distribution. Grain size ranges from 0.05mm- 1mm.

Transition zone towards dyke (5):

Hornblende (60-90%) is yellow- to light green pleochroic. Relief is moderately high and grains (0.3mm- 2mm) are anhedral to elongate subhedral. Interference colors are upper 2nd order, and extinction is inclined. Zoned grains occur; center has yellow-green pleohroism, while rim has pale green to colorless pleochroism.

Talc (10-20%) is yellow-brown with a lamellar or bladed habit. Grains (0.02mm -1.5mm) have medium relief, and perfect (001) cleavage. Interference colors are various upper 2nd- upper 3rd order colors, and extinction is pebbly. Preferred orientation is parallel to hornblende.

Chlorite (<10%) has a week pale green to green pleochroism. Grains (0.02mm- 2mm) have lamellar habit whit perfect (001) cleavage, and relief is moderately high. Interference colors

are lower 1st order or anomalous light brown. Chlorite grains are aligned parallel to hornblende and talc.

Figure 3.21: Micrograhpy of thin section 4.22a showing the zoned reaction pattern in XPL. Mineralogy and texture changes through zone 1 to 5 as explained in section 3.3.3. Base of thin section is 2 cm.

3.4.1 Structural summary

Structural geology and metamorphic geolog go hand in hand, so both aspects should be taken into consideration when investigating an area. For the purpose of this thesis structural data is mainly used to establish a framework for the tectonometamorphic studies in terms of correlation of metamorphic- and deformational events, and comparison with earlier work.

The types of structural elements registered in the different lithologies are presented in table 3, followed by brief descriptions.

Table 3.9: Overview of structural elements related to lithologies

		Folding			
Lithologies	**Fabric**	Large-scale	Small-scale	**Shear-zones**	**Faults**
Meta-anorthosite	*	*		*	*
Migmatite gneiss	*	*			*
Cpx-Grt amphibolite	*	*	*	*	*
Amphibole-rich rock	*		*	*	*
Serpentinite				*	*
Felsic dykes			*	*	*
Doleritic dykes	*			*	*

Fabric and folding:

Meta-anorthosite (1), Cpx-Grt amphibolite (2), amphibole-rich ultramafic rock (3) and dolerite (4) are all foliated, while the fabric in the migmatite gneiss is banding (5). In all four cases, fabric is parallel to the lithological layered sequence at the location where each of them is situated. However, due to the large amount of felsic dykes relative to the ultramafic rocks (loc.4) foliation measurements has a restricted range, and is strictly only valid for the lens in which they are taken.

Main structural trends for each rock type: gently dipping = <15°, moderately dipping= 15-45°, steeply dipping = >45°.

1) Main trend of foliation in meta-anorthosite is gently dipping to the SE or gently dipping to the NW, giving large scale flexural folding. Folding is upright and from field measurements the trend of axial plane is SW-NE.
2) Cpx-Grt bearing amphibolite has a NNE or SSW striking, gently- moderately dipping foliation, linked by flexural-open folding. Folding is upright and trend of fold-axis is SSW-NNE.
3) Measurements taken in the disrupted amphibolite-rich rock give a NW striking, gently dipping foliation.
4) Foliation in dolerite is steeply dipping and striking SW or W.
5) Foliation in migmatite gneiss is gently dipping towards the SE (fig.3.7)

Felsic dykes have also recorded folding. Intensity of folding decreases with dyke thickness. At location 1, fold style is tight to isoclinal and overturned (fig. 3.21 C). Axial plane is moderately dipping towards the W.

Shear zones:

Several large shear zones occur in the SMC. Sinistral sense of shear is determined from cross-sections at location 3 (fig. 3.22 A), indicating that the eastern block has moved upwards relative to western block, top-to-the SE. Small scale shearing in the Cpx-Grt bearing amphibolites is deforming folded felsic veins/dykes. Sense of shear is dextral, moving the western block up relative to the eastern block, top-to-the-E.

Faults:

All of the studied rock types have experienced brittle deformation. Normal faults are seen on the fold limbs of large scale flexural folds, dipping moderately either towards WNW or ESE direction (fig. 3.21 D). Normal faults are also seen steeply dipping towards NNE (fig 3.21 B)

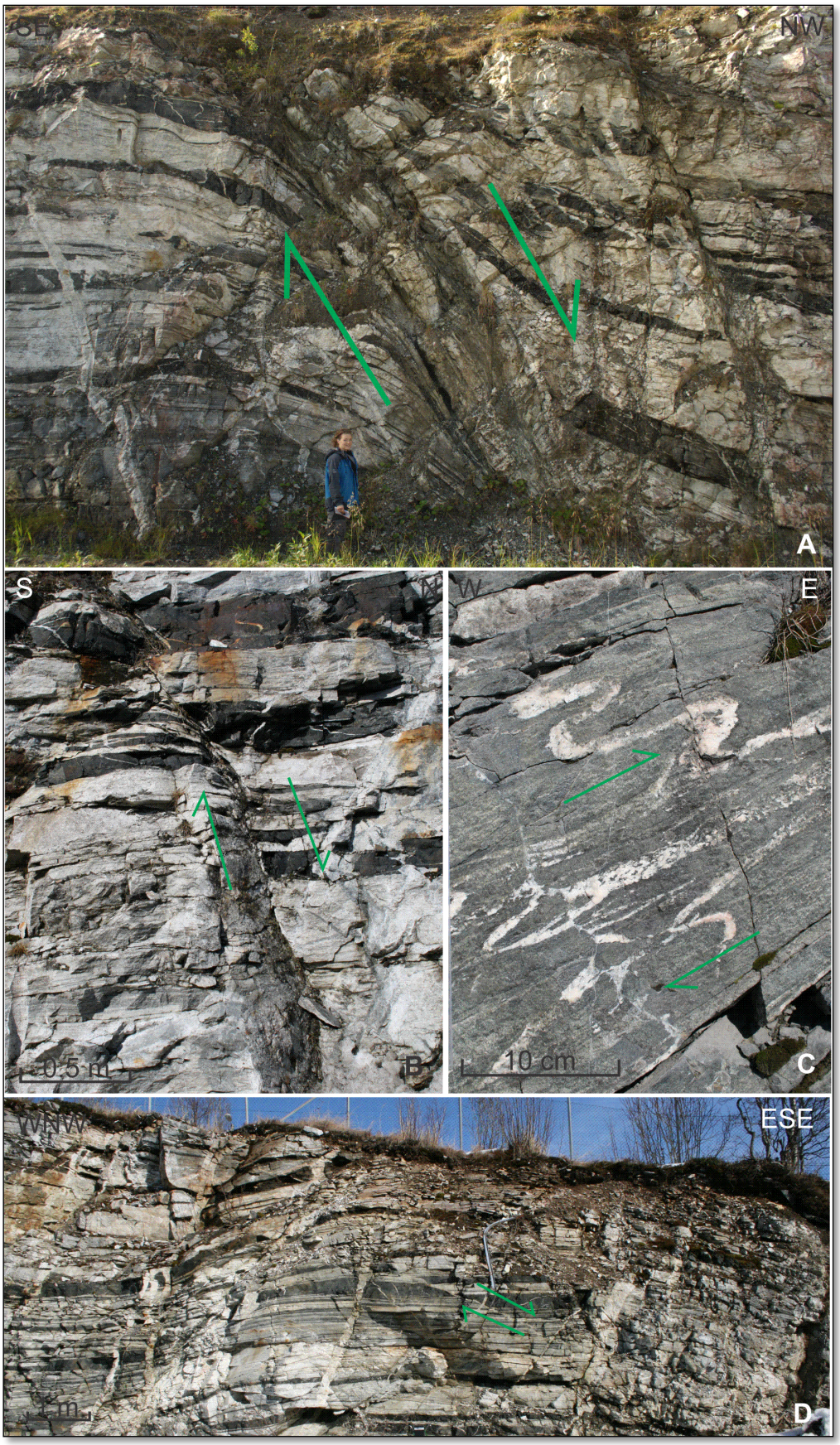

Figure 3.22: A) Large scale sinistral shear zone at loc. 3. B) Steeply dipping normal fault at loc.3. C) Small scale shear zone at loc.1. D) Gently dipping normal fault at loc 3. See structural descriptions in section 3.4.1 for details.

3.5 Summary and interpretations of petrographical observations

Textural interpretations in this summary are made on the basis of thematically listed referenced work:

Corona textures and coronites: Shand (1945). *Serpentinization:* Moody (1976). *Plagioclase alteration, deformation and recrystallization*: Goldsmith and Ehlers (1952); Vernon (1975); Olsen & Kohlstedt (1985). *Chloritization:* Yu-Chyi et al. (1984). *Porphyroblasts:* De Wit (1976). *Zoning and inclusions*: Tracy (1982). *Migmatites and partial melting*: Johannes & Gupta (1982); Brown et.al (1995); Sawyer (1999). *Reaction zones:* Marocchi et al. (2009). *General microtextural interpretation*: Shelly (1994), Putnis (2002).

Meta-anorthosite

Studied material of the meta-anorthosite has been divided into:

1) Samples predominantly of plagioclase, which have penetrating foliation defined by mica, epidote/clinozoisite and minor chlorite.
2) Samples that have no penetrating foliation, where plagioclase is present mostly as small aggregates in granular masses of zoisite. Mica and epidote/clinozoisite are present both as inclusions and with a cross-cutting relationship to zoisite. Chlorite has a cross-cutting relationship to all other phases except the white mica.

Variant 1 is interpreted to be least altered. Impurities in plagioclase are suggested to be a mix of alteration minerals as a result of sussurtization. In some cases replacement of plagioclase is even more complete seen as grains of epidote/clinozoisite, while in other zones plagioclase is almost pure with polygonal texture. The latter is interpreted to be a preserved magmatic feature. Chlorite is regarded to be a late phase which signifies that an Mg-phase has been present at an earlier stage.

In variant 2, the breakdown of plagioclase is much more extensive, and based on the intergranular relationship the main metamorphic mineral assemblage is suggested to be: Zo+ Pl+ Ep/Czo+Mca. Intra-crystalline features (corroded cores in anhedral pure plagioclase) signifies partial melting of the rock, which together with zoisite (indicating disequilibrium of

plagioclase at high pressure condition) makes the rock interesting for further analysis and pseudosection construction.

Leucocratic dykes

Two variations of the felsic dykes have been studied:

1) White colored dykes containing plagioclase with zoisite inclusions, epidote/clinozoisite, white mica and hornblende.
2) Purple-grey colored dykes with unaltered plagioclase as main mineral accompanied of hornblende and accessory phlogopite, chlorite and calcite.

Type 1 has a metamorphic overprint,where epidote/clinozoisite and white mica present due to breakdown of plagioclase. Euhedral zoisite needles are suggested to have grown in equilibrium with the melt. The occurrence of large anhedral plagioclase grains surrounded by smaller plagioclase grains with polygonal mosaic texture is regarded to be deformational sub-grain recrystallization. Type 2 contains few signs of breakdown processes, with the exception of chlorite replacing phlogopite. White veinlets are considered to be fluid-pathways causing decoloration. Calcite is suggested to be a late phase. For the purpose of this study these dykes are interesting because their composition indirectly holds information about the protolith the melt fractionated from, and they represent the thermal peak condition related to the migmatization process. The fresh dyke will be studied more thoroughly through analyses of bulk composition, calculation of normative composition and pseudosection construction.

Migmatite gneiss

Migmatite gneiss occurs with compositional banding. The discontinuity of the fabric without structural interference indicates that banding is a result of partial melting, where a melt phase have segregated from the country rock to form leucocratic bands (leucosomes) by *insitu* crystallization. This is supported by observation of cuspate grain shapes, melt film along grain boundaries between grains of hornblende (see figure 3.9). Micro-veins of unknown composition and cross-cutting relationship to the overall parallel banding are interpreted as a late feature.

Deformation is recorded in the rock as sub-grain recrystallization of the plagioclase, seen as large strained grains surrounded by clusters of smaller unstrained grains with mosaic texture. Clinozoisite is regarded to be a late product of the breakdown of plagioclase. For the purpose of this study the migmatite gneiss will not be studied in further detail because it apparently represents a mixture of neosome and paleosome.

Grt-Cpx bearing amphibolite

The inclusion trails in the poickilitic garnet porphyroblasts is the oldest recognized mineral assemblage and fabric in the amphibolite (S1). Hornblende, plagioclase, clinopyroxene, titanite, epidote/clinozoisite and opaque minerals are all observed as inclusions in studied garnets. Opaque minerals and titanite may be part of an early paragenesis or be a metamorphic product, while epidote/clinozoisite is suggested to be breakdown products of other phases (e.g plagioclase).

Poikilitic garnets are considered to pre-date the latest deformational event producing the (S2) foliation based on:

- Evidences of mechanical breakdown
- Discordant relationship between internal foliation (S1) and main foliation in the rock (S2)
- Pressure- shadows occur in relation to garnets.

The foliation parallel light colored veins are interpreted to be leucosomes as result of partial melting, segregation and *insitu* crystallization of mainly plagioclase. Evidences for this in thin section are melt pools, cuspate grain shape of plagioclase and clinozoisite/epidote between ferromagnesian minerals, which is interpreted to be pseudomorphs of plagioclase melt-film. Plagioclase grains in veins are zoned which indicates crystallization under changing conditions. The extent of saussuritization and deformation (recorded as sub-grain recrystallization) of plagioclase grains varies.

On the basis of zoned hornblende (olive green center and blue-green rim) and reaction rims (blue-green hornblende rim on clinopyroxene), the olive green hornblende is interpreted to pre-date the blue-green variant. Allanite is seen as inclusions in olive green hornblende and is for that reason suggested to be part of an early stage paragenesis. Radial fracture pattern in

epidote/clinozoisite is due to the metamicte allanite, and haloes surrounding allanite in hornblende is present for the same reason.

Thin, cross-cutting veins which composition was not identifiable with the use of microscope are suggested to be late features, as they clearly post-dates the leucosomes and main foliation.

Symplectitic growth of minerals (eg. epidote and quartz) signifies disequilibrium, and will be a subject of further discussion in section 5.3.2. The mineral assemblage (Amph +Pl +Cpx+Aln ± Ttn ±Op) recorded in garnet porphyroblasts together with evidence for partial melting makes the rock interesting for further XRF-analyses and pseudosection construction.

Meta-dolerite

The zoned nature of hornblende signifies that the brown-green variation pre-dates the green-blue one. Inclusions of plagioclase, allanite, titanite, zircon, epidote/clinozoisite, opaque minerals are all observed in the oldest generation of hornblende. Epidote/clinozoisite inclusions are interpreted to breakdown products of plagioclase. Other signs metamorphism and deformation in metadolerite are:

- rutile reaction rims on opaque minerals
- symplectitic growth of Ep/Czo in relation to plagioclase and hornblende (discussed more thoroughly in section 5.3.3)
- sub-grain recrystallization of plagioclase
- Epidote/clinozoisite rim around allanite
- Mechanical breakdown of hornblende

Mafic dykes have so far not been documented in the SMC, which makes the rock subject for further studies by XRF-analyses.

Amphibole-rich ultramafic rock

Amphiboles are zoned in many variations indicating that they have grown under changing conditions. There are few indications of phase transitions except from chlorite replacement of phlogopite and rutile rims on opaque minerals. Opaque minerals may have originated as part of an early paragenesis or may be metamorphic.

The inconsistent orientation and cross-cutting nature of acicular amphibole suggest late growth relative to the other hydrous phases. There are no clear trends relating amphibole habit to certain variations of zonation, but a yellow-brown core seems to favor a prismatic habit. Further discussion will follow in chapter 5.

Serpentinite

The extensiveness of the serpentinization amongst ultramafic samples varies:

Most altered zones consist predominantly of serpentine-group minerals, together with iddingsite and other breakdown products (e.g talc, chlorite and opaque minerals) of olivine and other unknown protolith phases. Least altered are zones where relict olivine is preserved as aggregates in a mesh-patterned system of veins consisting predominantly of serpentine- and opaque minerals. Spinel is observed inside olivine and is for that reason interpreted to be a part of an early paragenesis.

Reaction zone between serpentinite and felsic dyke

The studied reaction zone is interpreted to be a metasomatic sequence, where polymineralic transition zones separates near-monomineralic or near-bimineralic bands of mainly hydrous phases (from serpentinite towards dyke: talc+ antigorite zone, anthophyllite/gedrite zone, hornblende + tremolite/actionlite zone, phlogopite+ chlorite+ talc zone). This sequence will be subject of further discussion in chapter 5.

4 XRF- analyses, CIPW-norm calculations and pseudosection construction

This chapter presents results from XRF-analyses, CIPW-norm calculations and further construction of pseudosection with Perple_X 6.6.6 (Connolly, 2011) software package.

Two rock types were selected for further XRF- analysis based on their metamorphic parageneses and intergranular relations. Pseudosections were constructed in both cases:

(1) Meta-anorthosite, sample 3.6
(2) Cpx-Grt amphibolite, sample 1.1

Additionally, analysis of the purple-grey variety of felsic dykes was performed based on the freshness of the rock. CIPW-norm calculation and pseudosection construction was also performed:

(3) Felsic dyke, sample 4.24

XRF-analysis and CIPW-norm calculations were performed on the mafic dyke.

(4) Meta-dolerite, sample 3.5

X-ray fluorescence spectroscopy of major elements was performed according to the procedure presented in section 2.3. Results are presented in table 4.1 – 4.4, and their relation to location and thin section is presented in the appendix, table A2.

Perple_X was used with the aim to determine phase topological relations within the individual chemical system of three samples (sample number: 3.6, 1.1, 4.24) presented as pseudosections in P-T space. Constructions are made on the assumption that bulk-compositions reflect equilibrium mineral assemblages and reaction volumes.

Final pseudosections presented in this chapter are products of the process of running the Perple_X6.6.6 sub-programs BUILD, VERTEX and PSSECT, in addition to graphical modification in CorelDrawX5. Supplementary analyses of phases and solutions (composition and volume) were performed by the use of the sub-program- WERAMI. Details on thermodynamic data set, solution model file and general work flow of Perple_X6.6.6 are given in section 2.5.

CIPW-norms are calculated for dolerite and felsic dyke to get the normative composition as explained in section 2.4.

4.1 Meta-anorthosite

Table 4.1: Results from XRF- analysis of meta-anorthosite given in average wt% and calculated normalized molar proportions. FeO is calculated from stoichiometry. Loss of ignition is not tested.

Sample3.6	SiO_2	Al_2O_3	TiO_2	FeO	MnO	MgO	CaO	Na_2O	K_2O	P_2O_5	Tot
Wt (%)	45,47	29,81	0,07	0,98	0,02	0,16	17,61	2,01	0,11	0,02	96,23
N.mol. prop	46,75	18,10	0,00	0,81	0,00	0,24	19,37	2,00	0,07	0,01	87,35

Pseudosection construction:

Calculated normal molar proportions of oxides of major elements presented in table 4.1have been used for construction of P-T pseudosections. Before modeling phase topological relations, some considerations were made based on the mineralogy of sample 3.6:

- There are only traces of Fe-Mg minerals – all secondary, and the small amount of MgO present has thus been discarded from the calculations.
- Epidote is the only iron-rich phase in the analyzed sample. The iron component of epidote is ferric, and for that reason the FeO value from table 4.1 were balanced by stoichiometry with O_2 to form the equivalent amount of Fe_2O_3.
- The proportion of the potassium component is very small. There is no K-phase identified, and so it is reasonable to assume that this small amount is present as K-feldspar component in plagioclase.Thus it is reasonable to merge K_2O into Na_2O, which also will reduce the complexity of pseudosection.

Modifications where included when running BUILD. The only solution model used in calculations was for plagioclase, **[Pl(h)]** (Newton et al., 1980). H_2O and O_2 were added as thermodynamic components.

The topological relationship of different phases in the NCFASHO chemical system for meta-anorthosite (sample 3.6) is given in figure 4.1, for the P-T window 0.6-1.2 GPa and 500-750 ^oC.

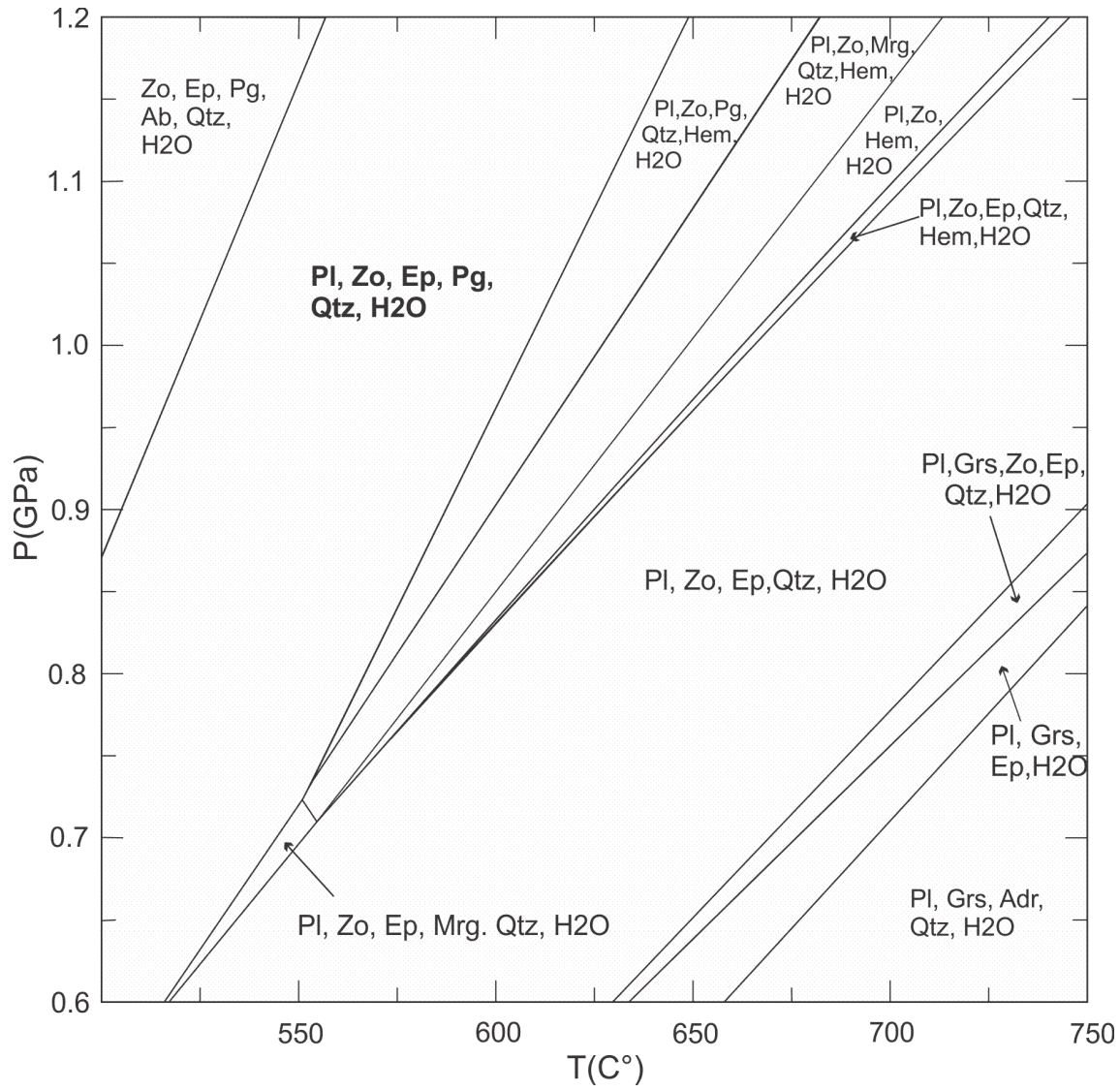

Figure 4.1: P-T pseudosection constructed from molar proportions of major elements of sample 3.6 (table 4.1) with the given modifications.

In figure 4.1,showing P-T pseudosection for meta-anothosite, quartz is present in minute quantities in all fields while the studied rocks do not contain any quartz. This may be due to the theoretical ideal composition of phases included in the calculations. For that reason quartz will not be included in further discussion of this rock.

There are two parageneses between 500-650 ^{0} C and 0.6-1.2 GPa, that coincide with petrographical observations:

1) Pl+Zo+Ep+Mrg + excess H_2O
2) Pl+Zo +Ep+Pg + excess H_2O

Assemblage 1 has a low T-P stability field. It favors the Ca-rich variety of mica, margarite. Assemblage 2 is stable over a large P-T interval, and paragonite (sodic) is the stable mica.

Further discussion on the pseudosection for the meta-anorthosite is presented in section 5.1.

4.2 Cpx-Grt bearing amphibolite

Table 4.2: Results from XRF- analysis of Cpx-Grt bearing amphibolite given in average wt% and calculated normalized molar proportions. FeO is calculated from stoichiometry. Loss of ignition is not tested.

Sample 1.1	SiO_2	Al_2O_3	TiO_2	FeO	MnO	MgO	CaO	Na_2O	K_2O	P_2O_5	Tot.
Wt (%)	44,38	13,77	1,93	12,76	0,25	6,07	12,44	2,34	0,55	0,16	94,64
N.mol.prop	43,08	7,88	1,41	9,16	0,00	8,78	12,72	2,20	0,34	0,07	84,23

Pseudosection construction:

Calculated normal molar proportions of major elements presented in table 4.2 were modified to reduce complexity of P-T pseudosection;

- XRF- analysis proved small amounts of K_2O in the bulk composition. The mineral content identified by optical microscopy suggests that the potassium component is likely to belong in amphibole and plagioclase. The solution model used for calculations does not include potassium in amphiboles, and consequently another phase that is suitable for potassium (e.g biotite) will be provided by the program. To avoid this, K_2O is merged with Na_2O.
- TiO_2 may enter hornblende and ilmenite in amphibolites. However, none of the solution models of amphibole include Ti, and TiO_2 is excluded from the calculations.

Modifications were included when running BUILD. H_2O was included as a thermodynamic component, and the following solution models were used for calculations: amphibole **[Amph(DHP)]** (Dale et al., 2000),, clinopyroxene **[Cpx(HP)]** (Holland & Powell, 1996), plagioclase **[Pl(h)]** (Newton et al., 1980), garnet **[Gt(WPH)]** (White et al., 2007) and melt **[melt(HP)]** (Holland & Powell, 2001; White et al., 2001).

P-T pseudosection for the Cpx-Grt bearing amphibolites in the NCFMASH system is presented in figure 4.2, for the P-T space 0.5 – 1.5 GPa and 500-1000^0 C.

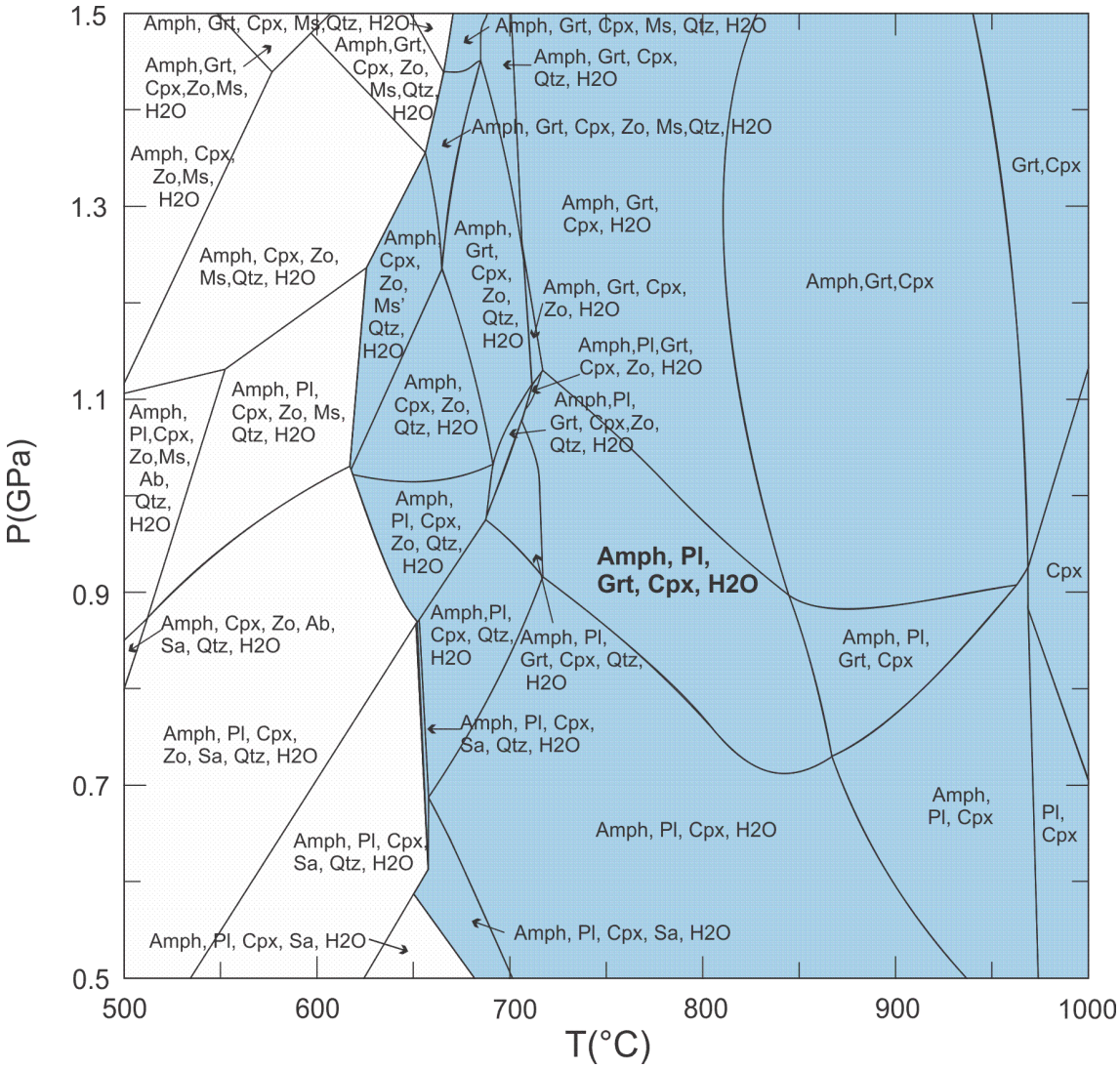

Figur4. 2: P-T pseudosection constructed on the basis of molar proportions of major elements given in table 4.2. Paragenesis written in bold letters coincides with petrographical observations. All fields with blue base have a melt phase present.

There is one paragenesis in figure 4.2 that coincides with petrographical observations:

Amph + Pl + Grt + Cpx + melt + excess H2O

The stability of the assemblage is between 0.7 - 1.1 GPa and 700 – 860 ^{0}C. The field has a lower temperature limit defined by the disappearance of quartz at approximately 710^{0}C and 0.9- 1.05 GPa. Excess water is not present over 850-860 ^{0}C and 0.75 – 0.9 GPa, and this is the upper temperature limit. At temperatures around 700-710 ^{0}C plagioclase is stable up to 1.1 GPa. With a temperature rise to about 850 ^{0}C plagioclase will not be stable at pressures above

0.9 GPa. This breakdown of plagioclase at reducing pressure conditions as temperature increases is the main restriction of upper pressure limit. The occurrence of zoisite, at 1.1 ± 0.1 GPa and 710- 720 ^{0}C, is the upper pressure limit for the lower temperature conditions of the field. In the low temperature area (710- 720 ^{0}C) garnet stabilizes at approximately 0.9 GPa. As temperatures rises garnet stabilizes at decreasing pressures. Minimum P-T condition for garnet stability defines the lower P-T stability for the mineral assemblage at approximately 0.7 GPa and 840 ^{0}C. Melting temperature for the given bulk is between 630-680 ^{o}C, and pressure change seemingly has little influence of the melting process in the selected P-T window.

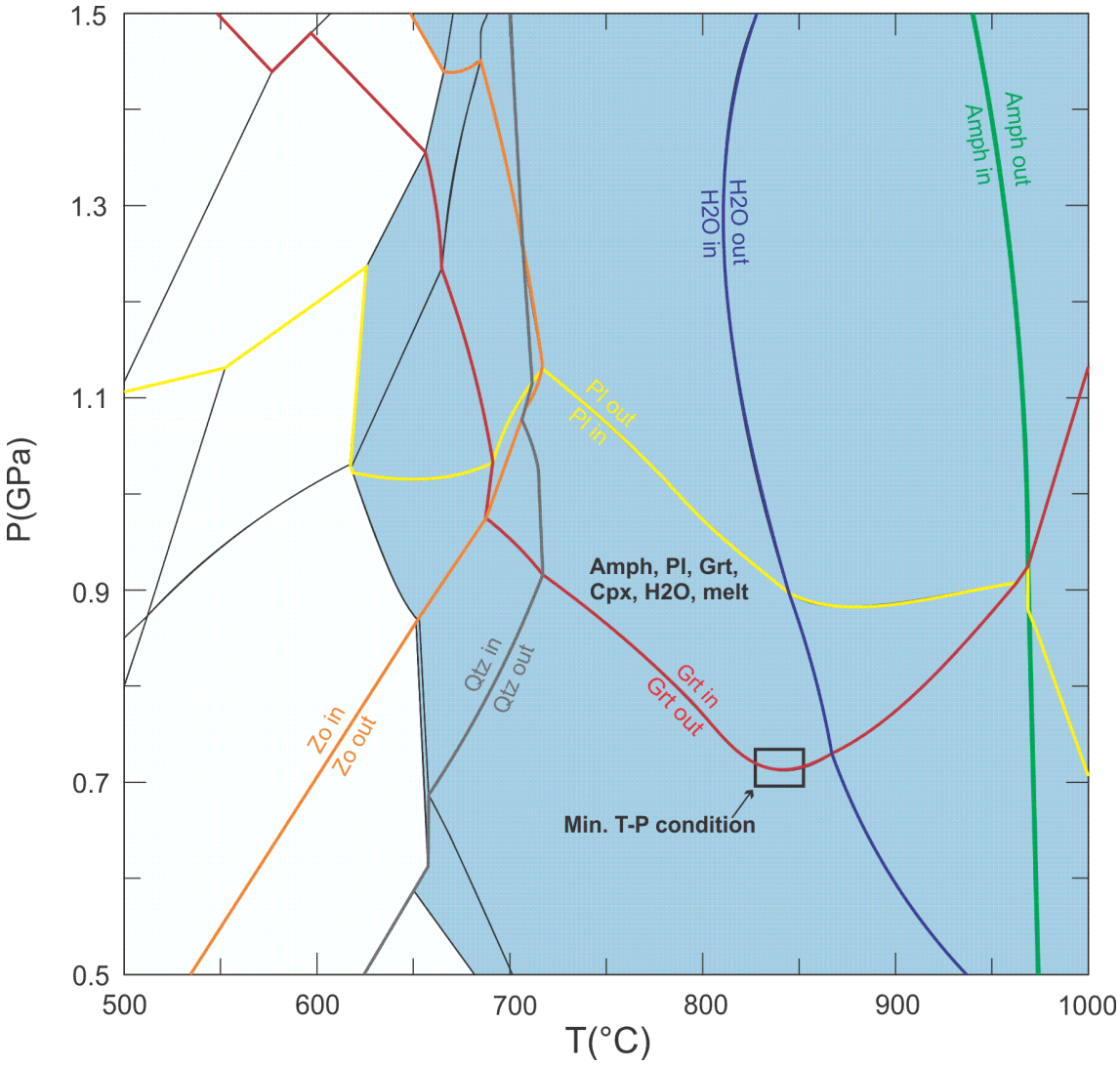

Figure 4.3: P-T pseudosection for the Cpx-Grt bearing amphibolite giving the stability field of the correct paragenesis in bold letters. All fields with blue base has melt phase present. Phase stability lines defining the field are given in colors: Orange= zoisite, grey= quartz, red= garnet, yellow= plagioclase, green = amphibole and blue= H_2O. Black box indicates minimum P-T condition for the stability of the paragenesis.

4.3 Felsic dyke

Table 4.3: Results from XRF- analysis of purple-grey felsic dyke given in average wt% and calculated normalized molar proportions. FeO is calculated from stoichiometry. Loss of ignition is not tested.

Sample 4.24	SiO_2	Al_2O_3	TiO_2	FeO	MnO	MgO	CaO	Na_2O	K_2O	P_2O_5	Tot.
Wt (%)	57,15	24,13	0,06	0,62	0,01	0,34	6,58	7,05	0,35	0,02	96,31
Norm.mol.prop	57,91	14,41	0,05	0,49	0,00	0,51	7,12	6,93	0,22	0,01	87,63

Table 4.4: Results of CIPW-norm calculation for felsic dyke based on bulk composition given in table 4.3.

CIPW 4_24	C	Or	Ab	An	Hy	Ol	Il	Ap
Wt(%)	0,24	2,04	59,65	32,51	1,12	0,57	0,12	0,04

Comments on CIPW norm calculations:

Neither quartz nor nepheline is present in the calculated modal composition of sample 4.24, suggesting that the fresh felsic dyke is silica-saturated.

Pseudosection construction:

P-T pseudosection felsic dyke was constructed from the calculated normal molar proportions of major elements presented in table 4.3, with one modification:

- The small proportion of TiO_2 was set to 0 to simplify the chemical system, and reduce complexity of the pseudosection.

Modification was included when running BUILD. H_2O was added as a thermodynamic component, and the following solution models were used: amphibole **[Amph(DHP)]** (Dale et al., 2000), clinopyroxene **[Cpx(HP)]** (Holland & Powell, 1996), plagioclase [**Pl(h)]** (Newton et al., 1980),, garnet **[Gt(WPH)]** (White et al., 2007) and melt **[melt(HP)]** (Holland & Powell, 2001; White et al., 2001), orthopyroxene **[Opx(HP)]** (Holland & Powell, 1999), omphasite **[Omph(GHP)]** (Green et al., 2007), mica **[Mica(CHA)]** (Coggon &Holland, 2002; Auzanneau et al., 2010).

Pseudosection for the felsic dyke in the NCKFMASH system is presented in figure 4.4, for P-T conditions 0.8- 1.3 GPa and 700-1000 ^{0}C.

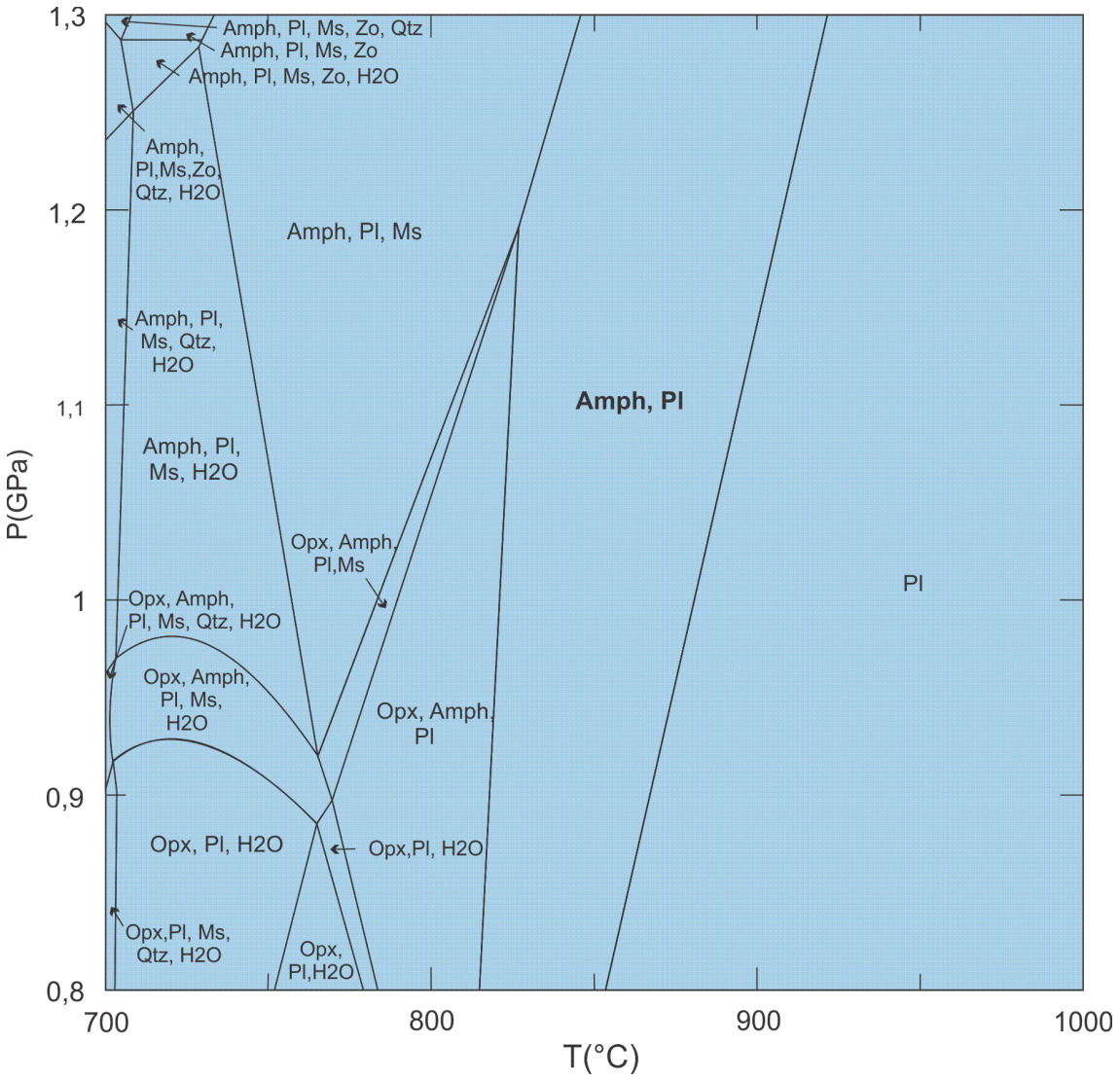

Figure 4.4: P-T pseudosection for felsic dyke constructed from data provided in table 4.3. All fields with blue base includes melt phase. The paragenesis given in bold letters is comparable with the dominating mineralogy identified by optical microscopy.

One paragenesis in the pseudosection presented in figure 4.4 is similar to the petrographical observations:

Amph + Pl +melt

The mineral assemblage is stable over a large field within the given P-T space. P-T range for the stability zone is approximately 820- 920 ^{0}C between 0.8- 1.3 GPa. Upper temperature limit of the paragenesis is defined by the stability of amphibole, which is stable up to 855 ^{0}C

at the lowest given pressure and 920 ^{0}C at maximum pressure conditions. The lower temperature limit is at 820-830^{0}C up to 1.18 GPa. At temperatures below this ortopyroxene, which is not an observed phase, is stable. For high pressure conditions the lack of muscovite in the paragenesis marks the lower temperature limit. Muscovite is not stable over 830- 845^{0}C at 1.18-1.3 GPa. A melt phase is consistently present in the pseudosection because the mineral assemblage is close to primary igneous, which means it exists in equilibrium with the melt it crystallizes from.

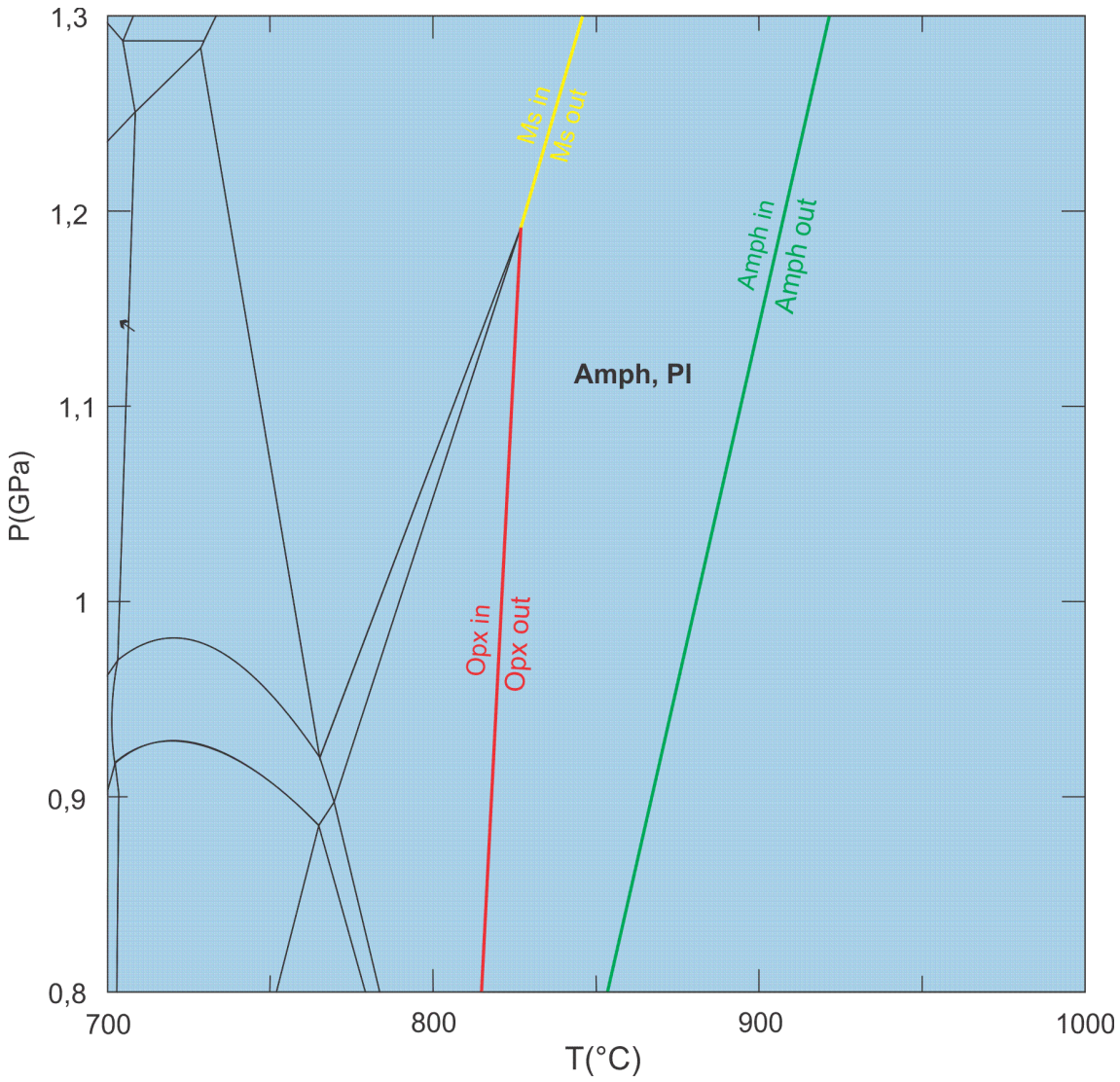

Figure 4.5: P-T pseudosection for the felsic dyke showing the stability field of the correct paragenesis given in bold letters. All fields with blue base has melt phase present. Phase stability lines defining the field are given in colors: red= ortopyroxene, green= amphibole and yellow= muscovite.

4.4 Meta- dolerite

Table 4.5: Results from XRF- analysis of dolerite given in average wt%. FeO is calculated from stoichiometry. Loss of ignition is not tested.

Sample3.5	SiO_2	Al_2O_3	TiO_2	FeO	MnO	MgO	CaO	Na_2O	K_2O	P_2O_5	Tot
Wt (%)	48,70	19,80	0,91	9,40	0,11	3,96	9,77	4,22	0,30	0,34	97,51

Table 4.6: Calculated modal composition of the meta-doleritic dyke from bulk composition given in table 4.5.

CIPW3.5	Or	Ab	An	Ne	Di	Ol	Il	Ap
Wt(%)	1,77	31,6	34,2	2,2	10,1	14,1	1,74	0,79

Comments on CIPW-norm calculations:

The modal composition of sample 3.5 contains nepheline, indicating that the doleritic dyke is silica undersaturated/nepheline normative.

5 Metamorphic development

In this chapter the metamorphic evolution of the selected rocks in the SMC will be discussed on the basis of results and preliminary textural interpretations presented in chapter 3 and 4, together with results obtained by earlier workers. Each rock type is discussed separately in the context of its chemical system, before some considerations and comments are presented for the SMC as a whole. Metamorphism in the felsic- and ultramafic are addressed first respectively through the CNASH- and MFSHTi system, and will serve as a reference point for discussion of metamorphism in the more complex mafic system, NCFMASHTi. Derived P-T implications will be summarized graphically in the context of earlier work at the end of the chapter.

Broks (1985), Krogh et al. (1990), Rindstad (1992), Selbekk et al. (2000), and Indrevær (2011) have all suggested a polymetamorphic evolution for the SMC. Based on field observations, petrography, pseudosection constructions and earlier work the metamorphic evolution of the studied rocks can be divided into:

M1: Peak P-T conditions representing syn-anatexis episode. M1 is regognized throughout the rock complex by partial melting and related reactions in meta-anorthosite, migmatite gneiss and Cpx- Grt bearing amphibolite.

M2: Cooling-phase with crystallization of anatectic melts, both *insitu* and in the felsic dykes, which results in metasomatic reactions between felsic and ultramafic rocks. Amphibole rims on anhydrous minerals (in Cpx-Grt bearing amphibolite) is also seen in relation to the cooling stage.

M3: Further low-grade retrogressive metamorphism, recognized by epidotization in CNASH-system rocks, through chloritization MFSHTi-system rocks, and serpetinization in the ultramafic rocks.

In addition a late short-lived prograde event indicated by antigorite growth in serpentinite will be discussed.

5.1 Felsic rocks

Meta-anorthosite and felsic dykes basically have similar mineralogy giving metamorphic reactions within the same chemical system. The main difference is the plagioclase composition, expressed by anorthite content: 100* (X_{An} / (X_{An} + X_{Ab})), between felsic cumulate rocks and later dyke resulting from anatexis.

5.1.1 Meta-anorthosite

Varying grade of transformation of the meta-anorthosite from the same unit was observed at location 3. Observations can be listed according degree of metamorphism, from least to most altered stages:

1. Coexisting plagioclase and hornblende with preserved magmatic textures
2. Saussuritized plagioclase, which occurs with epidote/clinozoisite and white mica
3. Coexisting plagioclase, granular zoisite, epidote/clinozoisite and white mica

In addition chlorite is present as retrograde phase.

The introduction of hydrous minerals signifies that metamorphic reactions have taken place in the presence of a fluid phase. The most altered samples were collected adjacent to the cross-cutting dykes, while samples with preserved magmatic features were situated in less structural-affected zones. This also suggests that infiltration of hot fluids have played a significant role in the metamorphism of the anorthositic protolith. In order to study the metamorphic paragenesis (3) of the meta-anorthosite in more detail EDS- analysis from Rindstad (1992) have been used. Her results gave a paragonitic composition of the white mica in meta-anorthosite. Thus, the most appropriate field in the pseudosection for the meta-anorthosite is designated by the paragenesis: Zo + Pl +Ep + Pg +(Qtz)[1] + excess H_2O (see figure 4.1).

[1] **Qtz is given in brackets for reasons given in section 4.1.1, p**

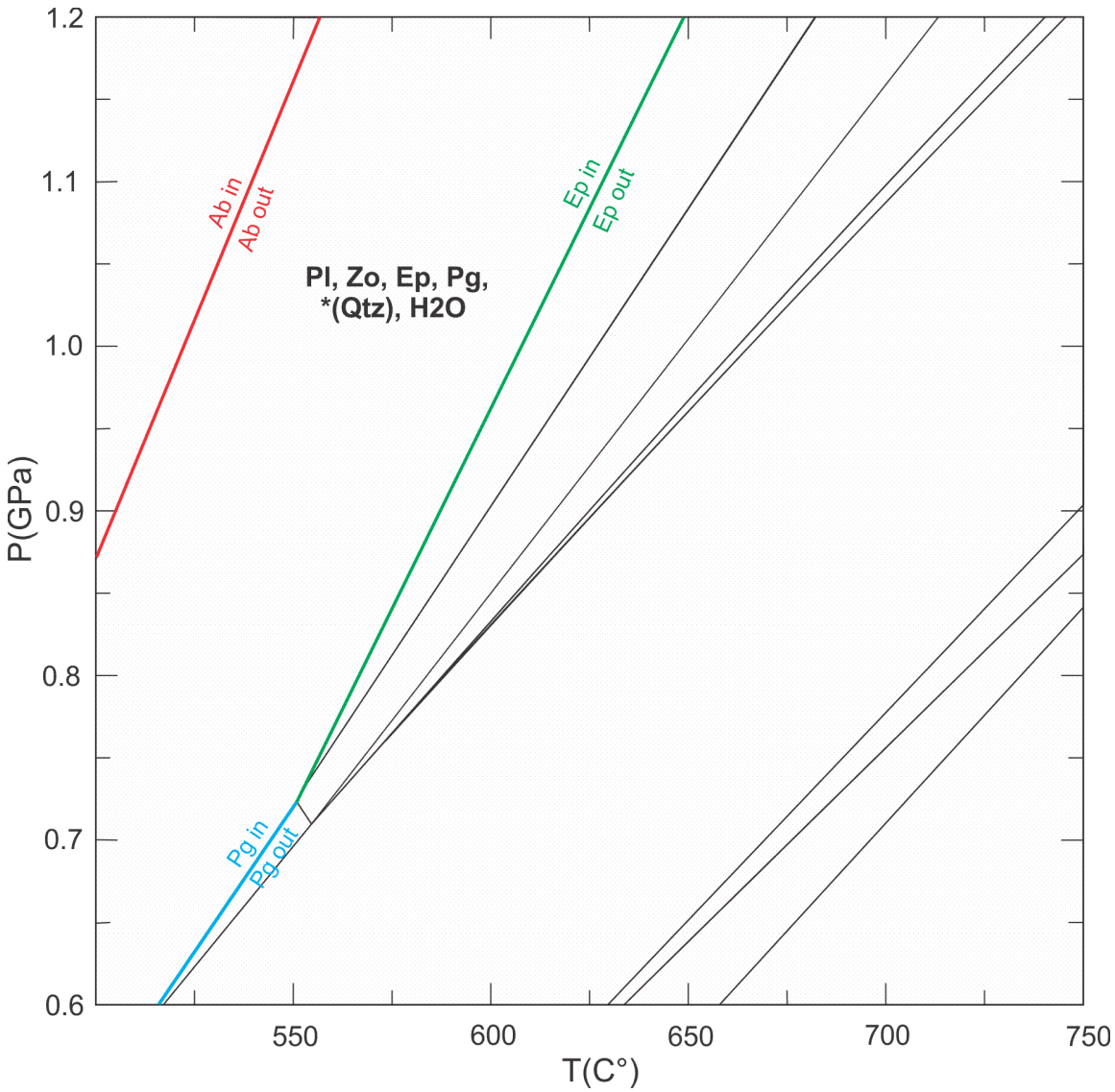

Figure 5.1: Diagram showing phase transition boundaries for P-T pseudosection given in figure 4.1. Upper temperature limits of epidote (green line), albite (red line) and paragonite (blue line) define the stability field of the paragenesis. *Qtz is given I brackets for reasons given in section 4.1.1, p

Figure 5.1 shows that the suggested mineral assemblage with excess H_2O is stable in the P-T range 0.6-1.2 GPa and 500-650^{0}C. From minimum pressure condition of calculation up to 0.73 GPa the paragenesis is stable between approximately 520-550^{0}C. At temperature above this paragonite is not stable for the given bulk composition. Above 0.73 GPa the observed paragenesis is stable between the low-T albite-in curve (straight P-T curve from 500^{0}C - 560^{0}C) and the higher-T epidote-out curve (from 550- 650^{0}C).

There is no melt phase present in the pseudosection, which is not in agreement with petrographical observations. Thin section studies holds evidences of partial melting

(explained in section 3.5). On all scales of study there is a complete lack of amphibole and Mg-rich breakdown products in the most altered samples of the meta-anorthosite, while in least altered samples amphiboles are seen distributed along grain boundaries of plagioclase. Partial melting initiates in plagioclase triple-junctions, which evolve into permeable melt-networks along grain boundaries, therefore it is not unlikely that amphiboles have been transported with drainage (Sawyer, 1999).

The relict textures of melt suggest that the apparent equilibrium assemblage (Zo + Pl +Ep/Czo + Pa + excess H2O) is partly a result of anatexis, where incongruent melting of the anorthitic given by the reaction:

(1) 4 CaAl2Si2O8 +H2O = 2CaAl3Si3O12(OH) + Al2O3 +SiO2

4 anorthite + H2O = 2 zoisite + smelte

(Selbekk & Skjerlie, 2001)

Selbekk and Skjerlie (2001) also suggested that zoisite from as neoformed zosite crystallized directly from melt at 900^{0}C and 1.25 GPa. The granular habit of zoisite which is seen in the meta-anorthisite does however signify an advanced stage in the breakdown process of plagioclase (Matthews & Goldsmith, 1984).

Small amounts of ferric iron (eg. from Fe $^{3+}$ substitution of Al $^{3+}$ or Si $^{4+}$ in magmatic plagioclase (Karsli et al., 2004), or partitioning of Fe^{3+} between amphibole and melt (King et al., 2000)) would explain the development of epidot/clinozoisite. The presence of paragonite indicates retrogression, and therefore the selected field in constructed P-T section (see figure 5.1) is showing the stable mineral assemblage subsequent to anatexis (Zo +Ep/Czo + Pg + Pl). However, the fact that paragonite is zoned and seen texturally to pre/syn- and post date zoisite does not supporting this entirely.

To understand the incongruent melting and breakdown process of plagioclase in more detail a pseudosection was constructed for pure plagioclase with composition $An_{65.}$ Normal molar proportions are given in table 5.1.

Table 5.1: Normal molar proportions of plagioclase An_{65}.

An_{65}	SiO_2	Al_2O_3	Na_2O	CaO	Tot
N. mol. prop	58,75	20,625	4,375	16,25	100

Solution models used in calculations were: feldspar, **[feldspar_B]** (Benisek et al., 2010), white mica **[Mica(CHA)]** (Coggon &Holland, 2002; Auzanneau et al., 2010) and melt **[melt(HP)]** (Holland & Powell, 2001; White et al., 2001). H_2O was added as thermodynamic components.

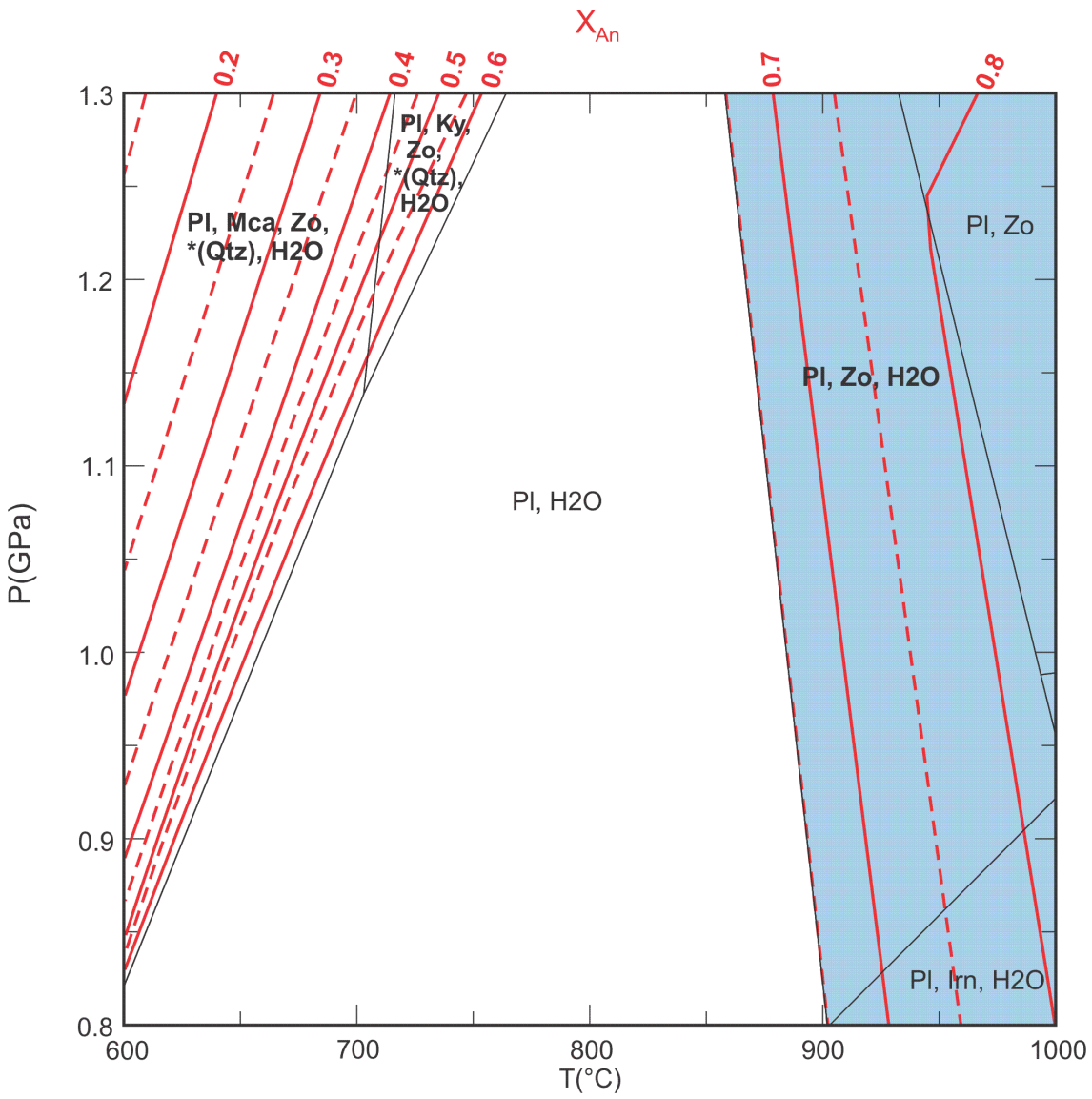

Figure 5.2: P-T-X pseudosection of plagioclase (An_{65}) stability. X_{An} ranges is from 0.15 – 0.8 in the selected P-T window (X_{An} values are given by continuous and dotted red contours, where continuous contours are labeled). Fields with blue base includes a melt phase. *Qtz is given in brackets for reasons given in section 4.1.1, pp.

P-T pseudosection (figure 5.2) illustrates that plagioclase with the chosen composition starts to melt along a straight curve with negative slope from 900-860°C with increasing pressure from 0.8- 1.3 GPa. Progressive incongruent melting enriches the residual plagioclase in the anorthite component and produces Na-rich melt and zoisite. In the solid state plagioclase breaks down at temperature below approximately 700-760°C at high pressures (1.15 – 1.3 GPa), and at lower pressures (0.8-1.15 GPa) from below 600-700°C.In the presence of fluids at temperatures below 720°C and given pressure conditions anorthitic plagioclase breaks down to form zoisite and mica. Retrogressive breakdown of plagioclase results in an increase in the albite component mainly due to formation of zoisite along with paragonitic mica. This means that the reason for paragonite being observed to pre/syn- and post date zoisite, is simply explained by the multi-stage growth of zoisite (where early retrogressive paragonite is overgrown by retrogressive zoisite). It is also possible that some of the white mica is relict, and in that case indicating an earlier hydrous metamorphic event of the cumulate protolith in "unaffected" zones (like where amphibole is present in the clearly magmatic part of the meta-anorthosite).

Selbekk & Skjerlie (2001) suggested that fluids infiltrating the SMC during partial melting of the rock sequence were enriched in sodium. There is no doubt that fluids have actively affected the meta-anorthosite. However, the sodium problem has not been addressed so far. An attempt was made to balance a reaction of anorthitic plagioclase in the presence of fluids with dissolved Na^+:

(2) 6 CaAl2Si2O8 + 2H2O + Na+ = 3 Ca2Al3Si3O12(OH) + NaAlSi3O10(OH)

6 anorthite + 2H2O + Na^+ = 3 zoisite + paragonite

Dissolved sodium in the fluid phase which infiltrated the SMC could have been an additional factor promoting formation of paragonite during breakdown of anorthitic plagioclase. However, the pseudosection (fig.5.2) shows that the assemblage zoisite + paragonite may form without introduction of extra Na. Selbekk & Skjerlie's (2001) experiments is as earlier mentioned performed on material from the Rognsund Intrusion (Seiland Igneouse Province, north-Norway) and the Na addition needed to get a result similar to what is observed in the SMC, may simply be a matter of higher Na in the natural bulk composition of the protolith in the SMC (Selbekk & Skjerlie, 2001).

5.1.2 Leucocratic dykes

The felsic dykes have been described as two separate types based on mineralogical differences, and textural evidences of alteration:

1. Pl + Hbl + accessory minerals - preserved igneous mineral assemblage in purple-grey dyke
2. Pl +Hbl + Zo + Ep/Czo + Mca - metamorphic paragenesis in apparent equilibrium in white dyke

In addition there is retrograde chlorite and late calcite.

The possibility of zoisite, epidote/clinozoisite and/or mica minerals coexisting with melt has already been discussed in section 5.1.1. However, seen as neither epidote-group minerals nor white mica occurs in unaltered dykes they are regarded a result of hydrous breakdown of plagioclase.

The systematic distribution of euhedral-subhedral needles, as inclusions in plagioclase, is interpreted to be a crystallographic orientation relationship between zoisite and the host plagioclase. This type of growth pattern reflects zoisite nucleation on twin boundaries or dislocations in the host grain, and is suggested to have restricted occurrence to when breakdown reaction of plagioclase is <10% complete (Wayte et al, 1989).

In the SMC, inter-dyke composition of plagioclase ranges from An_{15}- An_{50} (Landmark, 1951; Rindstad, 1992; Selbekk et al., 2000). The dykes have generally been studied on the basis of average composition, but sub-division of CIPW-norm calculations from Rindstad (1992) according to dyke type show that normative plagioclase composition varies An_{20}- An_{29} amongst white colored dykes, while purple-grey dykes range in composition from An_{29}-An_{39} (see appendix, table A3a, b). Results from Selbekk et al. (2000) are not differentiated according to dyke-type, and so calculations give a wide range in plagioclase composition, from An_{22}-An_{41}. The close to unaltered dyke from location 4 (sample number 4.24) has plagioclase with andesitic composition, An_{35}. The varying compositional nature of plagioclase between dykes may be a result of:

- An addition in Na during formation of the hydrous metamorphic mineral assemblage (e.g as suggested by reaction (2))
- Varying degree of partial melting in the rock from which melt segregated
- Or most likely a combination of the two

To summarize:

The meta-anorthosite is suggested to have a multi-stage reaction history, where;

- Granular zoisite indicates an advanced stage in the breakdown process of cumulate plagioclase related to the partial melting event, initially taking place at P-T peak of metamorphic conditions. Zoisite in textural equilibrium with Ep/Czo + Pg is a result of break down during retrogression.
- Epidote/clinozoisite may have grown at peak conditions, and during cooling phase.
- Paragonite is suggested to be a breakdown product of the more Na-rich melt-crystallized plagioclase during cooling, as no mica is present in the pseudosection above melting limit. Dissolved sodium in infiltrating fluids could have been a supplementary source for paragonite formation.

Felsic dykes formed due to anatexis of the SMC, and has experienced less extensive metamorphism. The zoisite in the metamorphic felsic dykes is suggested to be a secondary feature representing growth during cooling stage. The metamorphic history is seemingly only retrogressive.

5.1.3 P-T implications for the felsic rocks

Field- and geochemical investigation of the SMC by Selbekk et al. (2000), states that partial melting took place under H_2O-saturated conditions. Based on melting experiments (of the nepheline normative Rognsund Intrusion) Selbekk & Skjerlie (2001) suggested that felsic dykes in the SMC crystallized at 900^0C and 1.25 GPa.

Zones within the same meta-anorthositic unit interpreted to have different metamorphic evolution (1-preserved magmatic features, 2-evidences for partial melting and 3-high grade metamorphism) lead to an attempt of constructing a pseudosection from the bulk composition of a possible protolith. The aim was to constrain possible conditions for anatexis of the SMC

anorthosite, and investigate which minerals theoretically could coexist as an equilibrium paragenesis together with a melt phase at anatexis conditions. Well aware of the uncertainties related to modifications of compositions caused by recrystallization fluid-infiltration, calculation were done on the basis of major element oxide abundances of the SMC meta-anorthosite obtained by Rindstad (1992), given in table 5.2. Plagioclase normative composition of selected sample (P-11) was ~An 72 (bytownite).

Table 5.2: Bulk- analysis of least altered anorthosite (sample number P-11) obtained by Rindstad (1992) given in average wt% and calculated normalized molar proportions. FeO is calculated from stoichiometry. Loss of ignition is not tested.

P-11(Rindstad)	SiO_2	Al_2O_3	TiO_2	FeO	MnO	MgO	CaO	Na_2O	K_2O	P_2O_5	Tot.
Wt (%)	48,54	28,37	0,21	1,53	0,03	1,18	13,35	4,07	0,38	0,03	97,69
Norm.mol.prop	51,57	17,76	0,00	1,22	0,00	1,87	15,15	4,19	0,26	0,01	92,03

Considerations prior to calculation and procedure for constructing of pseudosection coincide in detail with what was explained for the meta-anorthosite (see section 4.1-pseudosection construction).

Solution models used in calculations was for feldspar**, [feldspar_B]** (Benisek et al., 2010) , pyroxene **[Omph(GHP)]** (Green et al., 2007), amphibole **[Amph(DHP)]** (Dale et al., 2000), garnet **[Gt(GCT)]** (Ganguly et al., 1966), white mica **[MaPa]** (Bucher-Nurminen et al.,1983), epidote **[Ep(HP)]** (Holland & Powell, 1998) and melt **[melt(HP)]** (Holland & Powell, 2001; White et al., 2001). H_2O and O_2 were added as thermodynamic components.
The topological relationship of phases in the NCFASHO chemical system for sample P-11(Rindstad, 1992) is given in figure 5.2, for the P-T window 0.9-1.3 GPa and 650-900 ºC.

Result is given in figure 5.2 below.

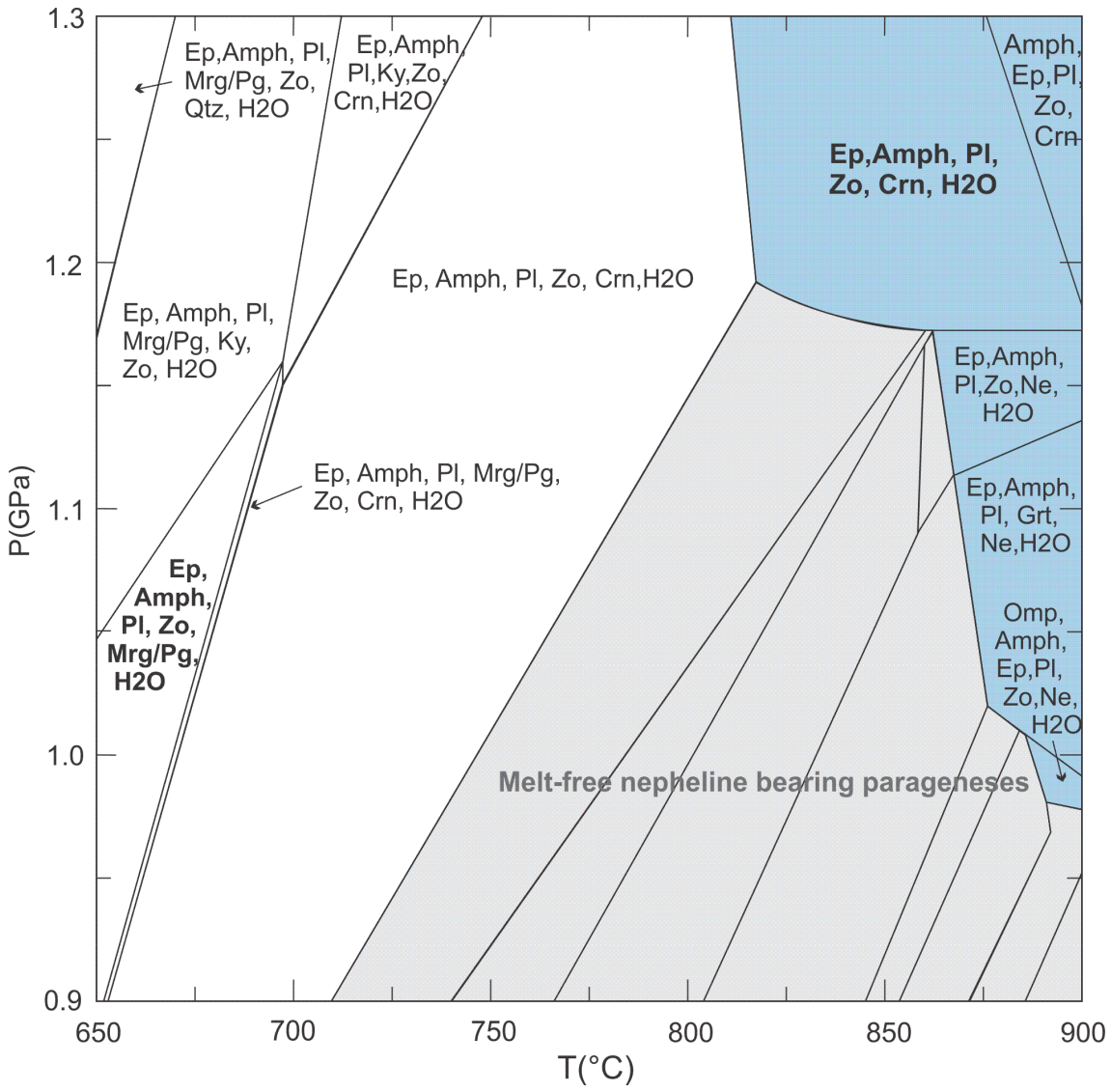

Figur 5.2: P-T pseudosection constructed on the basis of molar proportions of major elements given in table 5.1. All fields with blue base have a melt phase present. Suggested field for partial melting of the SMC protolith, and field for retrogreesed felsic dykes is given in bold letters.

Figure 5.2 illustrates that melting of the possible protolith initiates at approximately 1.18 GPa in the temperature interval 800-850 ^{0}C. With rising pressure in the given temperature range melt would be in equilibrium with the paragenesis: Pl + Ep/Czo + Amph + Zo + Crn+ excess H_2O. Wt (%) of corundum within the given field varies between 0.55 and 1.25 (obtained by running the analytical sub-program of Perple_X 6.6.6 - WERAMI). Thus, it can be regarded an accessory mineral in most of the field, and could easily have been missed during material sampling. Recent work by Kullerud et al. (2012) holds evidences of corundum in the equilibrium assemblage resulting from the migmatization process on a mainland locality within the SMC (Nordfjellet).

Mineral assemblage of least altered dyke type is stable over large field in its respective pseudosection:

- The mineral assemblage Pl+ Amph + melt (least altered dyke) has maximum temperature along a straight positive slope approximately 820- 920 ^{0}C between 0.8-1.3 GPa, in the NCKFMASH-system (see figure 4.4). This coincides with Selbekk and Skjerlie (2001) experimental estimation of melting conditions (900^{0}C and 1.25 GPa).

The paragenesis of the metamorphic felsic dykes is seen as a stabile mineral assemblage in the pseudosection for the possible protolith of the meta-anorthosite:

- For the selected P-T window in the NCFASHO-system the stability of Pl+Amph+ Zo + Ep+ Mca + excess H_2O is within the pressure range 0.9-1.05 GPa at 650^{0}C, and the maximum point is at 1.15 GPa and 675^{0}C (see figure 5.2). This coincides with conditions implied for the retrogressive mineral assemblage of the meta-anorthosite.

5.2 Ultramafic rocks

5.2.1 Amphibole-rich rock

Amphiboles are stable in a wide range of P-T conditions and chemical environment in magmatic and metamorphic rocks. Studies of metamorphism in amphibole dominated rocks makes the understanding of compositional zoning and trace element partitioning an important tool. The chemical zoning and overgrowth in amphiboles can be seen as a record of changing metamorphic conditions, which can be recognized through pleochroic characteristics (Binns, 1965; Bard, 1970; Raase, 1974). Changing optical properties, color and pleochroism, in amphiboles is primarily associated with iron- and titanium content, and transfer involving charged iron- and titanium ions (Faye & Nickel, 1970). An attempt has been made to interpret the observed zoning in amphibole-rich rock (see descriptions, section.3) in the context of metamorphic evolution. Rindstad (1992) classified hornblende in amphibole-rich layers to be ferro-pargasitic referring to Leake (1968). The protolith of the amphibole-rich ultramafic rock is unknown.

Optically differentiated amphiboles addressed according to pleochroism:

Non-pleochroic/colorless: Tremolitic amphibole (Mg-rich calcic amphibole).

Pale green-green: Actionolitic amphibole (Fe-rich calsic amphibole).

Amphiboles in the actinolite series are subdivide by ferro-actinolite content [(Fe + Mn)/(Fe + Mn + Mg)] into tremolite (0-10%), actionlite (10-50%) and ferro-actinolite (50-100%). Color gets darker with increasing Fe content (Hellner & Shurmann, 1966).

Green to olive green, yellow to green-brown: Variations of hornblende

For Ca-amphiboles there is a general link between increasing metamorphic grade and increase in Mg/(Mg+Fe), Ti, Al, Na and K content along with decrease in Si and total Fe+ Mg+Mn±Ca (Engel & Engel, 1962; Jenkins,1983; Ernst & Liu, 1998).The color parallel to elongation of hornblende changes from blue-green, green, brown-green to brown with increasing metamorphic grade. The color change is regarded to reflect a steady increase in Ti content relative to Fe as metamorphic grade increases (essentially a function of rising temperature)(Binns, 1965; Raase, 1972).

Amphiboles are chemically complex, and stability is strongly dependent of bulk composition, but in general there is a transition from actinolite series at low T-P conditions (greenschist to lower amphibolites facies to Ti-paragasite (Na-Ca-Ti hornblende) at pressure higher than 10 kBar. The stability field of amphiboles is extended to higher temperatures as the content of pargasite increase (Oba,1990). Some general stability limits of amphiboles:

Actinolite series lower stability: 375^0C at 1000 bar water pressure, 50 bar CO2 pressure (Hellner & Shürmann, 1966).

Tremolite upper stability: 800^0C at 0.5 GPa, 830^0C at 1GPa (Boyd, 1959).

Pargasite stability: 0.5 GPa- 955^0C, 1 GPa- 1045^0C (Boyd, 1959); 1042 ^{0}C at 0.45 GPa, 1053^0C at 0.75 GPa (Hollaway,1973).

The yellow-brown core seen in some amphiboles signifies higher Ti-content than its paler greenish tremolitic-actinolitic rim, which is an indicative for decreasing metamorphic grade. Prismatic amphiboles with green to green-brown hornblende core and tremolitic rim are interpreted to be a result of growth with decreasing P-T condition. Unzoned acicular actinolitic-tremolitic amphiboles with cross-cutting relationship to other amphiboles are suggested to be the latest stage of amphibole growth. The amphibole zoning together with late

chlorite growth on the expense of phlogopite gives an overall impression of a retrograde evolution in the rock. Rutile around the rim of opaque minerals is also interpreted to be late growth. Late growth of tremolite signifies low Fe/Mg in the bulk, which also means favorable conditions for rutile formation. The assemblage rutile + Fe-Ti oxide (e.g Ilmenite) + chlorite + indicates reducing environmnent (Spears, 1993).

5.2.2 Serpentinite

Parts of the rock sequence in the SMC are partially or completely altered to serpentinite, allowing insight in the metamorphic process of a retrogressive hydration of ultramafic rock.

Hydration has caused breakdown of olivine to serpentine-group minerals. In least altered state the unknown protolith is recognized through relict olivine ± green spinell, commonly characteristically fractured with infilling of chrysotile and magnetite. Pure olivine aggregates has been replaced by pseudomorphs of iddingsite with increased degree of alteration. Toward the most complete stage (close to reaction zone) antigorite + chrysotile + talc + opaque minerals becomes the apparent equilibrium assemblage.

Rindstad (1992) analysed relict olivine from partly serpentinized ultramafic rocks on the Tromsø Island. Her results gave $XFo_{(86)}$, with minor Mn (see appendix). Observed metamorphic paragenesis together with Rindstad's analyses justifies a suggestion of hydrous breakdown of olivine in the MFSH-system, where the fayalite component of olivine generally substitute for Mg or Al in serpentine-minerals (e.g Fe-lizardite), or is redistributed by partial oxidation into separate opaque phases (Moody, 1976). The forsterite component may decompose through the irreversibel metastable reaction:

(3) chrysotile + brucite = 2 forsterite + $3H_2O$ (Johannes, 1968; Evans 1977)

This gives a generalized hydration reaction which decomposes the ultramafic protholith through serpentinization under low temperature conditions (50-300^{0}C):

(4) MgFe olivine + H_2O = MgFe- serpentine + MgFe- brucite + magnetite + H_2 (aq) (Evans, 2010)

where brucite is a Mg-hydroxide which often cannot be indentified in thin section studies in serpentinite because of intimated growth with chrysotile, or very small grain size (Moody, 1976).
Magnetic character of the rock together with equation (4) supports that opaque minerals of the serpentinite are magnetite.

Above 300^0C, antigorite forms on the expense of chrysotile/lizardite or olivine. Intergranular relations show that antigorite has grown as the latest serpentine-mineral, and so it is likely that antigorite is a result of decomposition of the low-temperature serpentine-minerals, e.g through the reactions:

(5) 17 chrysotile/lizardite = antigorite + 3 brucite (Evans, 1977)

Chrysotile seen in the rock exists metastably. The magnetite is believed to be inherited from a low-temperature serpentinization event as diffusion rates are magnitudes higher during antigorite serpentinizations (approximately 400-600^0C), which eliminates the need to precipitate magnetite with elevated temperature (Evans, 2010).

The ultramafic protolith seemingly has experienced an event of elevated heating during serpentization, where phase transitions are interpreted to be a result of multi-stage reactions in the MFSH-system from low-temperature sub-greenschist facies to upper greenschist /lower amphibolite facies metamorphism.
In contact with the felsic dykes the metamorphic ultramafic rock has been modified by metasomatic processes, which leads to the next topic of discussion- the reaction zones.

5.2.3 Reaction zones between serpentinite and felsic dykes

Development of reaction zones on interfaces between serpentinite and felsic dykes is regarded to be a result of bimetasomatic reactions, often referred to as “blackwall alteration” (Carswell et al., 1974). Reaction bands are local, and restricted to the contact surface between the two lithologies. In the SMC reaction zones can be regarded as diffusive mass-transfer between the two chemical systems MFSH and CASH, where there is local equilibrium only between minerals and fluid within each band.The driving force is a gradient in chemical potential between the two compositionally different lithologies, which leads to diffusion of components in the presence of a fluid phase with the aim to minimize free energy (Larikova & Zaraisky, 2009). As metasomatic reactions usually are short lived, isothermic and isobaric the main aim has been to study diffusion of major phase forming elements based on mineralogical transitions across the reaction zone.

Uncertainties are many when investigation metasomatic rocks, but the studied reaction zoned has seemingly developed as a result of two-way diffusion of Al and Ca from the felsic dyke and Mg and Fe from the meta-ultramafic rock. An attempt was made locate the critical factors of diffusion in this setting from the preserved “frozen” phases in the zoned/banded sequence.

Diffusion of elements across the reaction zone is primary controlled by the free energy released by a particular replacement reaction as opposed to the free energy of possible alternative replacement reaction. If a reaction allows an element to sit in the lowest free-energy configuration possible (for the given system and P-T conditions) the diffusion of the element terminates, giving a diffusion front (Carswell et al., 1974).

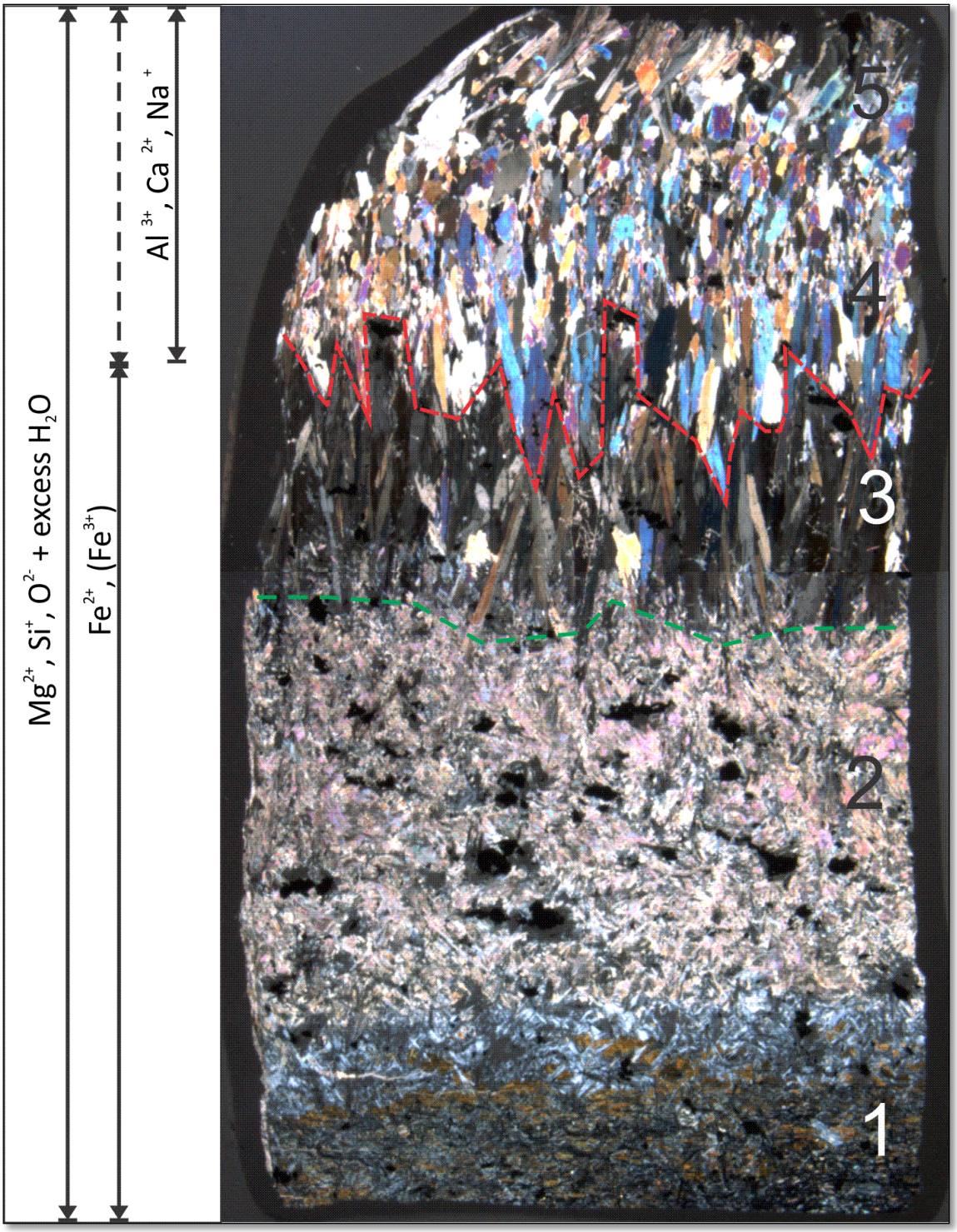

Figure 5.3: Suggested diffusion model for metasomatic reaction zone in the contact between serpentinite and felsic dyke. Mg, Si, O, H2O is present through the whole zone. Fe might be present across the whole reaction zone, or may terminate at the diffusion front of Al, Ca, Na (see main text for more detail).

- - - - approximate diffusion front of Al, Ca, Na. Might also be the initial contact of the two original litologies.

- - - - marks boundary for loss of magnetism, which might indicate oxidation of magnetite.

Comments to figure 5.3:

All zones have hydrous- , silicate- and magnesium phases, and so water, Si and Mg are not regarded to be critical components in the metasomatic sequence. This may be due to abundance of the components, element mobility and T-P restrictions for phase formation/stability during metasomatism (Larikova & Zaraisky, 2009).

Iron may also be present in all zones, rather certainly as a component in opaque minerals in zone 1-4, but possibly also in amphibole in zone 4-5. The magnetic character of the opaque minerals is lost in the transition from zone 2-3, even if occurrence of opaque minerals is continuous through zone 1-4. This may be due to oxidation of magnetite to hematite, indicating oxidizing conditions. In the oxidized state iron does not go into Al free-amphiboles, which is in agreement with observation of anthophyllite and tremolit/actinolite in zone 1-3. However, in zone 4, hornblende is present which defines the Al diffusion front. The occurrence of hornblende coincides with a decrease in opaque minerals. This may be because ferric iron is allowed in the crystal structure of hornblende in small amounts, or simply because less Fe is available as it is further from the meta-ultramafic source rock (all diffusive iron has been consumed).

The calcium diffusion front and aluminum front are unambiguous, and terminates with the occurrence tremolite/actinolite in the transition between zone 3 and 4.

The silica flux is not easily understood as excess silica is not expected, seen as all parts of the SMC investigated so far has shown to be silica-undersaturated or saturated. A possible source of Si from the MFSH-system by breakdown of the fayalitic component of olivine with excess water, producing magnetite and silica whit excess water:

(6) $3Fe_2SiO_4 + H_2O = 2Fe_3O_4 + 3SiO_2 + H_2O$

Fayalite + water = Magnetite + Silica + excess water

(Frost & Beard, 2007)

However, Si from this reaction is likely to be consumed by the simultaneous reaction that decomposes the forsterite component to chrysotile at low T, or talc at elevated temperatures (which is expected as reactions are related to the cooling of intrusions).

(7) $3Mg_2SiO_4 + 5SiO_2 + H_2O = 2Mg_3Si_4O_{10}(OH)_2$

Forsterite + Silica + water = Talc

(Frost & Beard, 2007)

Seen as silica is a phase component in rocks on both side of the reaction zone, it is an available component which can contribute to form new phases during metasomatism, and so it might not be a silica flux in fluids across the whole reaction zone.

The serpentinite was in section 5.2.2 suggested to be a result of serpentinization with a related increase of temperature (antigorite beeing the latest serpentine mineral). If the ultramafic was metamorphosed prior to metasomatism, the talc dominated zone (zone 2) could partly be a result of breakdown of Mg-Fe serpentine through reaction 6;

(8) $(Mg,Fe)_3Si_2O_5(OH)_4 + H_2O + O_2 = 0.25Mg_3Si_4O_{10}(OH)_2 + 0.5Fe_3O_4 + H_2O + 0.25\ Mg^{2+}$

serpentine + water + oxygen = talc + magnetite + water + free magnesium

If relict olivine still was present when metasomatism occurred the talc-rich zone is most likely a combination of reactions (6), (7) and (8).

Brucite which has been mentioned as a possible product of serpentinization through reaction (5) has a simple chemistry, and could easily contribute to the growth of talc, magnetite of simply dissolve and go into solution (giving free magnesium- and iron ions).

If relict olivine was present during metasomatism it is worth noting that:

(9) Talc + Forsterite = Anthophyllite + H_2O (Marocchi et al., 2009)

Considering the bulk chemistry of the felsic dyke Na diffusion is expected. Hornblende is the sodium hosting phase in the reaction zone, and the Na front in regarded unambiguous with the transition between zone 3 and 4, where hornblende gives way to anthophyllite or tremolite/actinolite.

Interpretations where diffusion fronts of Ca, Na and Al coincides with the clear decrease of opaque minerals leads to the suggestion that this is the position of the original contact between the two lithologies. If that case the main diffusion has been from the serpentinitic side of the reaction zone.

5.2.3 P-T implications for the ultramafic rocks

Talc, chlorite, hornblende and actinolite/tremolite are all stable over large P-T intervals, which leave anthophyllite and as the most useful phase for implying P-T condition of the metasomatic reaction. In the MSH- system pure anthophyllite would have a restricted stability field between approximately 600^0C and 800^0C at pressures below 1.2 GPa (Chernosky et al., 1985). Studies by Marocchi et al. (2009) showed that lowering of the anthophyllite activity (Fe2+ - Mg substitution) gave a much wider stability field, from approximately 400- 1000^0C at 1.5 GPa.
To help constrain the P-T window it would be helpful to construct pseudosections from the mineral assemblages in the polymineralic transition bands in the reaction zone, however it is beyond the scope of this thesis. The chloritization of the amphibole rich ultramafic rock and the serpentinization has given the rocks an extensive retrogressive expression. However, as mentioned there are aspects of the serpentinitic rocks which are somewhat anomalous and will be further discussed in chapter 6.

Low-T serpentine implies very low temperatures during retrogression. The chrysotile-antigorite transition is approximately 280°C at pressurs below 20 kbar (Auzende et al. 2006). In the SMC late antigorite signifies elevation in temperature after development of the low-grade serpentine minerals. Some considerations on whether this is a result of the temperature rise caused by intrusion of the numerous felsic dykes (meaning low-temp serpentization would predate migmatization), or if it is a later phenomenon related to the regional Caledonian orogenic metamorphism has been done:

- The amount of high temperature serpentine (antigorite) increases towards the dykes interpreted as an indicative that the late antigorite formed as a result of intrusive activity. However, the significant temperature rise expected during the intrusive event would have exceeded the maximum temperature limit of chrysotile/lizardite, something that would erase the low-temperature minerals.
- Felsic dykes occurring as strongly deformed, while in other cases without signs of deformation may indicate that intrusion have occurred as several events. Therefore local heating giving antigorite growth after low-T serpentine minerals could be reasonable.

- Preservation of metasomatic reaction bands signifies either that the period of heating in the rock has been relatively short or water access has been restricted, meaning that low-temperature serpentine minerals could have been preserved.

Further discussion is best done in the context of the tectonometamorphic development of the SMC, and will be presented in section chapter 6.

5.3 Mafic rocks

5.3.1 Migmatite gneiss

In the migmatite gneiss there are clear evidences of partial melting and insitu crystallization. Micro-textural interpretations given in table 3.3, makes it likely that Hbl + Pl + Ti is the oldest recognized paragenesis. Subsequent metamorphism is mainly recognized through the hydrous phases: Ep/Czo + Zo. The granular habit of zoisite is, like explained for the meta-anorthosite(in section 5.1.1), is regarded to be a result of a more advanced stage in the plagioclase breakdown process seen in relation to partial melting at high P-T conditions (Matthews & Goldsmith, 1984). The embaying character of Ep/Czo may be related to the compositional differences of relict plagioclase versus insitu crystallized plagioclase, based on that in places is a connetion/network of Ep/Czo sourrunding corroded plagioclase. Water release during insitu crystallization could have contributed to plagioclase breakdown in the form of epidote/clinozoisite and zoisite.

The chemical zoining of epidote minerals, from epidote core to clinozoisite rim (recognized in XPL) reflects small changes in Fe-Al content, which is normal growth zoning resulting from the continuous breakdown of hornblende and plagioclase under epidote-amphibolite facies conditions (Spears, 1993).

5.3.2 Grt-Cpx amphibolites

Internal paragenesis in garnet, Amph +Pl +Cpx+ Aln ± Ttn ±Op, represents the least hydrated state recognized in the amphibolites. Amphibole is the only hydrous phase present. Amph + Pl + Grt + Cpx ± Ttn ±Op + melt and excess water signifies high temperature upper amphibolites facies metamorphism.

The partial melting event indicates peak P-T conditions. As noted in section 5.1.1 the product of incongruent melting of anorthitic plagioclase is expected to be enriched in the albite component (pure, little alteration), while the residual plagioclase (visually altered by saussurization) is enriched in the anorthite component. Ep/Czo is interpreted to be the main breakdown product of plagioclase arising from the cooling event subsequent to metamorphic peak conditions.

Clinopyroxene still being present in the matrix signifies that the high P-T event was restricted in terms of time or water access. Ep/Czo and hornblende rim around anhydrous minerals signifies a later hydration of the rock. Probably the upper amphibolite facies assemblage retrogrades from H_2O that is relased when melt crystallized (White & Powell, 2002). As earlier noted in section 5.2.1, blue-green hornblende growth around the rim of olive-green hornblende (and in this case also around clinopyroxene) also implies retrograde metamorphism, as the changes in pleochroic color arises from decrease of Ti content relative to Fe with degreasing metamorphic grade, from amphibolite- towards upper greenschist facies (Binns, 1965; Raase, 1972).

The symplectite intergrowth with epidote and quartz often in close relation to garnet and clinopyroxene has similarities to observations in the Grt-amphibolite in the Tromsdalstind sequence described by Krogh et al. (1990). In that case the occurrence was interpreted to be a degradation product of eclogite garnets. An alternative explanation for epidote-quartz symplectite formation, not involving garnet, is expressed by the reaction:

(10) Ep + Mg-Fe Hbl + Qtz → Mg-Fe Cpx+ Pl + Fe^{2+} rich Hbl + H_2O (Schumacher, 1991)

Schumacher (1991) argued that break down of epidote during prograde metamorphism took place through reaction (8) at approximately 665°C and minimum 6.2 kbar. The reversal reaction could explain symplectitic growth of epidote and quartz in close relation to clinopyroxene. It is also consistent with the zoned nature of hornblende, and would support restricted local occurrence of quartz together with epidote.

5.3.3 Meta-dolerite

The bulk and CIPW norms of the meta-dolerite were compared to analytical results from Selbekk at al. (2000) of metagabbro from the SMC. There was a sticking compositional agreement. In addition the meta-dolerite has a silica-saturated signature. It is likely that the meta-dolerite originated from the same magma source as the metagabbro.

The oldest recognizable mineral assemblage in the meta-dolerite is: Pl + Hbl + Zrn + Aln + Op ± Ttn

The green-brown (type 1) hornblende is suggested to be an original doleritic mineral, aswell as its allanite, titanite, zircon, opaque and plagioclase inclusions. The blue-green variety of hornblende, often around the rim of type (1) indicates retrogressive growth (Binns, 1965; Raase, 1972).

Another rimmed mineral is allanite (when occurring outside hornblende), which is linked to the epidote group by coupled substituition of REE3+ and ferric iron for calcium and ferrous iron in epidote, and for calcium and aluminum in clionozoisite (Giere and Sorensen, 2004). During igneous formation of allanite the RRE content decreases during crystallization, giving a rim of epidote/clinozoisite. However, textural relations in the meta-dolerite give reason to believe that there is a metamorphic reaction history producing the rim around allanite. Often the rim is symplectitic and intergranular boundaries towards hornblende and plagioclase are complex. Sometimes hornblende seemingly is overgrown by the rimmed allanite. Texturally symplectites resemble the ones in the Grt-Cpx amphibolite. However, the host mineral is generally clinozoisite rather than epidote and worms are seemingly plagioclase. Sometimes the symplectites are pseudomorphs textures where both the host mineral and the vermicular mineral are epidote/clinozoisite. Titanite often accompanies these textures as a late phase. In the contact between the SMC and the Tromsdalstind sequence Indrevær (2011) described a similar feature which he related to the breakdown of plagioclase. Carswell et al. (2000) described and linked epidote/clinozoisite with plagioclase worms or pebbles to be a product of decomposition of sodic pyroxene. Seen as neither garnet nor pyroxene is observed in the meta-dolerite the reaction history creating the symplectites is best justified by a simplified unbalanced reaction based on observations:

(11)Hbl^1 (Ti-Al enriched) + Pl^1 + Aln +H2O = Hbl^2 (Ti-Al depleted) +Pl^2 + Ep/Czo +Ttn

Hbl^1 + Pl^1+ Aln from the doleritic protolith breaks down in the presence of fluids to less Ti-Al rich hornblende[2], plagioclase[2], progressively more Al-rich epidote/clinozoisite and titanite. Plagiocalse [2] is expected to be less Ca-rich than reactant plagioclase because crystallization of epidote/clinozoisite around allanite consumes Ca. Ti-Al reduction in hornblende as a result of the continuous reaction is signified by change pleohroism. With decrasing metamorphic grade less Ti goes in to the mineral structure of hornblende (Binns, 1965; Raase, 1972), and it is not uncommon to see precipitation of titanite as a result of this (Spears, 1993). Phase transition of hornblende and plagioclase according to reaction (9) is continous, and indicates retrogressive metamorphism from amphibolites facies to epidote-amphibolite facies (Spears, 1993).

Another sign of metamorphism in the dolerite rutile rim around opaque minerals, suggested being a result of oxidation alteration of ilmenite (Temple, 1966).

5.3.2 P-T implications for the mafic rocks

Evidences of partial melting, relict anhydrouse phases and the presence of high P-T mineral assemblages signify that the mafic rocks have experienced high grade metamorphism. Partial melting occurs at temperatures between 625-675^{0}C, and 0.5-1.5 GPa.

Pseudosection for the Cpx-Grt bearing amphibolites gives minimum P-T stability for the mineral assemblage, Amph + Pl + Grt + Cpx + melt with excess H2O, at approximately 0.7 GPa and 840 ^{0}C. Maximum pressure stability of the paragenesis is 1.1 GPa at approximately 720^{0}C, and maximum temperature 860^{0}C at about 0.72 GPa. Maximum temperatures are well above the amphibole- granulite facies transition, but evidence of a granulite facies mineral assemblage is lacking. Subsequent to P-T peak conditions mafic rocks has experienced hydrous retrogressive metamorphism. All three rock types have preserved evidences of retrogressive reactions that can be related to lower amphibolites/ epidote-amphibolites facies conditions.

5.4 Correlations

Before considering the tectonometamorphic evolution of the SMC the P-T constraints derived through pseudosection constructions was graphically compared with the metamorphic evolution implied by Rindstad (1992), Selbekk & Skjerlie (2001) and Kullerud et al. (2012). Some comments on structural elements useful for tectonometamorphic interpretation of Tromsø Nappe and Nakkedal Nappe are summarized briefly at the end of this section.

P-T correlation:

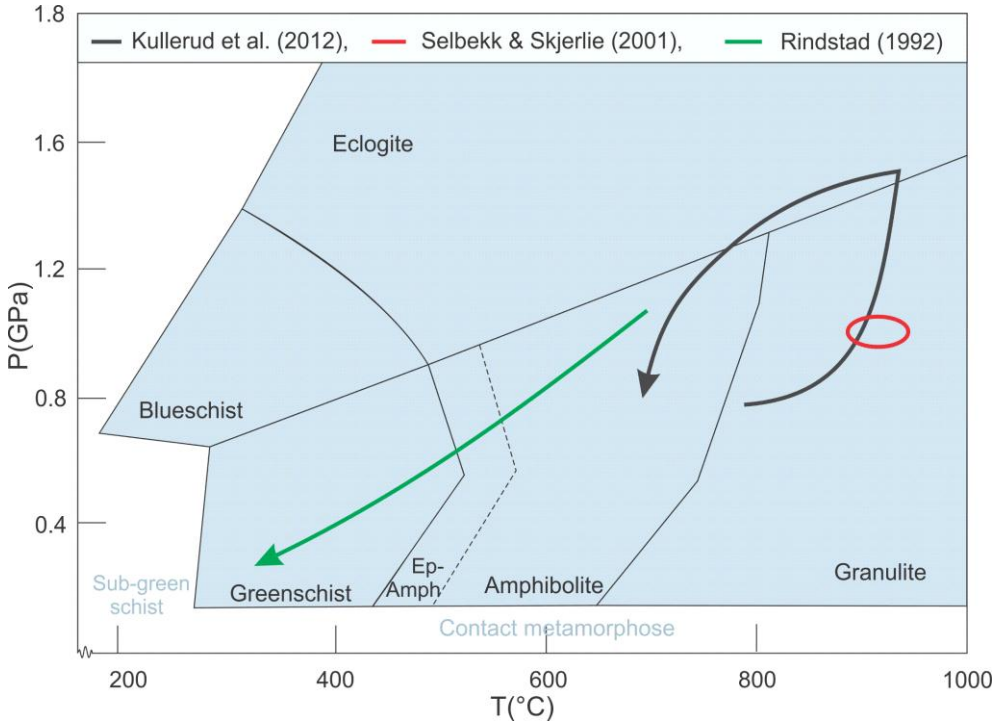

Figure 5.4: Comparison of earlier work in the SMC. P-T path by Kullerud et al.(2012) is based on psedosection-modelling of sampled material from the SMC. P-T constraints bySelbekk & Skjerlie (2001) is based on melting experiments of the Rongsund Intrusion. Rindstad's (1992) P-T estimations are constrained by geothermobaromertic calculations on sampled material from the SMC.

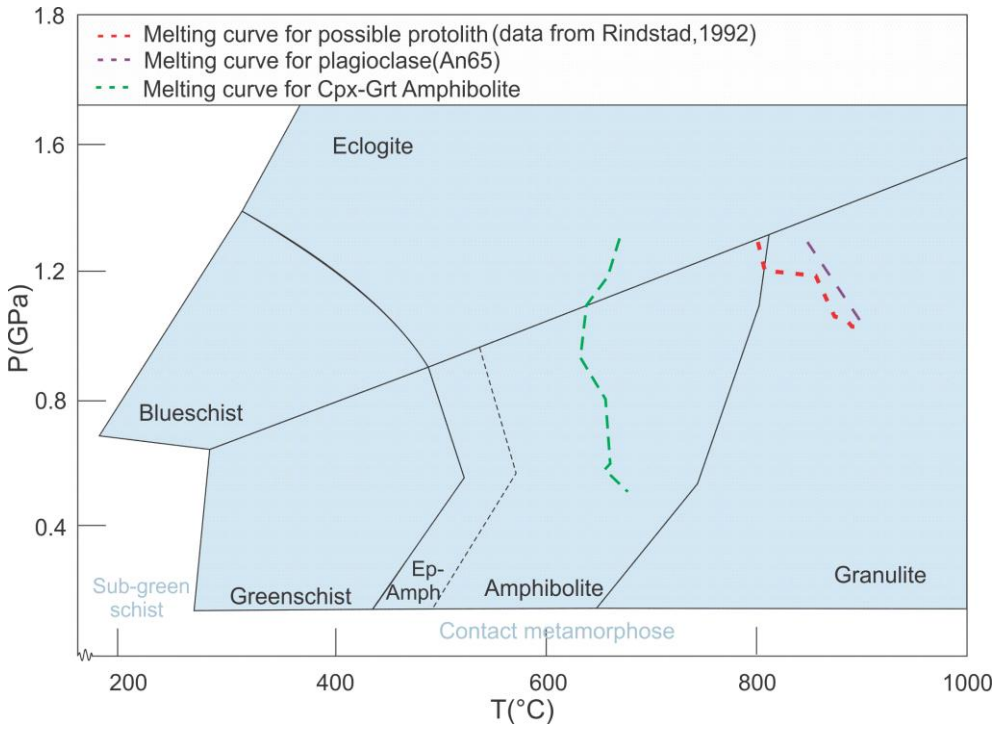

Figure 5.5: Diagram illustrating melting conditions for Cpx-Grt bearing amphibolite, possible anorthositic protolith and pure plagioclase (An_{65}) derived by pseudosection construction.

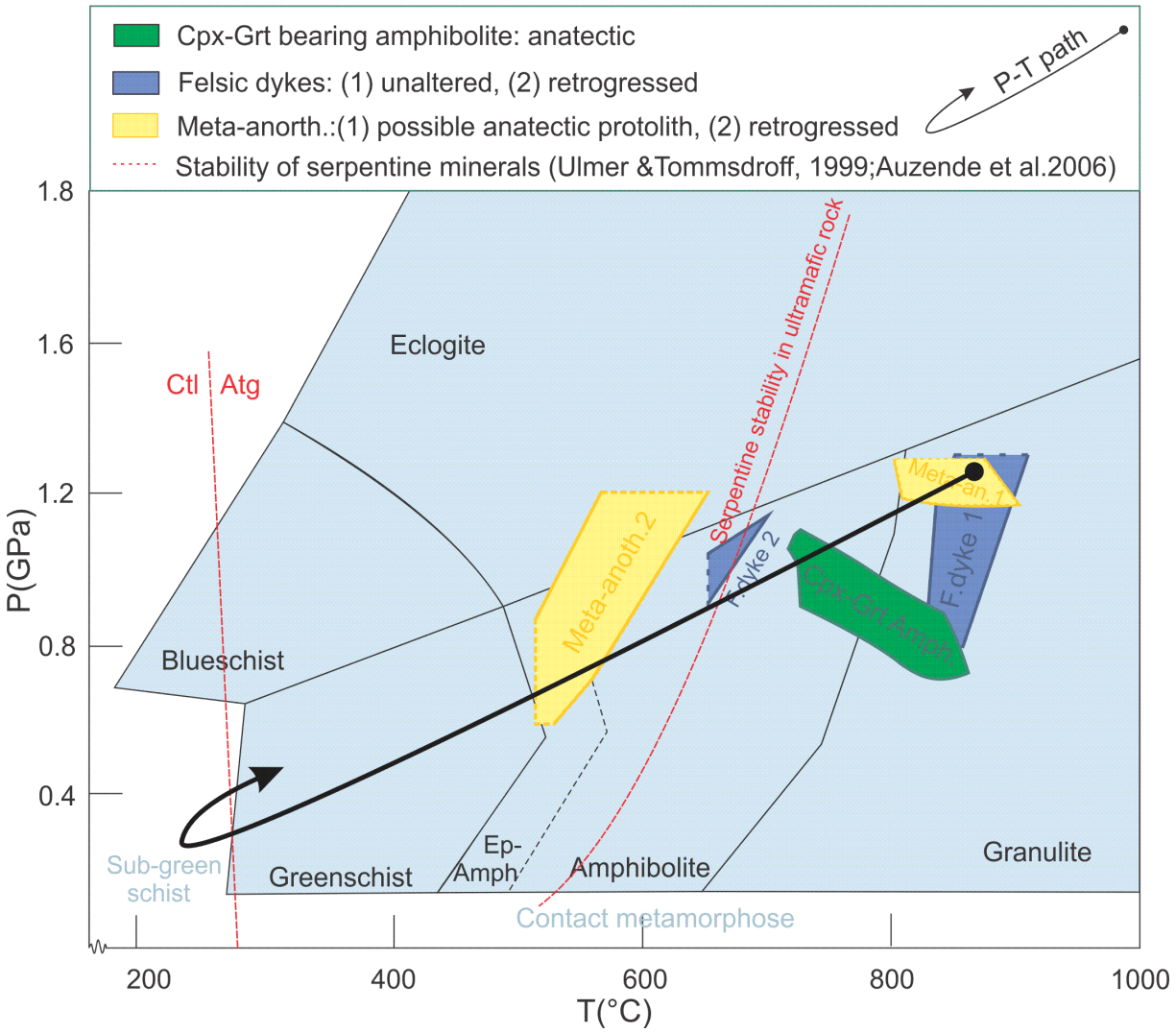

Figure 5.6: Diagram with suggested P-T path for the metamorphic evolution of the SMC based on the shown P-T constraints for meta-anorthosite, Cpx-Grt beraing amphibolite and felsic dykes. Rock type stability field corresponds to their respective pseudosections in chapter 4 and 5. Dotted lines on stability fields indicate restriction due to selected P-T interval for calculations. Late prograde event is based on metamorphism in ultramafic rocks (see section 5.2.2 and 6.2 for details). Serpentinization of ultramafic rocks is constrained by stability lines for serpentine minerals obtained by referenced workers.

Structural correlation:

Indrevær (2011) mapped the contact between the Tromsø Nappe and the Nakkedal Nappe NE of the Tromsdaltinden with emphasis on shear kinematics and relationship with metamorphism. Foliation data for the Cpx-Grt bearing amphibolites (given in section 3.4) coinsides with the main trend of the foliation in the Grt-Mca schist on the Tromsø Nappe side of the tectonical (called S_3 by Indrevær, 2011). This supports that the high P-T paragenesis of the Cpx-Grt bearing amphibolites related to the anatextic event predates the episode where the two nappes were juxtaposed.

Sense of shear of the large shear zones is the same as stretching lineations on the Tromsø nappe side of the tectonic contact (Indrevær, 2001). Large scale flexural folds and brittle faults also clearly post-date the main foliation close to the contact in the SMC, and is regarded late regional deformation after tectonic coupling of the two nappes. The overall trend of collected data for the latest structural elements is in agreement with what is generally accepted as late Caledonian features (Bergh et al., 2010).

6 Tectonmetamorphic evolution

Indications for that the SMC originated at as cumulate rock sequence have been presented by earlier workers (e.g Rindstad 1992, Selbekk et al., 2001). However there are few constraints regarding the pre-anatectic evolution of these rocks and the magmatic processes they derived from. The Tromsø Nappe sequence has been investigated more thoroughly over the years and it is helpful to consider the Upper Most Allochthon as a whole. In order to do so metamorphic events in the Tromsø Nappe has been compared with metamorphic events from the SMC:

Metamorphic events in the Tromsø nappe (TN)	(TN) P-T implications	Age - correlation (Ma)	(SMC) P-T implications	Metamorphic events in the Skattøra migmatite complex (SMC)
M1(TN): Eclogite facies metamorphism in TD related to the Taconian phase (Krogh et al., 1990; Corfu et al., 2003; Ravna & Roux, 2006).	690±30°C, 15.8-19.9 kbar (Broks, 1985), 735°C, 3.36 GPa(Ravna & Roux, 2006), 730-780°C, 3.2-3.5 GPa (Janák et al., 2012)	470 Taconian M1(SMC) M1(TN) E(2)	900°C, 1.0 GPa (Selbekk & Skjerlie, 2001), 875-900°C, >1.2 GPa (Kullerud et al.2012), Implications from this thesis: 800-850°C, >1.8 GPa(meta-anorth.),625-675°C, 0.5-1.5 GPa (Cpx-Grt Amph.).	**M1(SMC)**: Anatexis of the SMC (Broks, 1985; Rindstad, 1992; Selbekk et al., 2000, Selbekk & Skjerlie, 2001, Kullerud et al.2012)
E1: Partial melting during uplift (Stevenson 2005;2006;Ravna & Roux, 2006)	760-845°C, 2.0-2.2 GPa (Stevenson, 2005;2006).	445 M3(TN+SMC)		
M2 (TN): Prograde event during uplift, and related partial melting **(E2)** (Ravna et al. 1990; Ravna &Roux, 2006).	630±30°C, 7.8± kbar (Broks, 1985),743-950°C, 1.0-1.3 GPa(Stevenson, 2005; 2006). 680°C, 0.9 GPa (Indrevær, 2011).	Scandian phase 420	Implications from this thesis: 0.6-1.2 Gpa, 500-650°C (meta-anothosite),650-675°C 0.9-1.05 Gpa(felsic dyke).	**M2 (SMC):** Cooling during uplift, hydration related metamorphism and metasomatism.
M3(TD+SMC): Serpentinization and chloritiztion 560-630°C, 5-10 kbar (Broks, 1985), T-implication by Krogh et al.(1990): <500°C, T-implications from this study: <300°C.				

Figure 6.1: Summary of metamorphic events in Tromsø Nappe and Skattøra Migmatite Complex. Ages for the given metamorphic events are presented in table 6.1.

Nappes in the Upper Most Allochthon have for a long period been considered exotically derived from Laurentia margin, but recently an alternative origin has been presented by Kullerud et al. (2012); The Tromsø Nappe is suggested to have been a part of the Baltic continental margin, which experienced a stage of subduction prior to the Scandian collision phase. However, the tectonic contact between the Nakkedal Nappe and Tromsø Nappe has for long been known and pre-orogenic evolutions of the two nappes must be considered independently. The tectonic setting during formation and evolution of the rocks in the Upper Most Allochthon, together with respective ages has been implied by earlier workers:

Table 6.1: Age constraints for metamorphic events in Tromsø Nappe and Nakkedal Nappe.

Tromsø Nappe	Nakkedal Nappe
-The presence of carbonates and metapelites in the Tromsø Nappe sequence are interpreted to have originated as platform sediments (Krogh et al. 1990). - Metavolcanic-, metagabbroic- and metacarbonatitic rocks are indicators of an early active magmatic setting (Krogh et al., 1990). - **M1**: Indications of high pressure and subduction at 452.1 ± 1.7 Ma in the Tromsø Nappe. Age constraints are given by zircon-and titanite dating performed on eclogites of basaltic and gabbroic origin (Corfu et al., 2003). Leucosomes related to the eclogites suggests subsequent rapid uplift (~3,6cm/y) and two episodes (E1 and E2) of partial melting (Stevenson 2006; Ravna & Roux 2006). **-M2:** prograde event suggested to reflect the tectonic coupling of the Tromsø Nappe with Nakkedal Nappe. E2 partial melting is related to this stage. Age estimated to be: 450 ± 0.9Ma (Corfu et al., 2003, Ravna and Roux, 2006).	-The alkaline nature of the SMC rocks seen in relation to the quartz-feldspathic metasedimentary rocks of the Nakkedal Nappe complex points in the direction of a rifted margin setting (Selbekk et al., 2000). There is a general agreement that the SMC originated as a nepheline-normative layered cumulate sequence (Rindstad, 1992; Selbekk et al., 2000; Kullerud et al., 2012) Age is unknown. **-M1**:Formation of the leucocratic dyke swarm in the SMC indicates H2O-infiltration 456 ± 4 Ma ago. Age is based on U-Pb dating method of titanite from a migmatite leucosome (Selbekk et al., 2000). **-M2**: Hydration and retrogressive metamorphism is related to exhumation, decompression and cooling subsequent anatexis.
M3: Based on correspondence between late foliation and folding M3 is regarded as a post-main orogenic event during the Scandian phase. Krogh et al. (1990) suggested ages of the late cooling stage from K-Ar dating on retrogressive hornblende: 436 ± 11 Ma and 448 ± 20Ma (SMC), 437± 16 Ma (Tromsø Nappe).	

The P-T path from the constructed P-T pseudosections shown in figure 5.6 correspond reasonably well with earlier work by Rindstad (1992), Selbekk et al. (2000), Selbekk & Skjerlie (2001) and Kullerud et al.(2012). The correspondence give a foundation for suggesting a tectonometamorphic development in agreement with was has been suggested through figure 6.1 and table 6.1.

In addition a late prograde heating stage is suggested; based on the observed late reworking in the serpentinitic ultramafic rocks (for details see section 5.3.2).

In the context of the SMC the late antigorite growth was considered most likely to be a result of late dyke intrusion. Selbekk & Skjerlie (2001) suggested a tectonic model where uplift caused progressively deeper seated rocks to rise above solidus, and thus rock would: melt, cool and be intruded from melt formed below, something that fits nicely with observations. Included in Selbekk & Skjerlie's (2001) model there was a suggestion that the extensive partial melting events seen in the SMC was a result of dehydration of deeply seated eclogites of the Tromsø Nappe.

Another possibility arises when considering the Upper Most Allochthon as a whole:

Studies of the P-T evolution of metaperidotites in the Takab region, Iran, by Hajialioghli et al. (2007) gave a fairly similar P-T path as the one suggested for the SMC in figure 5.1. The Takab peridotites are suggested to have formed in the oceanic upper mantel (high P-T and ~72 km depth) before being retrograded under very low T (<280^{o}C). Subsequently a lower amphibolite facies prograde metamorphism in an orogenic setting is suggested. Hajialioghli et al. (2007) approached the problem of such a dramatic T- decrease (and the extreme decompression it would involve) by giving an alternative explanation where the peridotites were situated in the vicinity of a constructive plate boundary during an early convergent/collision/obduction event.

The suggested late prograde stage in the SMC could then possibly be linked to the prograde loop in the Tromsø Nappe(M2(TD) in figure 6.1). In that case the late heating of the serpentinite in the SMC would be related to the tectonic coupling of the Tromsø- and Nakkedal Nappe.

In order to favor any alternative the SMC needs to be investigated more thoroughly, through analytical differentiation between the polymorphs serpentine-minerals in the SMC-serpentinite and dating.

For future work on constraining magmatic ages in the SMC the dolerite dykes are suggested to be studies in more detail, as they contain significant amount of titanite, rutile and zircon.

7 Conclusions

On the basis of this study the following conclusions are made:

- Inclusions in peritectic garnet and relict clinopyroxene in the investigated amphibolitic-gneiss gives evidence of an early anhydrous stage in the evolution of the SMC.
- From anhydrous conditions the polymetamorphic metamorphic evolution consist of :
  (1) Hydration- where high P-T results in anatexis. Minimum temperatures must have exceeded the wet-melting curves for the protolithic rocks in the SMC. Based on P-T pseudosections melt is suggested present in the CNASH-system above approximately 1.18 GPa in the temperature interval 800-850 ^{0}C, and in the NCFMASH- system initial melting occurs between 625-675^{0}C, and 0.5-1.5 GPa.
  (2) Subsequent cooling and melt crystallization which lead to hydration reactions within units and metasomatic reactions in contact zones between dykes and host rock units.
  (3) Retrogression to very low T-P (greenschist/sub-greenschist conditions)

  In addition a late prograde growth of antigorite in the serpentinites is suggested. Further studies are necessary before arguments related to these observations with certainty can be used in discussion in a larger context.

- Felsic dykes has varying composition, which is put in relation to either addition of sodium through the infiltrating fluids or varying degree of partial melting. Crystallization of melt caused hydration- and metasomatic reactions in their vicinity.
- Incongruent melting of anorthositic plagioclase in the presence of fluids gives residual plagioclase enriched in the anorthite component, zoisite and melt which is enriched in sodium.
- Meta-dolerite has been identified in the SMC on the Tromsø Island, and is considered a new feature. Based on bulk chemistry and CIPW- norm calculations it has been compared to meta-gabbroic part of the SMC. Results show close similarities, and the meta-dolerite is suggested to have originated from the same magma source as the cumulate rocks in the SMC. The amount of accessory mineral hosting (L)RRE is significant .

REFERENCES

Ashworth, J.R., 1985. Introduction in: Migmatites, pp. 1-35. *Blackie, Glascow.*

Andresen, A., Fareth, E., Bergh, S.,Kristensen, S.E., Krogh, E.J., 1985. Review of the Caledonian lithotectonic units in Troms, North Norway. *The Caledonian Orogen-Scandinavian and Related Areas, pp.569-578.Wiley & Sons, Chichester*.

Auzanneau E., Schmidt M.W., Vielzeuf D. & Connolly J.A., 2010. Titanium in phengite: a geobarometer for high temperature eclogites. *Contributions to Mineralogy and Petrology, Vol.159, No.1, pp.1-24.*

Auzende, A.L., Guillot, G., Devouard, B. & Baronnet, A., 2006. Behaviour of serpentinites in convergent context : Microstructural evidence. *European Journal of Mineralogy, 18, 21–33.*

Bard, J. P., 1970. Composition of hornblendes formed during the Hercynian progressive metamorphism of the Aracena metamorphic belt (SW Spain). *Contr. Mineral. and Petrol. 28, 117-134*

Beard, J.S & Lofgren, G.E, 1989. Effect of Water on the Composition of Partial Melts of Greenstone and Amphibolite. *Science, New Series, Vol. 244, No. 4901, pp. 195-197*

Benisek A., Dachs E. & Kroll H., 2010. A ternary feldspar-mixing model base on calorimetric data: development and application. *Contribution to Mineralogy and Petrology, Vol.160, Number 3, pp. 327-337.*

Bergh, S. & Andresen, A., 1985. Tectonometamorphic Evolution of the Allochthonous Caledonian Rocks between Malangen and Balsfjord, Troms, North Norway. *Norges geologiske undersøkelse, Bulletin, 401, pp.193-204.*

Bergh, S.G., Kullerud K., Armitage, P.E.B., Zwaan, K.B., Corfu, F., Ravna, E.J.K. & Myhre P.I., 2010. Neoarchean and Svecofennian tectono-magmatic evolution of the West Troms Basement Complex, North Norway. *Norwegian Journal of Geology, Vol. 90, pp.1-28.*

Binns, R.A., 1965. The mineralogy of metamorphosed basic rocks from the Willyama complex, Broken Hill district, New South Wales. Part I. Hornblende. *Mineral. Mag. 35, pp. 306-326.*

Binns, R.A, 1978. Caledonian nappe correlation and orogenic history in Scandinavia north of lat 67°N. *Geological Society of America, Bulletin,89.*

Boyd, F.R., 1959. Hydrothermal investigations of amphiboles. *Reaseachers in geochemistry, Vol.1, Jhon Wiley and Sons, New York, pp. 377-396.*

Brattli, B., 1992. Mikroteksturer i magmatiske og metamorfe bergarter. *Institutt for geologi og bergteknikk, NTH, Trondheim.*
Broks, T.M., 1985. Cand.Sient. Oppgave i endogen geologi - Bergrunnsgeologiske undersøkelser innen Tromsø dekkekompleks i området Tromsdalen-Ramfjord-Breivikeidet, Troms., *Institutt for biologi og geologi, Universitetet i Tromsø.*

Brown M., Averkin, Y.A. &Mc Lellan, E.L., 1995. Melt segregation in migmatites. *Journal of Geophysical Research, Vol. 100, No. B8.*

Bruker AXS GmbH, 2004. Introduction to X-ray Fluorescence Analysis, User Manual. Bruker AXS GmbH, Germany.

Bryhni, I. & Andrèasson, P.G., 1985. Metamorphism in the Scandinavian Caledonides. In: *DG Gee, BA Sturt (eds) The Caledonide Orogen-Scandinavia and related areas.Jhon Wiely and Sons, Chichester, pp. 763-782.*

Bucher-Nurminen, K., Frank, *E*., & Frey, M., 1983. A model for the progressive regional metamorphism of margarite bearing rocksin the Central Alps. Amer. *Jour. Sci. 283-A, 370-395.*

Bucher, K. & Frey, M., 1994. Petrogenesis of Metamorphic Rocks. 6th ed., pp.251-285. *Springer-Verlag: Germany.*

Carswell D.A., Curtis C.D. & Kanaris-Sotiriou R., 1974. Vein metasomatism in Peridotite at Kalskaret near Tafjord, South Norway. *J. of Petrology, Vol.15, pp. 383-402.*

Carswell, D.A, Wilson, R.N. & Zhai, M., 2000. Metamorphic evolution, mineral chemistry and thermobarometry of schist and orthogneisses hosting ultra-high pressure eclogites in the Dabieshan of central China. *Lithos, Vol.52, 1-4, pp.121-155.*

Chernosky, JV, Day, HW., & Caruso, L.J.,1985. Equilibria in the system MgO-SiO,-H,0: experimental determination of the stability of Mg-anthophyllite. *American Mineralogist, 7 O, 223-236.*

Coggon R. & Holland T.J.B, 2002. Mixing properties of phengitic micas and revised garnet-phengite thermometers. *Journal of Metamorphic Geology, Vol.20, 7, pp. 683-698.*

Connolly, J.A.D & Petrini, K., 2002. An automated strategy for calculation of phase diagram section and retrieval of rock properties as a function of physical condition. *J. metamorphic Geol., 2002, 20, pp. 697-708.*

Connolly, J.A.D., 2009.The thermodynamic equation of state: what and how. *Geochem Geophys Geosyst. 10:Q10014*

Corfu, F.;Ravna, E. J. K. & Kullerud, K., 2003. A Late Ordovician U-Pb age for the Tromsø Nappe eclogites, Uppermost Allochton of the Scandinavian Caledonides. *Contributions to Mineralogy and Petrology. 145, 502-513.*

Corfu, Fernando; Roberts, R.J; Torsvik, T.H.; Ashwal, L.D. & Ramsay, D.M., 2007. Peri-gondwanan elements in the Caledonian nappes of Finnmark, northern Norway:

implications for the paleogeographic framework of the Scandinavian Caledonides.. *American Journal of Science 307, s 434- 458*

Dale J., Holland T. & Powell R. (2000). Hornblende-garnet-plagioclase thermobarometry: a natural assemblage calibration of the thermodynamics of hornblende. *Contributions to Mineralogy and Pertrology, Vol.140, 3, pp. 353-262.*

Davidsen, B., 1991. XRF-analyser ved IBG, UiTø; Metod, begrensninger og feil-grenser ved analyser av geologiske preparater. *Kompendium ved avdeling for endogen geologi, IBG, Universitetet i Tromsø.*

De Wit, M. J., 1976. Metamorphic textures and deformation: A new mechanism for the development of syntectonic porphyroblasts and its implications for interpreting timing relationships in metamorphic rocks. *Geological Journal, Volume 11, Issue 1, pages 71–100.*

Engel, A.E. & Engel, C.G., 1962. Hornblendes Formed During Progressive Metamorphism Of Amphibolites, Northwest Adirondack Mountains, New York. *Geological Soisiety of America Bulletin,Vol.73. No.12.*

Ernst W.G & Liu J., 1998. Experimental phase-equilibrium study of Al- and Ti-contents of calcic amphibole in MORB—A semiquantitative thermobarometer**.** *American Mineralogist, Volume 83, pages 952–969.*

Evans, B.W., 1977. Metamorphism of alpine peridotite and serpentinite. *Ann. Rev. Earth Planet. Sci, 5, pp.397-447.*

Evans, B.W., 2010. Lizardite versus antigorite serpentinite: Magnetite, hydrogen and life (?).*The Geological Society of America, Vol.38, 10, pp.879-882.*

Faye, G.H & Nickhele, E. H., 1970. The effect of charge-transfer processes on the colour and pleochroism of amphiboles. Can. Mineralogist, 10, pp. 616–635

Frost, B.R. & Beard, J.S., 2007. On Silica Activity and Serpentinization. J. of Petrology, Vol. 48, 7, pp. 1351-1368.

Ganguly J., Cheng W. & Tirone M., 1966. Thermodynamics of aluminosilicate garnet solid solution: new experimental data, an optimized model, and thermometric application. *Contributions to Mineralogy and Pertrology, Vol.126, 1-2, pp. 137-151***.**

Giere, R.& Sorensen,S.S., 2004. Allanite and Other REE-Rich Epidote-Group Minerals. *Reviews in Mineralogy & Geochmistry, Vol.56, pp. 431-439.*

Glazner, A.F., 1984. A short CIPW norm program. *Computers & Geosciences, Vol.10, No.4, pp. 449-450.*

Goldsmith, J.R & Ehlers, E.G., 1952. The Stability Relations of Anorthite and Its Hexagonal Polymorph in the System CaAl2Si2O8-H2O. *The Journal of Geology, Vol. 60, No. 4 , pp. 386-397.*

Green, E.C.R, Holland, T.J.B & Powell, R. (2007) An order-disorder model for omphacitic pyroxenes in the system jadeite-diopside-hedenbergite-acmite, with applications to eclogite rocks. *American Mineralogist, 92, pp. 1181-1189.*

Heinrich, E. W., 1965. Microscopic Identification of Minerals. *New York, McGraw-Hill Book Company, 414 p.*

Hellner, E. & Shürmann, K., 1966.Stability of metamorphic amphiboles:the tremolite-ferroactionlite series. *The Journal of Geology, Vol. 74, No. 3.*

Holland, T.J.B. & Powell, R., 1996. Thermodynamics of order-disorder in minerals: I. Symmetric formalism applied to minerals of fixed composition. *Am. Mineral, 81, pp.1413-1423.*

Holland, T.J.B. & Powell, R., 1998. An internally consistent thermodynamic data set of petrological interest. *J. of Meatmorphic Geology, Vol.16, 3, pp.309-343.*

Holland T. & Powell R., 2001. Calculations of Phase Relations Involving Haplogranitic Melt Using an Internally Consistent Thermodynamic Dataset. *Journal of Pertology, Vol.42, 4, pp. 673-683.*

Hollaway, J.R .,1973. The system pargasite-H2O-C2O: A model for melting of a hydrous mineral with a mixed-volatile fluids-I. Experimental results to 8 kbar. Geochim.Cosmochim., 37, pp.651-666.

Indrevær K., 2011. The Tromsø Nappe Contact with the Nakkedal Nappe Complex NE of the Tromsdaltind: Shear kinematics and relationship with metamorphism. *Master's thesis in geology, University of Tromsø, Norway.*

Janák, E., Ravna, E.J.K. & Kullerud, K., 2012. Constraining peak P-T conditions in UPH eclogites: calculated phase equlibria in teh kyanite- and phengite-bearing eclogite of the Tromsø Nappe, Norway. *Journal of Metamorphic Geology, Vol. 30, 4, pp.377-396.*

Jenkins D.M., 1983. Stability and Composition Relations of Calsic Amphiboles in Ultramafic Rocks. *Conrtibution to Mineralogy and Petrology, 83, pp.375-384.*

Johannes, W., 1968. Experimental investigation of the reaction forsterite + H2O→serpentine + brucite. *Contribution to Mineralogy and Petrology, 19, pp.309-315.*

Johannes, W. & Gupta, L.N., 1982. Origin and Evolution of a Migmatite. *Contribution to Mineralogy and Petrology, 79, pp.114-123.*

Karsli O., Aydin F. & Sadiklar B., 2004. Magma Interaction Recorded in Plagiocalse Zoning in Granitoide Systems, Zigana Granitoid, Eastern Pontides, Turkey. *Turkish Journal of Earth Sciences , Vol. **13**, 2004, pp. 287-305*

King P.L., Hervig R.L., Holloway J.R., Delaney J.S & Dyar M.D, 2000. Partitioning of Fe3+/Fe total between amphibole and basanitic melt as a function of oxygene fugacity. *Earth and Planatary Sience Letters, Vol.178, 2000, pp.97-112.*

Kirkland C.L.; Daly, J.S. & Whitehouse, M.J. 2007. Provenance and terrane evolution of the Kalak Nappe Complex, Norwegian Caledonides: implications for Neoproterozoic palaeogeograpy and tectonics. *J. Geol.,115, , pp. 21-41*

Kretz, R., 1983. Symboles of rock-forming minerals. *American mineralogist, 68, 277-279.*

Krogh, E.J., Andersen, A., Bryhni, I., Broks, T.M. & Kristensen, S.E., 1990. Eclogites and polyphase P-T cycling in the Caledonian Uppermost Allochthon in Troms, northern Norway. *J. metamorphic Geol., 8, 289-309.*

Kullerud, K., Nasipuri, P., Ravna, J.E.K. & Selbekk, R.S.,2012. Formation of corundum megacrysts during H2O-saturated incongruent melting of feldspar: P-T pseudosection-based modelling from teh Skattøra migmatite complex, North Norwegian Caledonides. *Contrib. Mineral Petrol., 2012.*

Landmark, K., 1973. Beskrivelse til de geologiske kart "Tromsø" og "Målselv". II. Kaledonske bergarter. *Tromsø Museum Skrifter. 15, 1-263.*

Larikova T.L. & Zaraisky G.P., 2009. Experimental modeling of corona textures. *J. metamorphic Geol., 27, pp. 139-151.*

Leake, B. E., 1968. A catalog of analyzed calciferous and sub-calciferous amphiboles together with their nomenclature and associated minerals. *Geol. Soc. Am. Spec. Papers 98.*

MacKenzie, W.S. & Adams, A.E., 1994. A colour Atlas of Rocks ans Minerals in Thin Sections. *Manson Publishing Ltd, London.*

Marocchi M., Mair V., Tropper P., Bargossi B.M., 2009. Metasomatic reaction bands at the Mt. Hochwart gneiss-peridotite contact(Ulten Zone, Italy): insight into fluid-rock interaction in subduction zones. *Miner Petrol, 95, pp. 251-272.*

Matthews, A. & Goldsmith J.R., 1984. The influence of metastability on reaction kinetics involving zoisite formation from anorthite at elevated pressures and temperatures. *Am. Mineralogist, Vol. 69, pp.848-857.*

Mehnert, K.R., 1968. Migmatites and the Origin of Granitic Rocks. *Amsterdam: Elisevier, 393 pp.*

Moody, J., 1976. Serpentinization: a review. *Lithos, 9, pp. 125-138.*

Newton, R.C., Charlu, T.V.& Kleppa, O.J., 1980. Thermochemistry of high structural state plagioclases. *Geochimica et Cosmochimica Acta, 44, pp.933-941.*

Oba, T., 1980. Phase relations in the Tremolite-Pargasite Join. *Contrib. Mineral. Petrol. 71, pp.247-256.*

Oba, T., 1990. Experimental study on the tremolite-pargasite join at variable temperatures under 10kbar. *Earth Planet Sci., Vol.99, No.1, pp. 81-90.*

Olsen, T.S. and Kohlstedt, D.L., 1985. Natural deformation and recrystallization of some intermediate plagioclase feldspars. *Tectonophysic.r, 111:* 107-l 31.

Pettersen, K., 1868. Geologiske Undersøgelser i Tromsø Omegn, i DKNVS Skr. i 19. Aarh., bd. 5, hf. 2, s. 113–240.

Putnis, A., 2002. Mineral replacement reactions: from macroscopic observations to microscopic mechanisms. *Mineralogical Magazine, Vol. 66, 5, pp. 689-708.*

Ravna, E.J.K, Roux M.R.M., 2002. A detailed P–T path for eclogites in the Tromsø Nappe, N Norwegian Caledonides:a complex history of subduction, exhumation, reheating and recrystallization. *AGU Fall Meeting (2002), Abstr., V51B–1253.*.

Ravna, E.J.K. & T erry, M.P., 2004. Geothermobarometry of UHP and HP eclogites and schists: an evaluation of equilibria among garnet-clinopyroxene-kyanite-phengite-coesite/quartz. *Journal of Metamorphic Geology* 22, 579-592.

Ravna, E.J.K. & Roux M.R.M., 2006. Metamorphic evolution of the Tønsvika eclogite, Tromsø Nappe-Evidence for a new UHPM province in the Scandinavian Caledonides. *International Geology Reviews, Vol. 48, 2006, p. 861-881.*

Raase, P., 1974. Al and Ti Contents of Hornblende, Indicators of Pressure and Temperature and Regional Metamorphism. *Conrtibution to Mineralogy and Petrology, 45, pp.231-236.*

Rindstad, L., 1992. Petrografiske, metamorfe og geokjemiske undersøkelser av Skattøragneise på Tromsøya med særlig vekt på de leucosome gangenes opprinnelse. *Unpublished. Cand scient thesis, University of Tromsø.*

Roberts, D. & Gee, D.G., 1985. An introduction to the structure of the Scandinavian Caledonides. In: Gee, D.G., Sturt, B.A. (Eds.), The Caledonide Orogen—Scandinavia and Related Areas. *Wiley, Chichester, pp. 55– 68.*

Roberts, D., 2003. The Scandinavian Caledonides: event chronology, palaeogeographicsettings and likely modern analogues. *Tectonophysics.,365, 283-299.*

Sawyer,E.W.,2008. Atlas of Migmatites.*The Canadian Mineralogist Special Publication 9, NRC Research Press, Ottawa, Ontario, Canada, 371 pp.*

Swayer, E.W., 1999. Criterian for the Recognition of Partial Melting. *Phys. Chem. Earth, Vol.24, No.3, pp.269-279.*

Selbekk, R.S., Skjerlie, K.P. & Pedersen, R.B., 2000. Generation of anorthositic magma by H2O-fluxed anatexis of silica-undersaturared gabbro: an example from the north Norwegin Caledonides. *Geol. Mag., 137, pp.609-621.*

Selbekk, R.S. & Skjerlie, K.P., 2001: Pertogenesis of theAnorthosite Dyke Swarm of Tromsø, North Norway: Experimental Evidences for Hydrous Anatexis of an alkaline Mafic complex. *Doctor Scientiarium Thesis, Department of Geology, University of Tromsø, Norway.*

Shand, S.J., 1945. Coronas and Coronites. Bulletin of The Geological Society of America. *Vol. 56, pp. 247-256.*

Shelly, D., 1993.Igneous and metamorphic rocks under the microscope. *1st ed., Chapman & Hall, London, pp.137-139.*

Schumacher R., 1991. Composition and phase relation in calsic amphibole in epidote- and clinopyroxene bearing of the amphibolites and lower granulite facies, central Massachusettes, USA. *Contrib Mineral Petrol, 108, pp. 196- 211*.

Spears, F.S., 1993. Meatmorphic Phase Equilibria and Pressure-Temperature-Time Paths. *Minerlogical Soceity of America, Whasington D.C, U.S., Ch.9, pp.289-293.*

Stevenson , J.A., 2005. High pressure partial melting of eclogite and garnet amphibolites rocks during decompression and heating, Tromsø Nappe Norway. *EOS(Transection of the American Geophysical Union, Vol.85, Abstarct T23C-03.*

Stevenson, J.A., 2006. Partial melting of eclogite, Tromsø, Norway. *Ph.D., Yale University, 323 pp.*

Temple. A.K., 1966. Alteration of ilmenite. *Economic Geology, Vol. 61, no. 4, pp.695-714*.

Tracy, R.J., (1982). Compositional zoning and inclusions in metamorphic minerals. *Reviews in Mineralogy and Geochemistry, January 1982, v. 10, p. 355-397*

Ulmer, P. and Trommsdorff, V. 1995. Serpentine Stability to Mantle Depths and Subduction-Related Magmatism. *Science, 268, pp. 858–861*.

Van Grieken, R. & Markowicz, A. A,2002. Handbook of X-ray spectrometry. *Marcel Dekker, New York.*

Vernon, R.H. 1975. Deformation and recrystallization of a plagioclase grain. *American* Mineralogist, 60, 884-888.

Wayte, G.J., Worden, R.H., Rubie., D.C & Droop, G.T.R., 1989. A TEM study of disequilibrium plagioclase breakdown at high pressure: the role of infiltrating fluid. *Conrtibutions to Mineralogy and Petrology, 101, 426-437.*

White R.W, Powell R. & Holland T.J.B, 2001. Calculation of partial melting equilibria in the system Na2O-CaO-K2O-FeO-MgO-Al2O3-SiO2-H2O(NCKFMASH). *Journal of Meatmorphic Petrology, Vol.19, 2, pp.139-153.*

White R.W, Powell R. & Holland T.J.B, 2002. Melt loss and preservation of granulite facies mineral assemblages. *Journal of Metamorphic Geology, 20, 621-632.*

White R.W, Powell R. & Holland T.J.B, 2007. Progress relating to calculation of partial melting equilibria for metapelites. *Journal of Metamorphic Geology, 25, 511-527.*

Yau, Y., Anovitz, L.M., E.J & Peacor, D.R., 1984. Phlogopite-chlorite reaction mechanisms and physical conditions during retrograde reactions in theMarble formation, Franklin, New Jersey. *Contributions to Mineralogy and Petrology, 88, 299-306.*

Zwaan, K. B.; Fareth, E. & Grogan, P. W. 1998. Geologisk kart over Norge, berggrunnskart TROMSØ, M 1:250.000. *Norges geologiske undersøkelse*

Internet resources:

www.perplex.ethz.ch/perplex_66_seismic_velocity.html

www.norgei3d.no

www.volcanoes.usgs.gov/yvo/aboutus/jlowenstern/other/software_jbl.html

APPENDIX

Table A1: Overview of samples and their belonging locality, thin section number, XRF-analysis number, figure numbers in main text, rock type and main minerals

Loc.	Hand specimen	Figure	Thin section	Figure	XRF	Rock type	Main minerals
1	1_1	3.10	1_1	3.11, 3.12	1_1, 1_1B	Mafic, amphibolite.	Amph, Pl,Grt,Cpx
	1_2		1_2			Mafic, amphibolite.	Amph, Pl,Grt,Cpx
2	2_3					Mafic, amphibolite.	Amph, Pl
3	3_4	3.3A	3_4	3.4A		Meta-anorthosite	Pl,Zo, Mca (Pg), Ep/Czo
	3_5	3.13	3_5	3.6A, 3.14	3_5(A,B,C)	Mafic dyke/felsic dyke	Pl,Zo, Amph/ Pl, Amph, Zo, Ep/Czo
	3_6	3.3B	3_6	3.4B	3_6, 3_6B	Meta-anorthosite	Pl,Mca, Zo, Ep/Czo
	3_7					Mafic, amphibolite.	Amph, Pl
	3_8					Amphibolite/leucosome	Amph, Pl
	3_9		3_9A			Felsic dyke	Hbl, Pl, Chl
			3_9B			Felsic dyke	Pl,Mca, Ep, Hbl
4	4_10					Reaction zone F -UM	Pl,Tlc,Amph,Chl
	4_11					Reaction zone F -UM	Pl,Srp, Amph, Tlc, Chl
	4_12					Reaction zone F -UM	Pl,Srp, Amph, Tlc
	4_13	3.16	4_13	3.17A		Ultra mafic	Amph, Chl, Bt
	4_14					Ultra mafic	Amph, Chl, Bt
	4_15	3.18	4_15	3.19D		Serpentinite	Ol, Srp,Tlc, Sp, Amph
	4_16					Reaction zone F -UM	Amph, Tlc, Pl, Chl
	4_17		4_17			Reaction zone F -UM	
	4_18		4_18	3.17B		Ultra mafic	Amph,Bt,Tlc
	4_19					Felsic dyke	Pl, Hbl
	4_20					Felsic dyke	Pl, Hbl
	4_21	3.8	4_21	3.9(A,B)		Migmatite gneiss	Amph, Pl, Ep/Czo
	4_22	3.20	4_22A	3.19C, 3.21		Reaction UM/F	Srp, Tlc, Ol, Tlc,Amph
			4_22B			Serpintenite	Srp, Tlc
	4_23		4_23	3.19(A,B)		Reaction UM/F	Srp, Tlc,Amph, Chl
	4_24	3.6	4_24	3.6B	4_24, 4_24B	Felsic dyke	Pl, Hbl

Table A2: Reference values, standard values and results of XRF-analyses given in wt.(%)

Sample	Ref.values	Std: AVG-1	Std: AVG-1B	1_1	1_1B	3_6	3_6B	4_24	4_24B	3_5A	3_5B	3_5C
Rock type				Cpx-Grt amph	Cpx-Grt amph	M-anort	M-anort	F-dyke	F-dyke	M-dolerite	M-dolerite	M-dolerite
SiO_2 (%)	58,84	59,14	59,19	44,5	44,25	45,99	44,94	57,32	56,98	48,64	48,72	48,75
Al_2O_3 (%)	1,05	17,02	17,05	13,76	13,78	30,23	29,38	24,18	24,08	19,78	19,79	19,84
TiO_2 (%)	17,15	1,01	1,017	1,934	1,933	0,065	0,065	0,061	0,061	0,91	0,92	0,91
Fe_2O_3 (%)	6,77	6,68	6,69	14,22	14,15	1,03	1,15	0,67	0,7	9,28	9,43	9,49
MnO (%)	0,09	0,094	0,094	0,252	0,248	0,018	0,019	0,012	0,012	0,11	0,11	0,12
MgO (%)	1,53	1,46	1,46	6,15	5,98	0,14	0,17	0,34	0,33	3,94	3,97	3,96
CaO (%)	4,94	4,86	4,85	12,57	12,31	17,58	17,63	6,59	6,56	9,76	9,78	9,77
Na_2O (%)	4,26	4,13	4,11	2,36	2,32	2,02	1,99	6,67	6,68	4,2	4,23	4,22
K_2O (%)	2,92	2,92	2,92	0,55	0,54	0,11	0,1	0,35	0,34	0,3	0,3	0,3
P_2O_5 (%)	0,49	0,492	0,495	0,161	0,163	0,02	0,02	0,015	0,018	0,34	0,34	0,35
Total	**98,04**	**97,806**	**97,876**	**96,48**	**95,69**	**97,21**	**95,47**	**96,22**	**95,77**	**97,26**	**97,59**	**97,71**

Table A3 a) Normative plagioclase composition of white dykes in the SMC based on CIPW-norm data from Rindstad (1992).

White	1/1	2	1/3	L-6	24/2	DP-T	1/2	L-11	L-20	11
An	21,43	22,83	22,68	19,44	18,66	22,72	20,56	28,42	22,43	19,07
Ab	71,86	71,8	73,9	70,29	73,49	67,14	67,71	68,48	73,55	66,18
An/(Ab+An)	**0,23**	**0,24**	**0,23**	**0,22**	**0,20**	**0,25**	**0,23**	**0,29**	**0,23**	**0,22**

Table A3, b) Normative plagioclase composition of grey dykes in teh SMC based on CIPW-norm data from Rindstad (1992).

Grey	L-12	1/7	1/8	1	7	L-3	L-2	24/1	6
An	30,74	33,08	34,25	35,01	28,42	31,27	25,04	35,07	30,65
Ab	59,76	54,72	51,58	52,16	56,48	50,49	60,06	56,31	53,4
An/(Ab+An)	**0,34**	**0,38**	**0,40**	**0,40**	**0,33**	**0,38**	**0,29**	**0,38**	**0,36**

Table A4: Normative plagioclase composition for dykes in SMCbased on CIPW-norms data from Selbekk et al. (2000).

Sample no.	S2-96	S25-96	S26-96	S30-96	S12-97	S14-97	S15-97	S17-97	S20-97	S23-97	S24-97	S25-97	S26-97	S29-97	S28-97	S41-97	S42-97
An	22,80	34,40	32,00	20,30	30,90	19,60	21,30	21,90	26,90	21,40	20,90	28,70	31,90	35,20	34,70	32,70	28,70
Ab	72,40	50,50	57,10	72,20	60,90	70,20	71,40	70,30	67,30	73,10	73,90	60,90	57,30	52,90	60,70	60,80	66,20
An/(Ab+An)	**0,24**	**0,41**	**0,36**	**0,22**	**0,34**	**0,22**	**0,23**	**0,24**	**0,29**	**0,23**	**0,22**	**0,32**	**0,36**	**0,40**	**0,36**	**0,35**	**0,30**